Solar radio bursts and Space Weather

Christophe Marqué

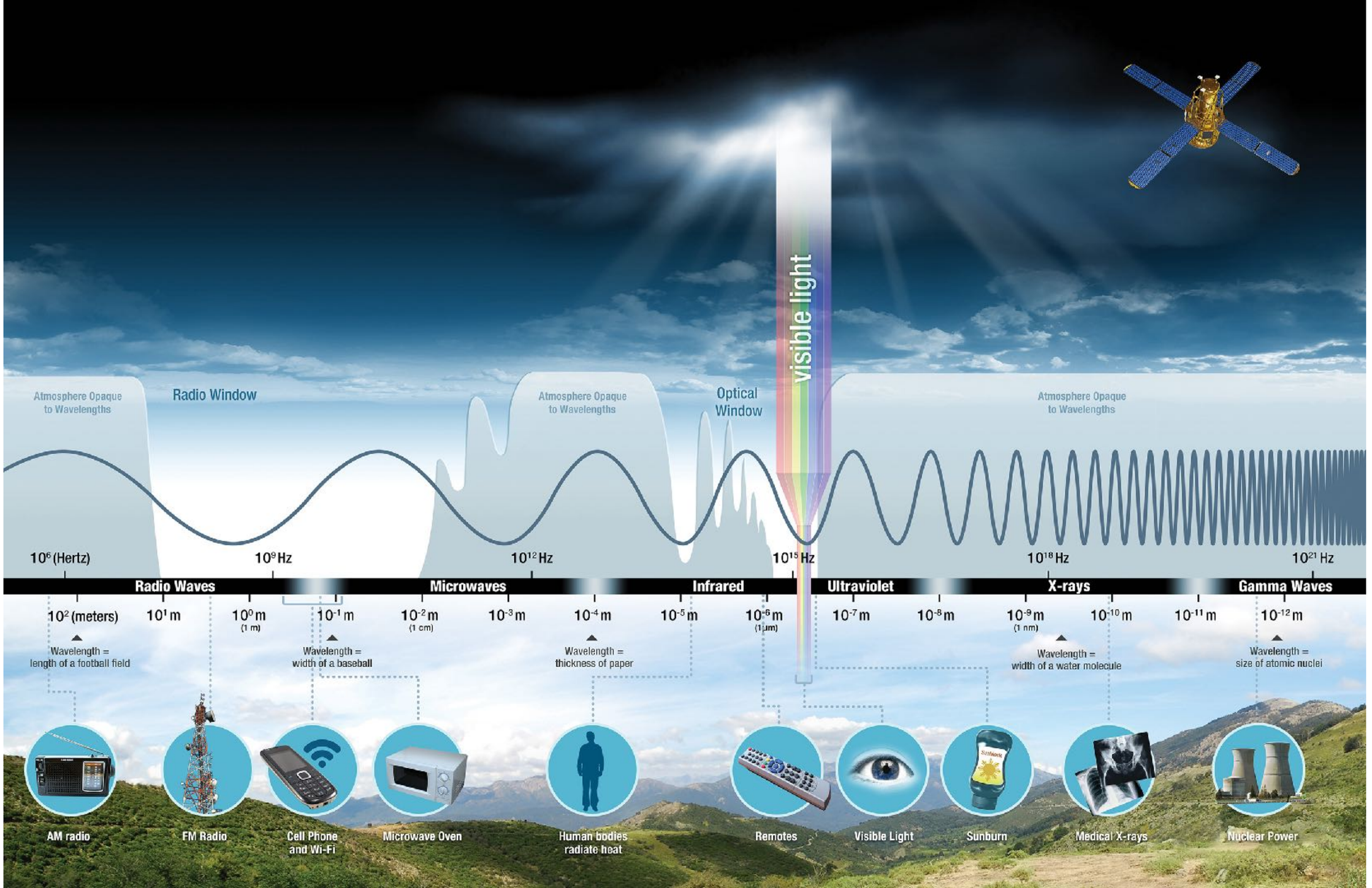
visible light
Atmosphere Opaque to Wavelengths
Radio Window
Atmosphere Opaque to Wavelengths
Optical Window
Atmosphere Opaque to Wavelengths
10^{6} (Hertz)
10^{9} Hz
10^{12} Hz
10^{15} Hz
10^{18} Hz
10^{21} Hz
Radio Waves
Microwaves
Infrared
Ultraviolet
X-rays
Gamma Waves
10^{2} (meters)
10^{1} m
10^{0} m (1 m)
10^{-1} m
10^{-2} m (1 cm)
10^{-3} m
10^{-4} m
10^{-5} m
10^{-6} m (1 µm)
10^{-7} m
10^{-8} m
10^{-9} m (1 nm)
10^{-10} m
10^{-11} m
10^{-12} m
Wavelength = length of a football field
Wavelength = width of a baseball
Wavelength = thickness of paper
Wavelength = width of a water molecule
Wavelength = size of atomic nuclei
AM radio
FM Radio
Cell Phone and Wi-Fi
Microwave Oven
Human bodies radiate heat
Remotes
Visible Light
Sunburn
Medical X-rays
Nuclear Power

The Sun is among the strongest radio sources in the sky

but ...

it was first detected in 1944 by G. Reber, 11 years after the discovery of cosmic radiations by K. Jansky

FIGURE 3

F_a versus frequency (10^8 to 10^{11} Hz)

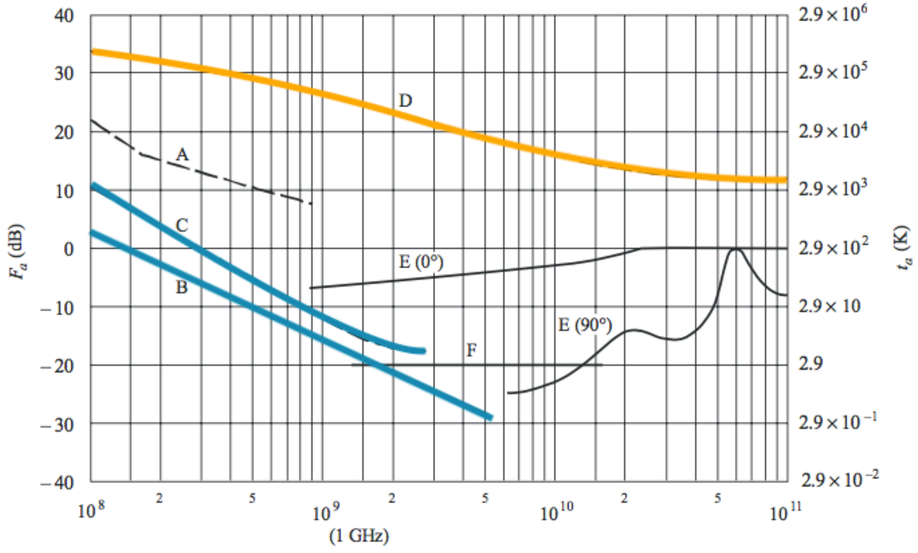

A: estimated median city area man-made noise
B: galactic noise
C: galactic noise (toward galactic centre with infinitely narrow beamwidth)
D: quiet Sun (½° beamwidth directed at Sun)
E: sky noise due to oxygen and water vapour (very narrow beam antenna); upper curve, 0° elevation angle; lower curve, 90° elevation angle
F: black body (cosmic background), 2.7 K
minimum noise level expected

P.0372-03

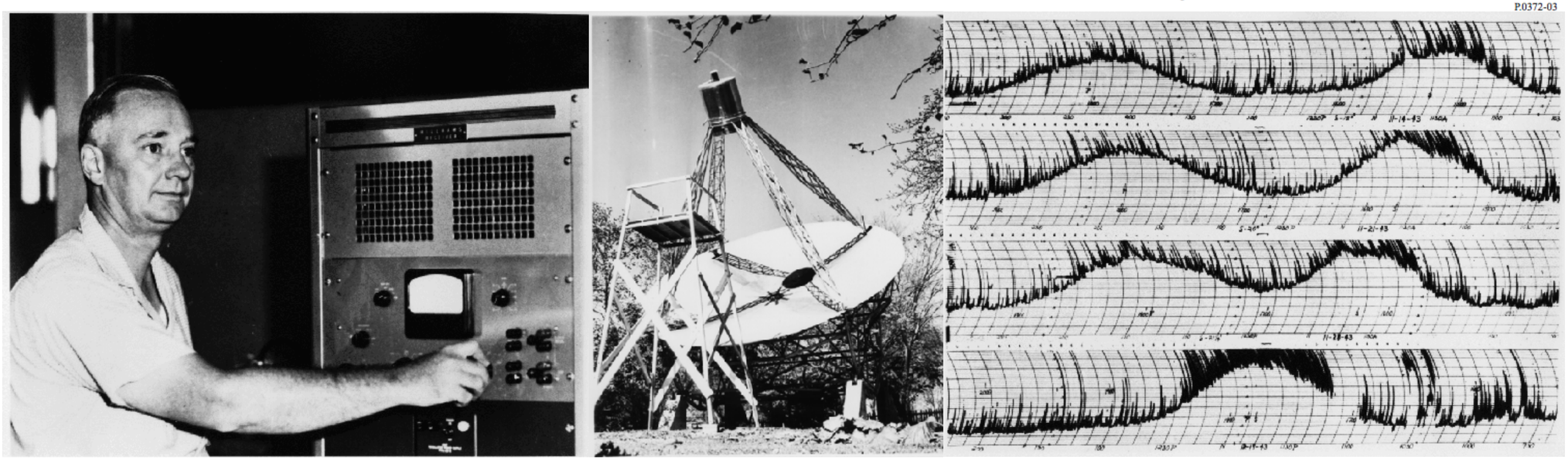

All layers of the solar atmosphere are accessible to radio observations

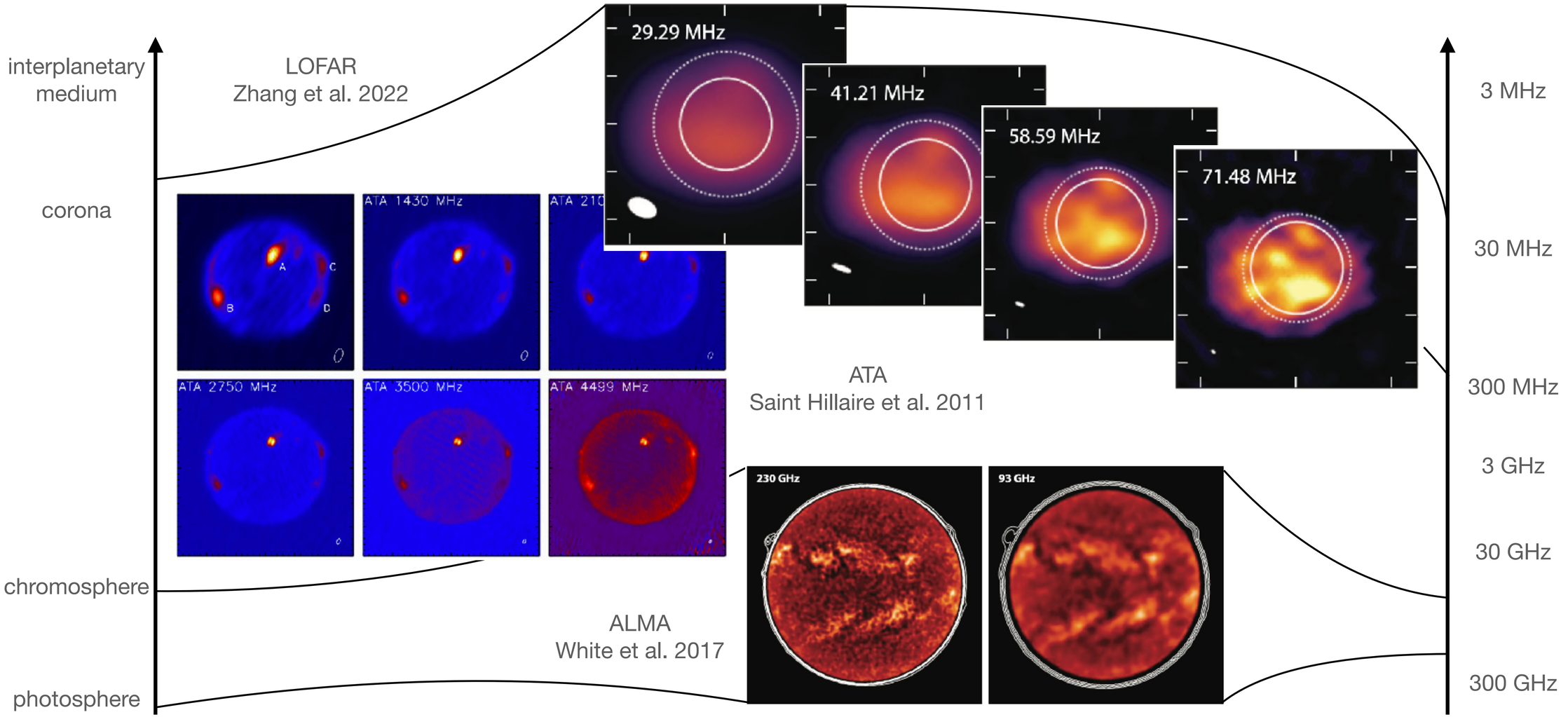

Imaging observations

- Diameter of the Sun : 32 '
- AR size: few arcmin
- Telescope resolution $\propto \lambda/D$

Main technique is interferometry

ALMA single dish 12 m 230 GHz	ALMA single dish 12 m 93 GHz	ATA 6000 MHz	ATA 1430 MHz	LOFAR LBA 71 MHz	LOFAR LBA 30 MHz
20"	1'	0.75'	3.1'	5'	15'
12 m	12 m	~300 m	~300 m	~ few km	~ few km

Interferometry

- Array of antenna
- Correlation of signal from pairs of antenna give one measurement point in the Fourier domain
- Difficulties
  - The Sun is large
  - Variable
  - High dynamic

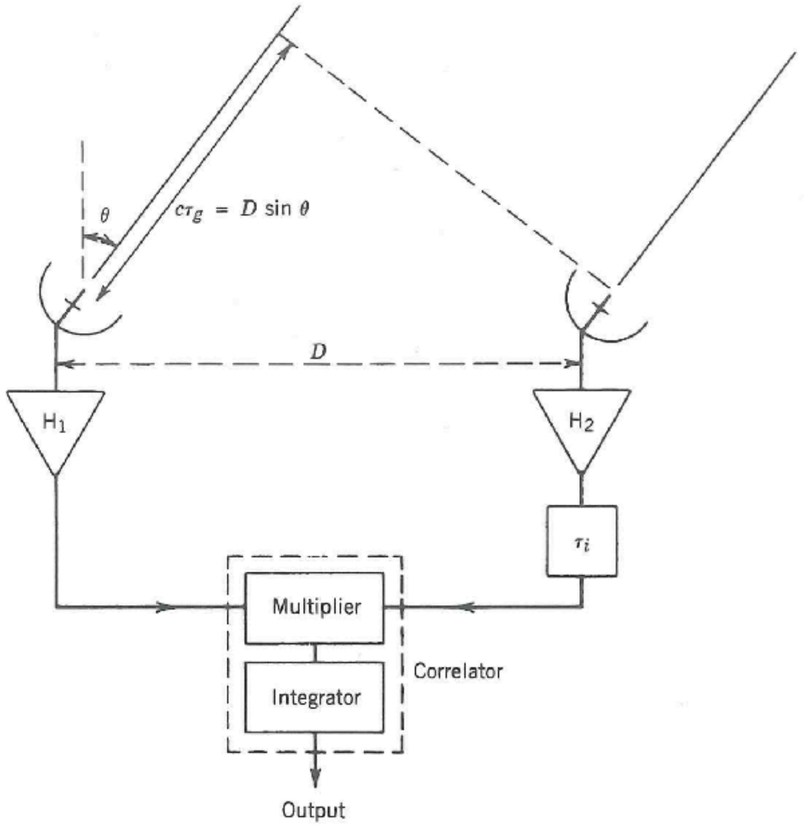

Interferometry

- Array of antenna
- Correlation of signal from pairs of antenna give one measurement point in the Fourier domain
- Difficulties
  - The Sun is large
  - Variable
  - High dynamic

Snapshot u-v coverage

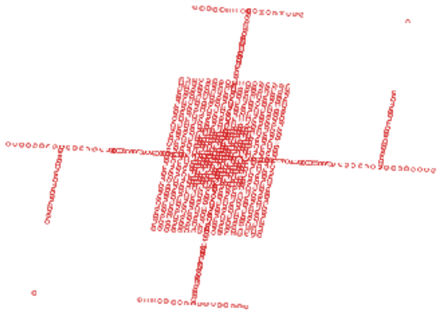

Earth-rotation u-v coverage

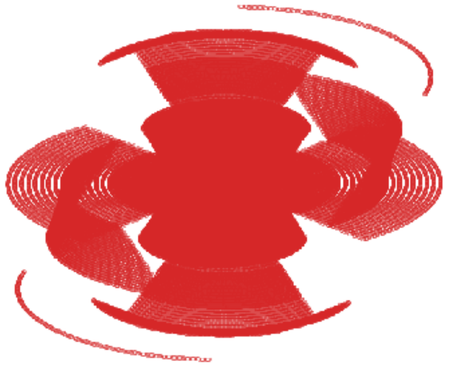

Snapshot image

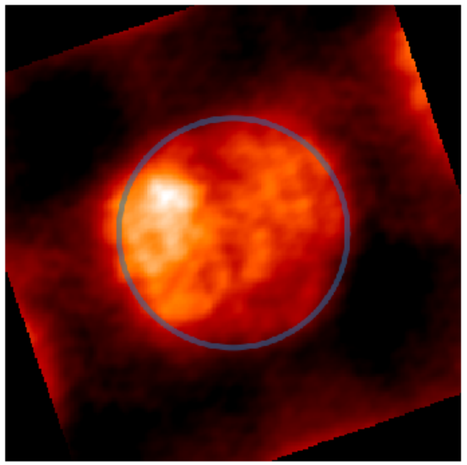

Earth-rotation image

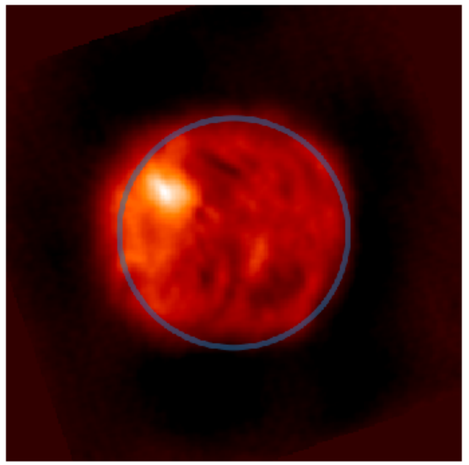

Nançay radioheliograph



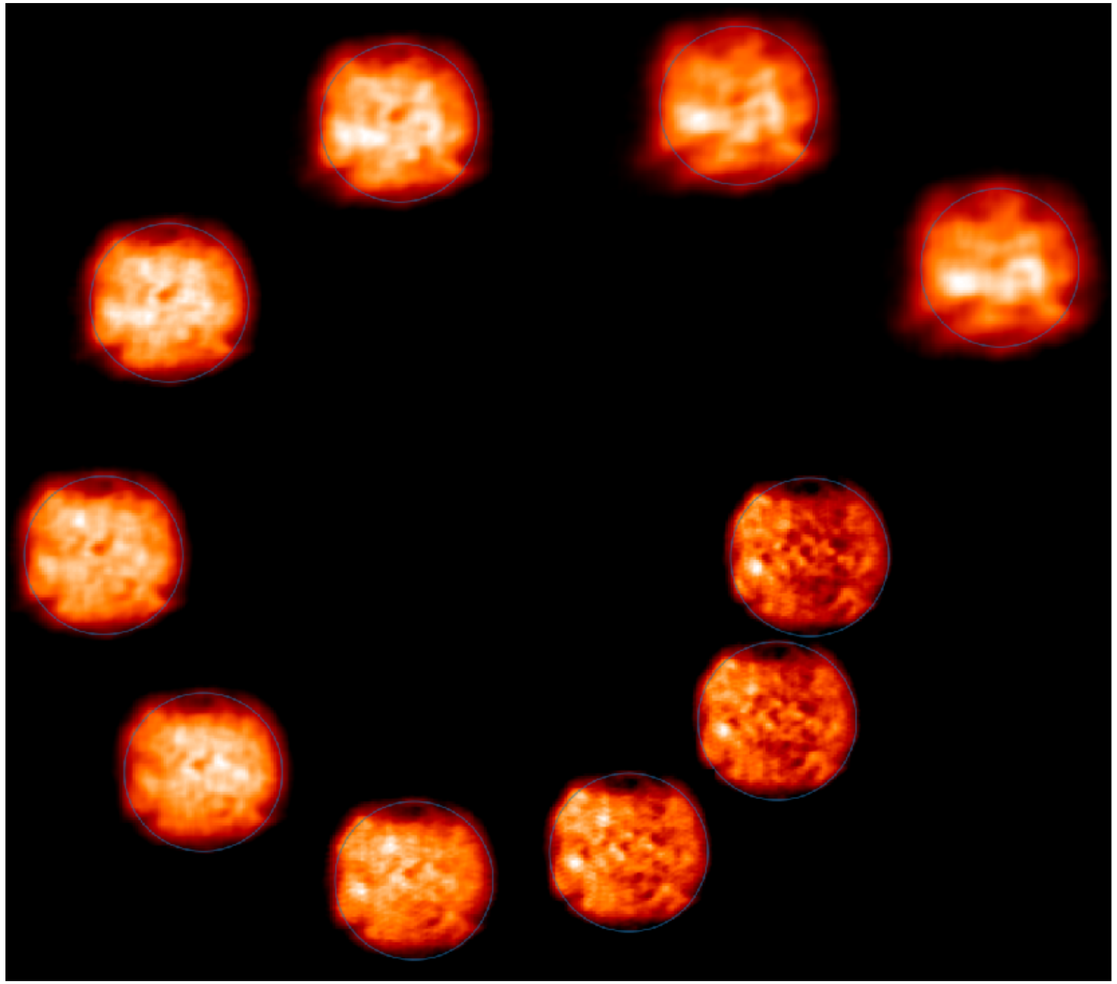

LOFAR



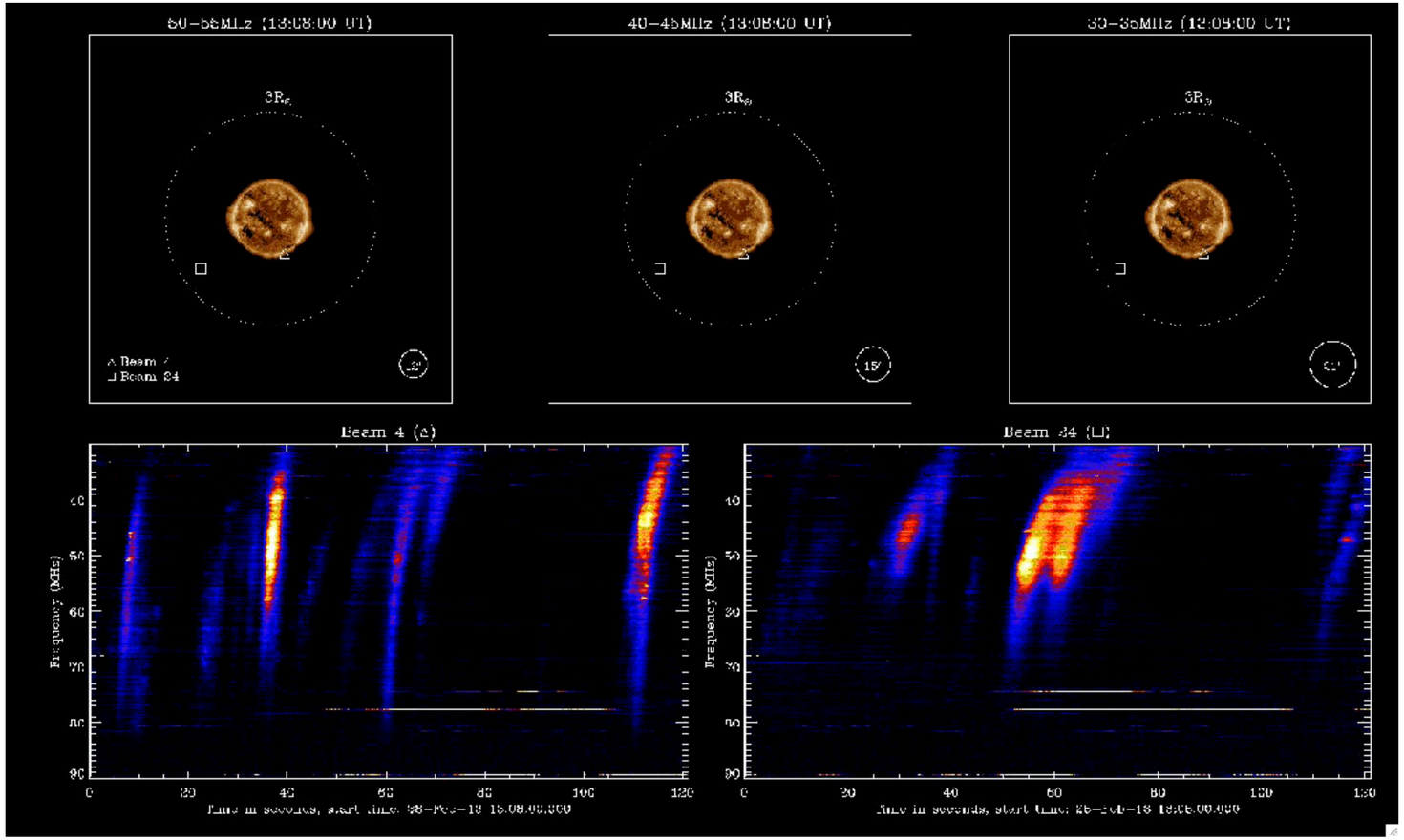

Morosan et al. 2014

LOFAR



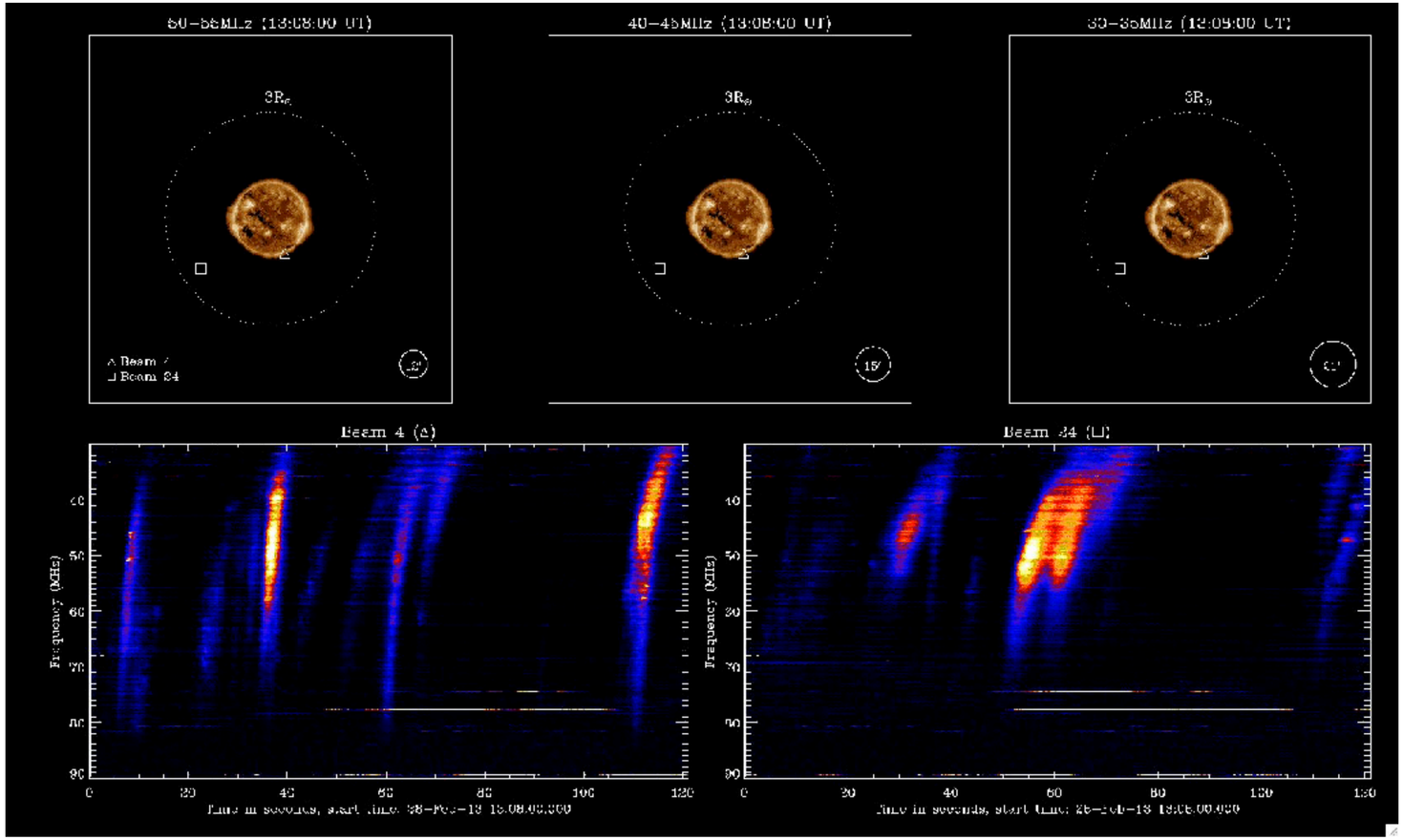

Morosan et al. 2014

Dynamic spectra

- Pseudo images time / frequency
- Temporal evolution of the solar radio spectrum
- Useful for detection and study of radio bursts
- Different kinds of bursts have been detected:
- At low frequencies < 500 MHz :
    - type I, II, III, IV, V

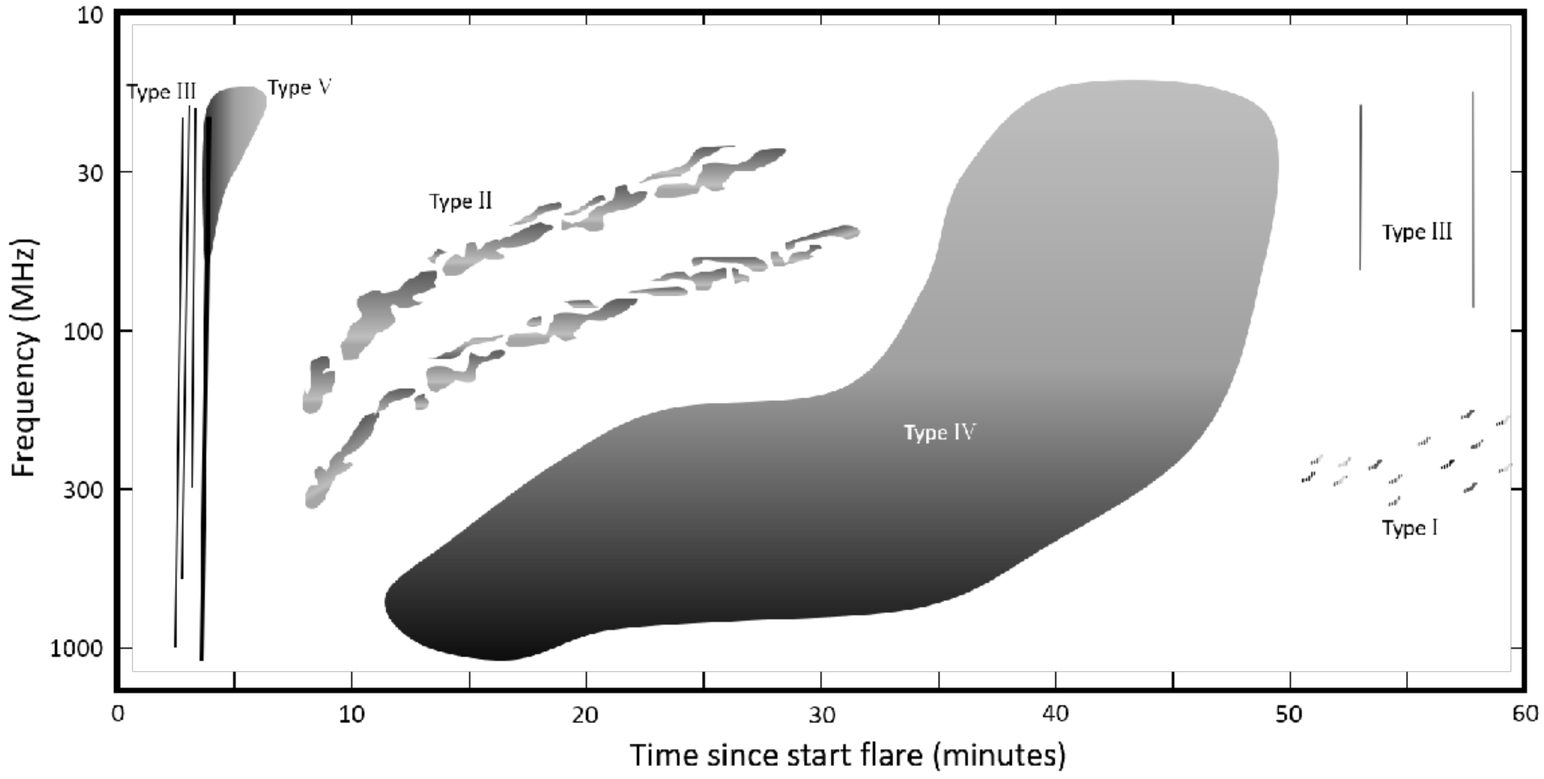

Radio bursts

Solar radio bursts are produced by non thermal electrons accelerated during eruptive events of all magnitudes

For frequencies (f) below ~ 1- 2 GHz, the dominant emission is called plasma emission, where energetic electrons trigger local plasma oscillations which are then converted into E. M. radiations $f \propto \sqrt{n_e}$

Above, gyroemissions, gyrosynchrotrons or bremstrahlung emissions dominate

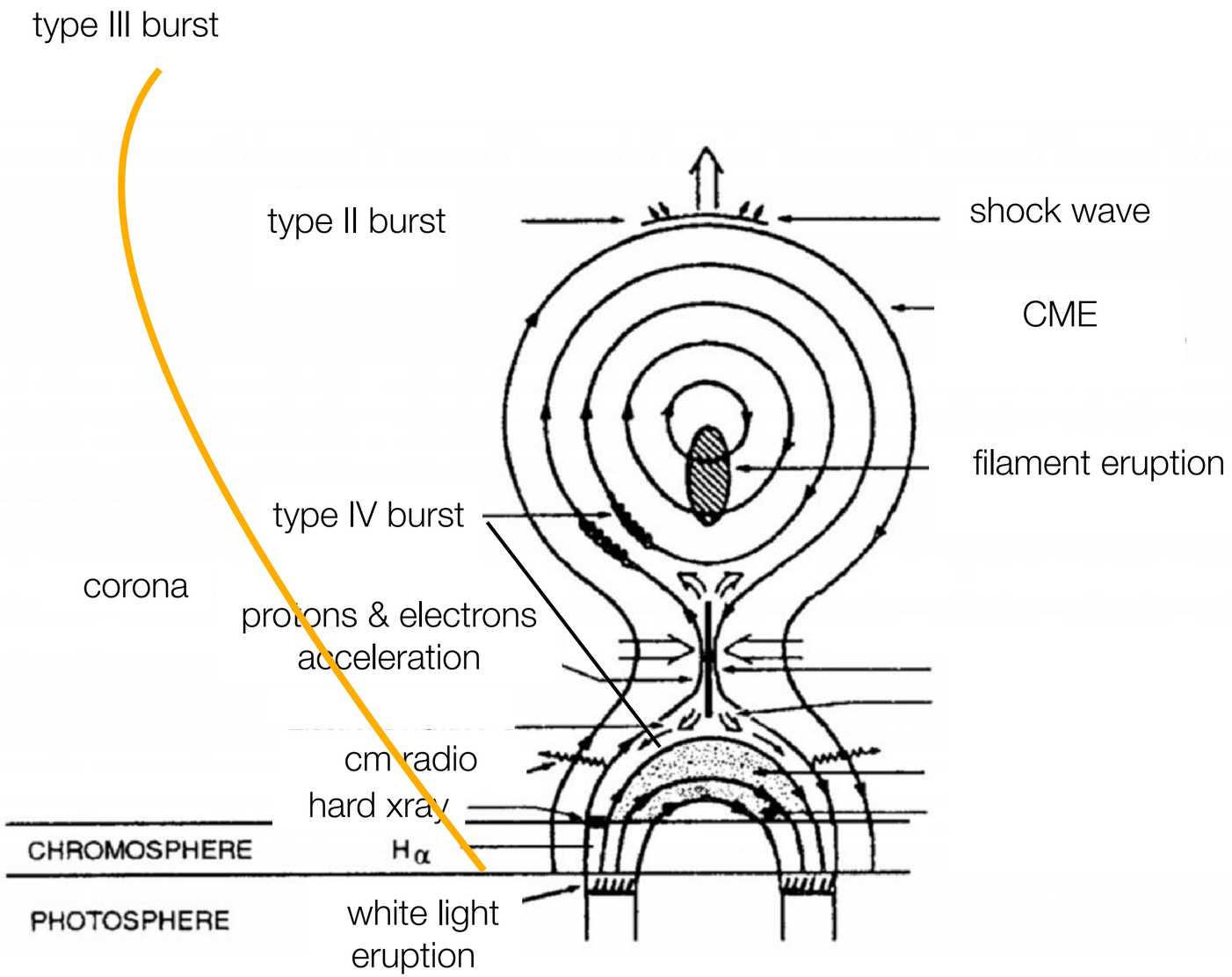

Adapted from Lantos, P.

Converting frequency into distance

Poor man's method

- 1d electron density models
- Based on eclipses (Baumbach-Allen (1937-1947), Saito, Newkirk) (close to the Sun 1 - 2 Rs)
- Systematic studies of IP radio bursts (Leblanc et al. 1998) or radio sources occultations (Erickson, 1964) (R > 2 -10 Rs)
- In all cases this is inaccurate !

Leblanc, 1998

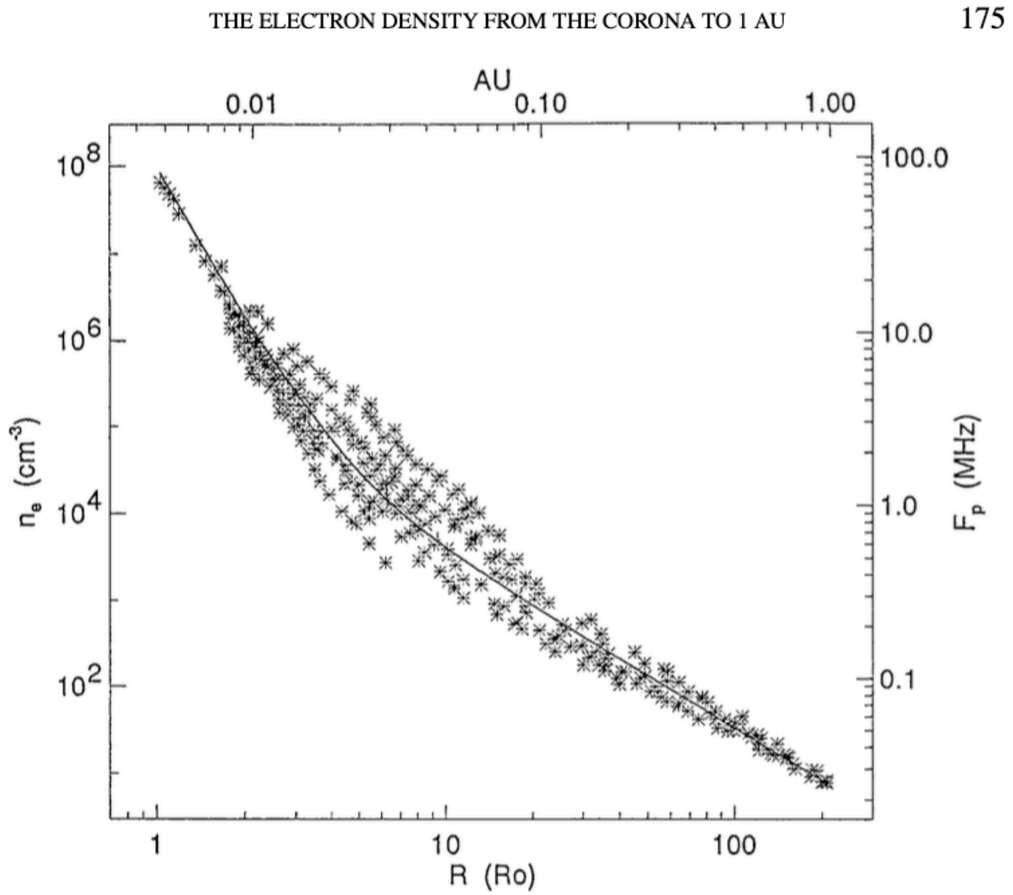

Figure 5. Electron density model vs radial distance derived from all 11 events, where the density at 1 AU has been normalized to 7.2 cm^{-3} (f_p = 24 kHz). The solid line is the best fit whose equation is given in the text. The small cluster of points in the upper left comes from 25–75 MHz observations of Nançay for one event.

Type I & noise storms

Non flaring radio bursts linked to sunspots

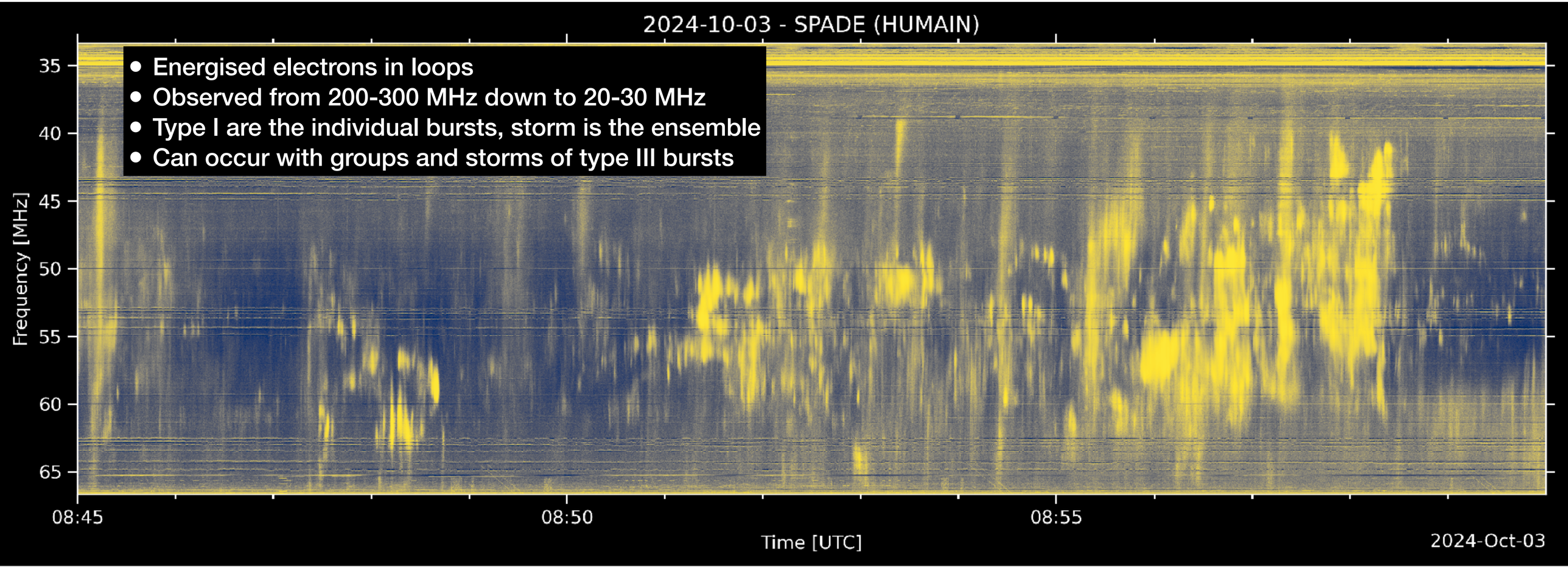

Anatomy of a noise storm

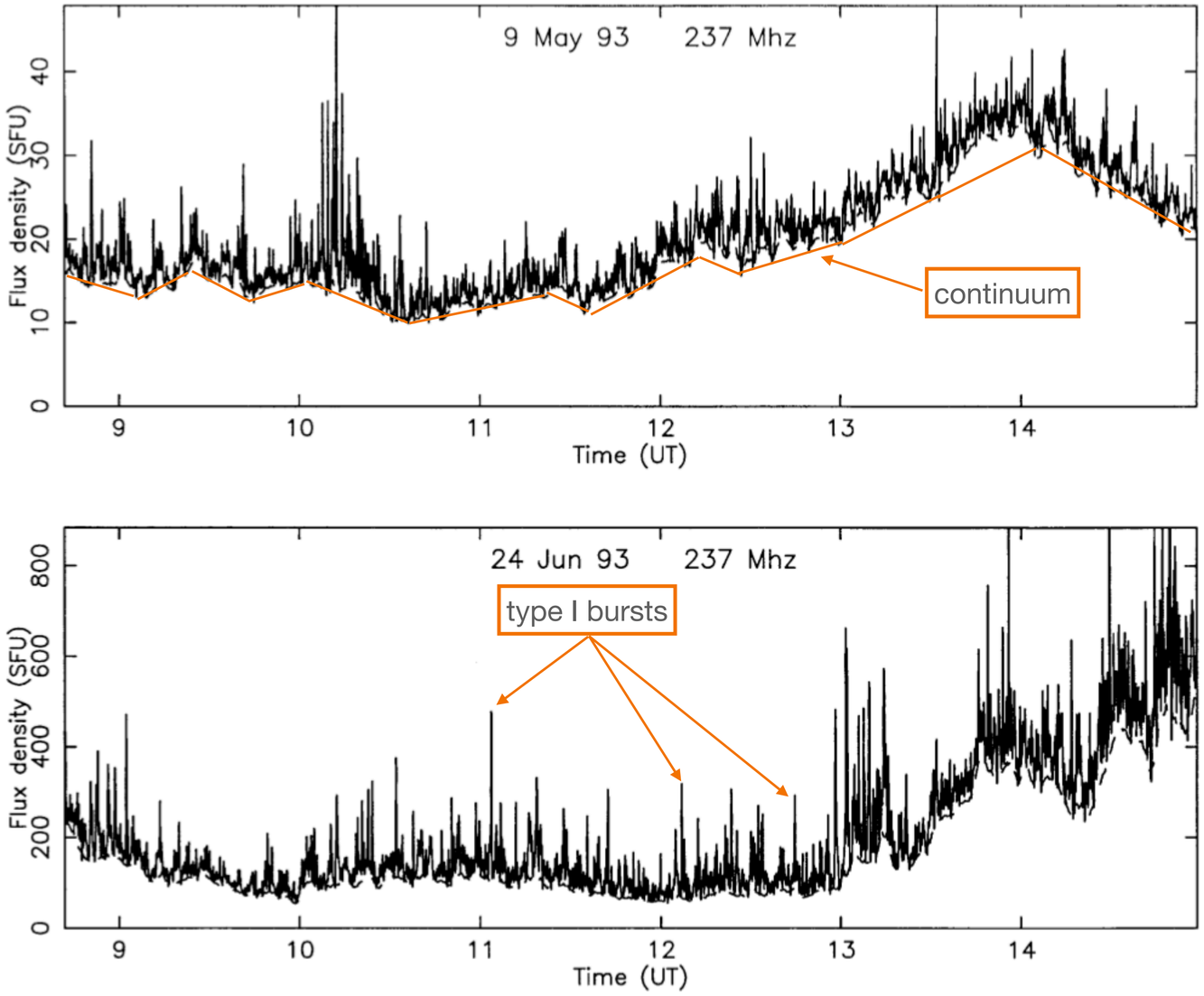

from Mercier & Trotter, 1997

VLA observations

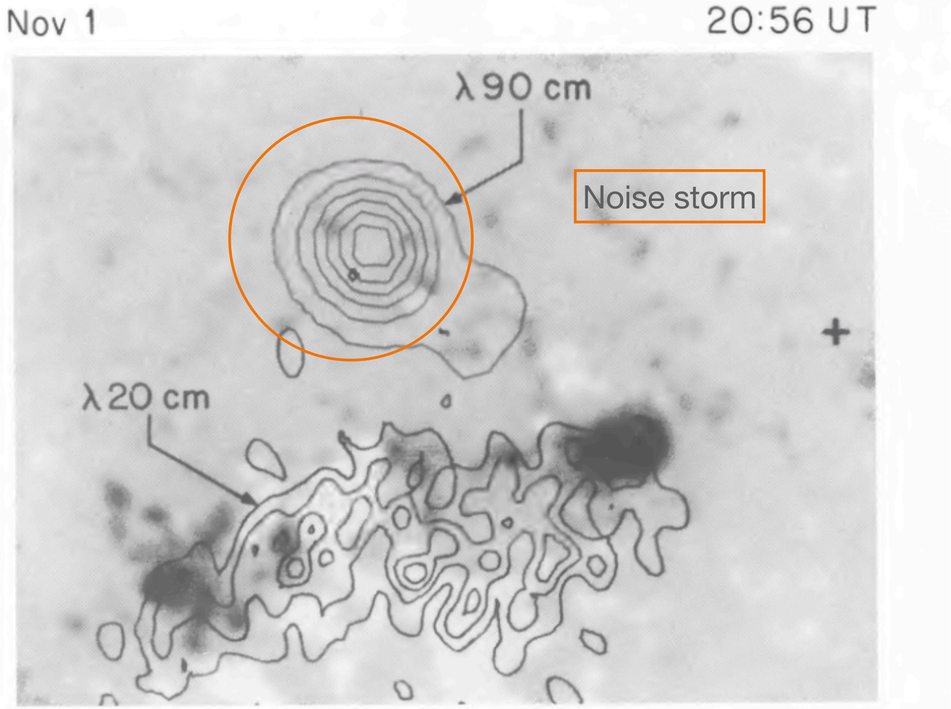

Habbal et al., 1989

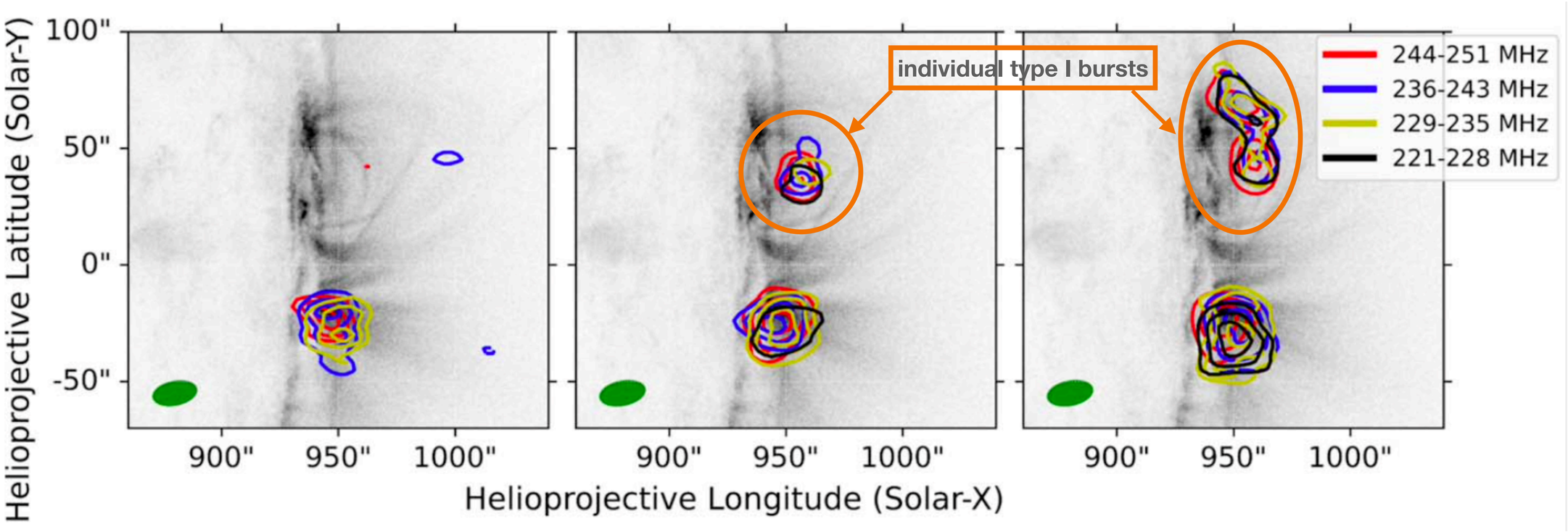

Mondal et al., 2024

Type II burst

- Slow drift downward in frequency
- < 200 - 300 MHz
- Fundamental, 2nd Harmonic, 3rd Harmonic, band-split
- Observed in corona and interplanetary medium
- Flare / CME related
- Shock waves

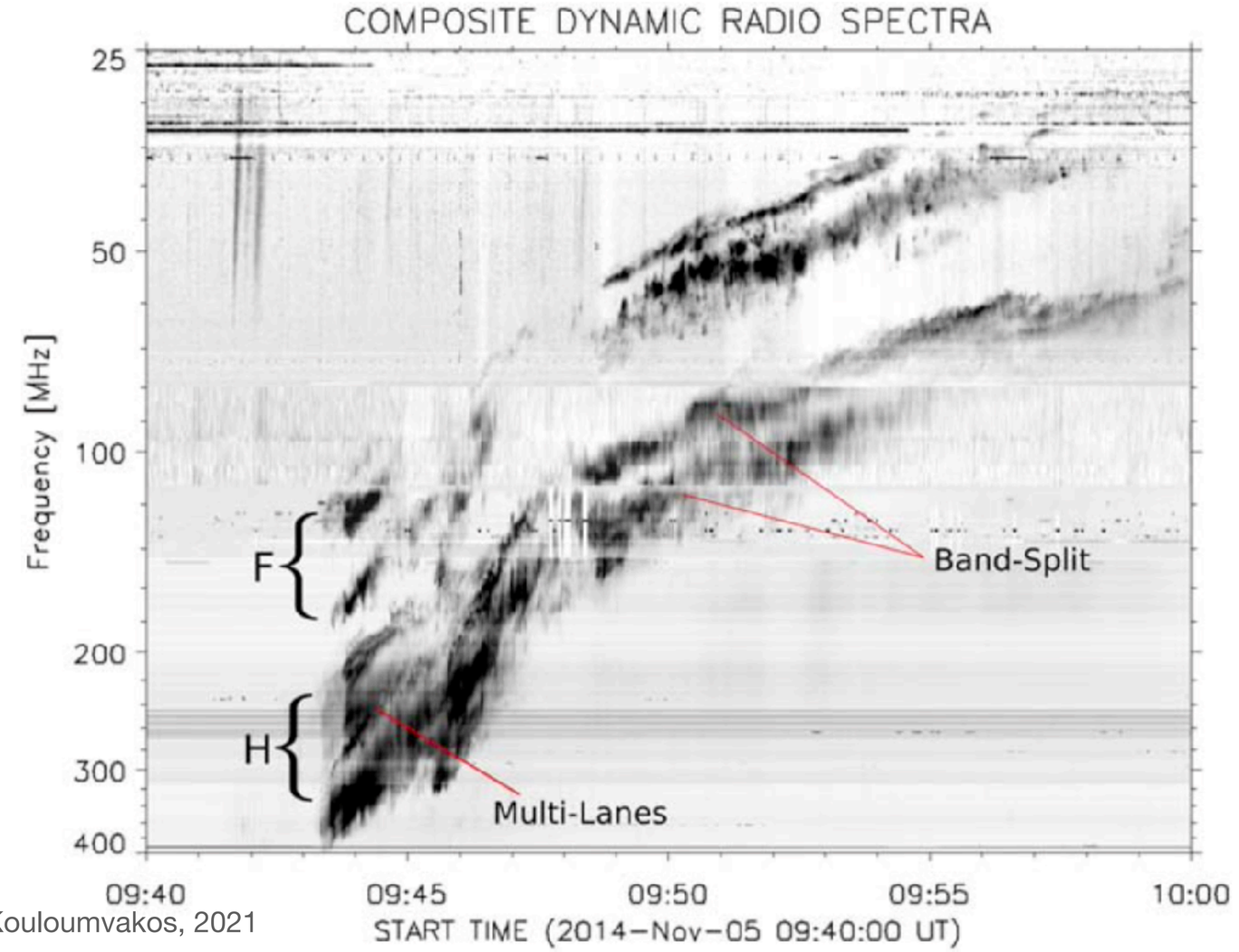

Kouloumvakos, 2021

Type II burst

- Slow drift downward in frequency
- < 200 - 300 MHz
- Fundamental, 2nd Harmonic, 3rd Harmonic, band-split
- Observed in corona and interplanetary medium
- Flare / CME related
- Shock waves

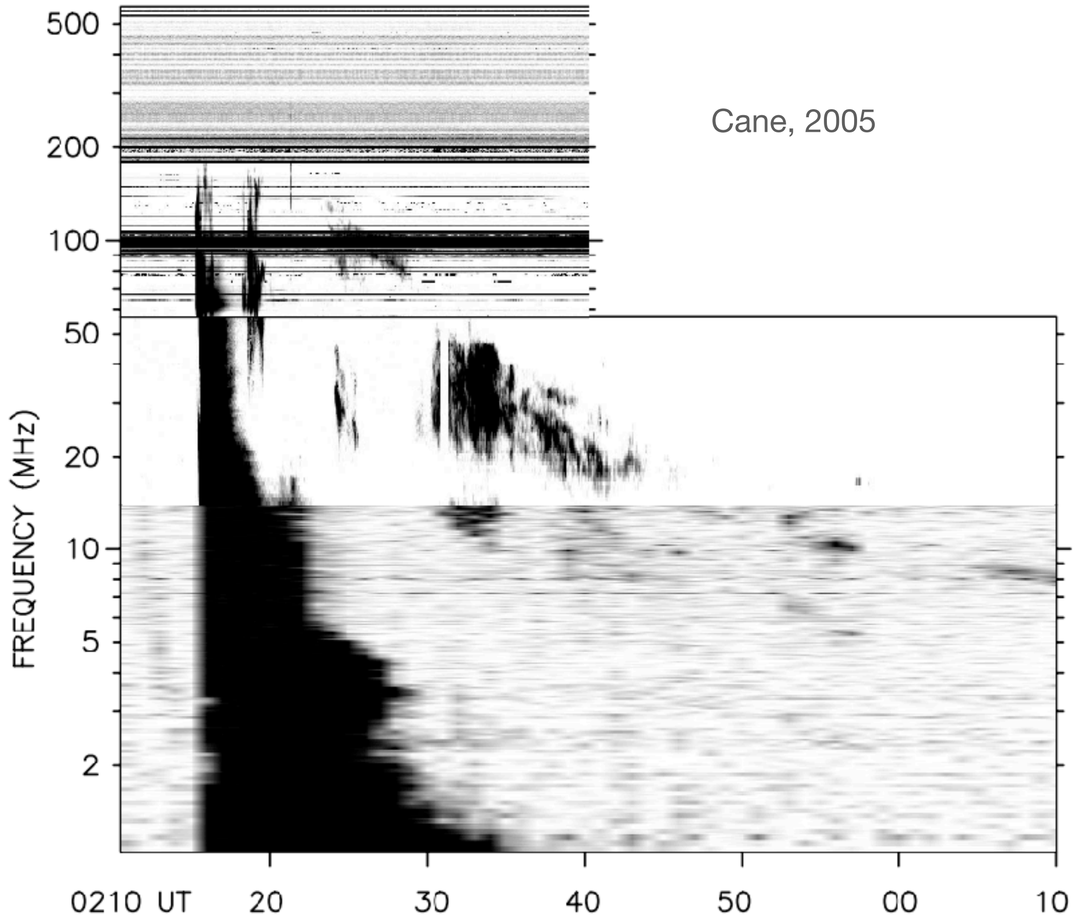

Cane, 2005

FIG. 3.—60 minute plot, 2003 March 19 02:10 UT. This is a continuation of another metric type II into the RAD2 range. The activity at 02:18 UT and 60 MHz, 02:24 UT and 30 MHz, and 02:32 UT and 14 MHz may be an intermittent type II fundamental. The stronger activity may be the harmonic emission.

HUMAIN SPADE

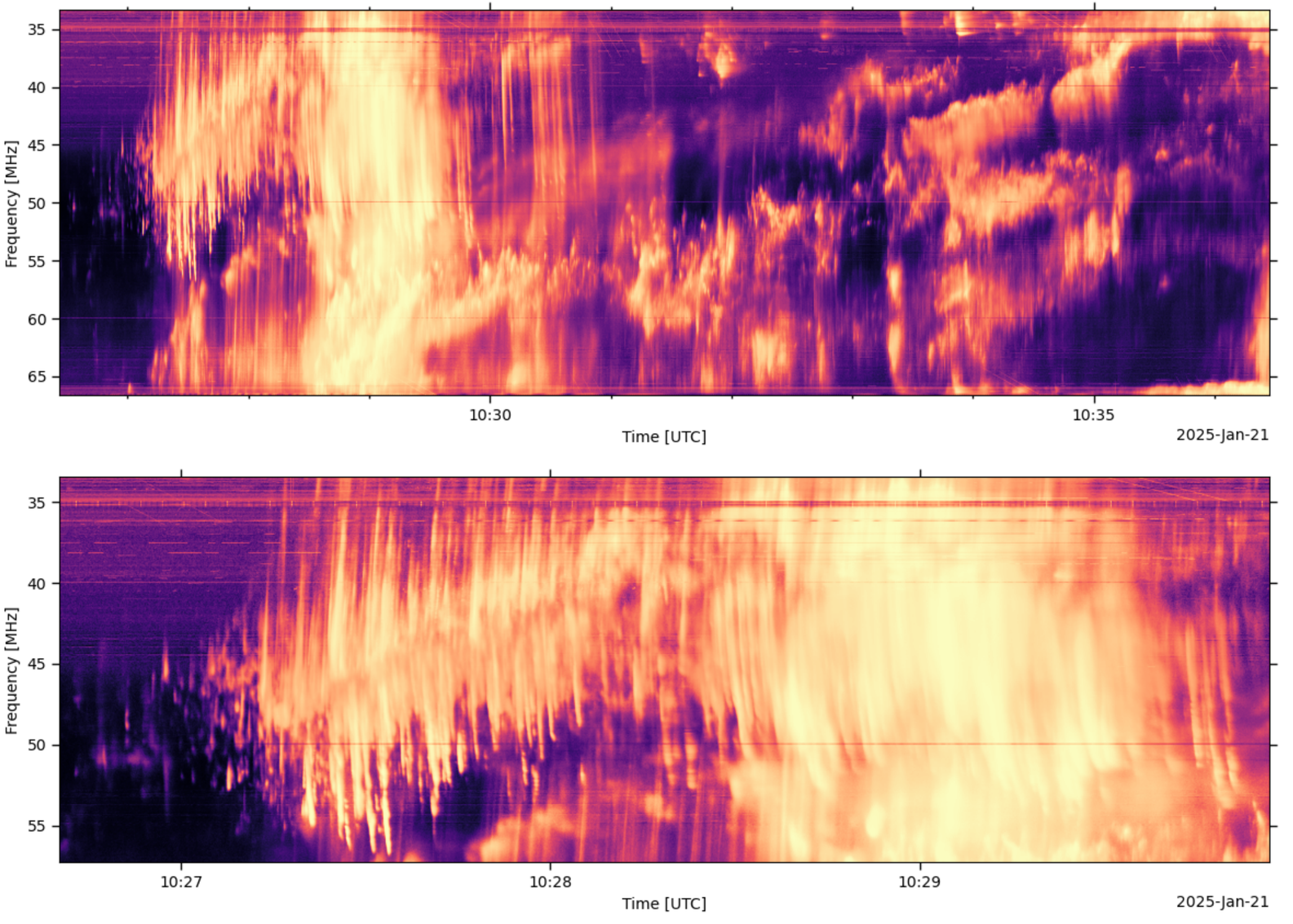

HUMAIN SPADE

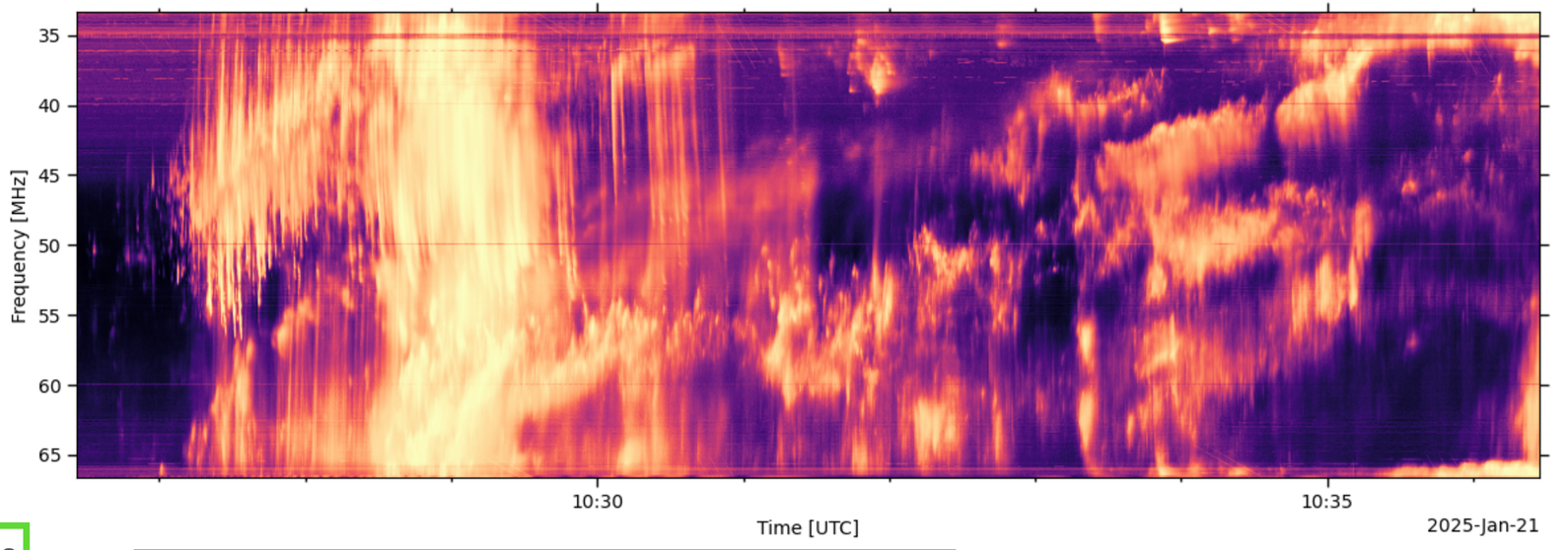

Herringbones

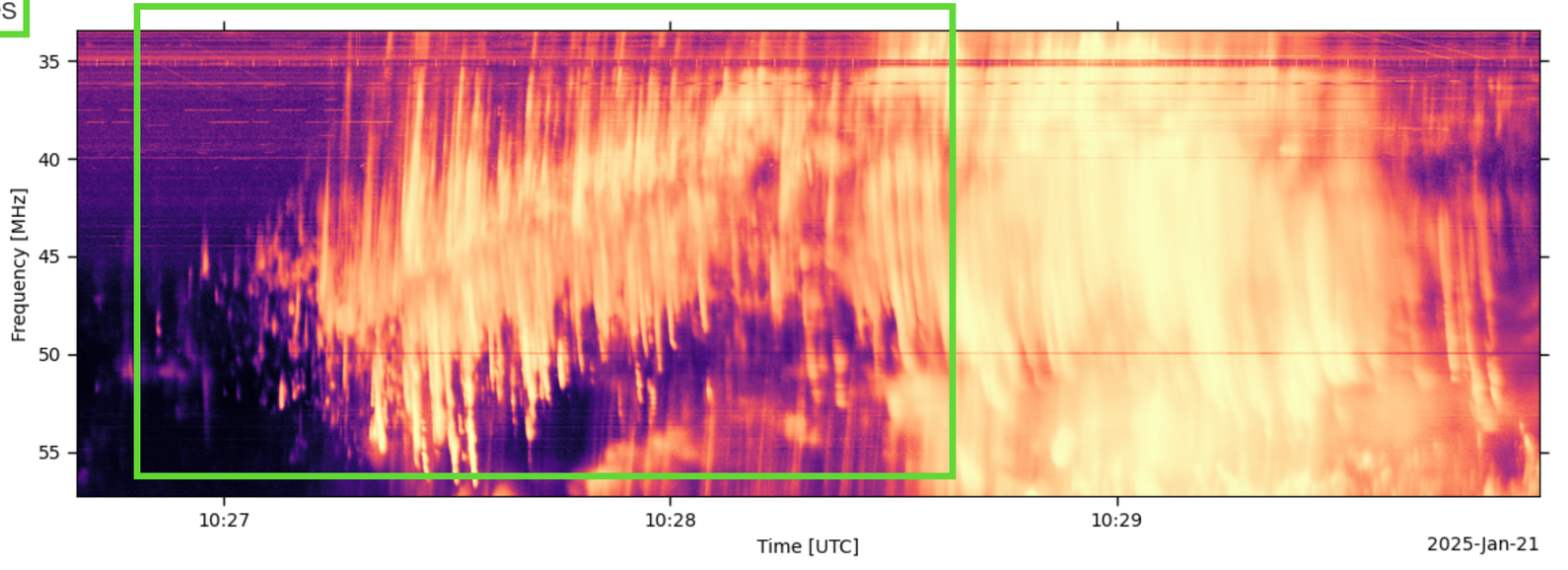

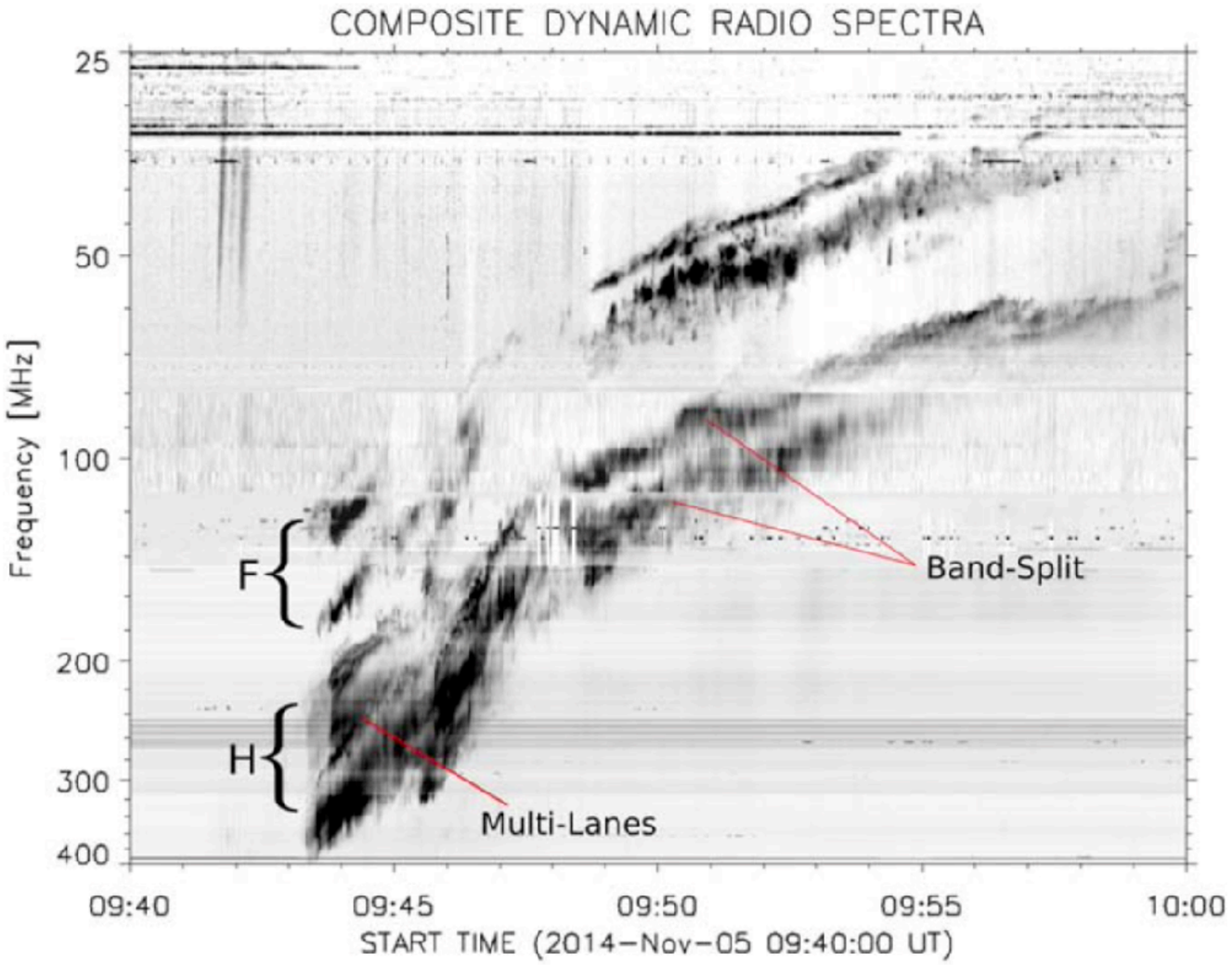

- Drift rate --> speed
- Models points at weak shock waves M_A ~1.5, quasi perpendicular shock (Mann, 1995)
- Empirical modelling (Vrsnak et al., 2001, 2002):
  - Band split --> Density jump at shock interface, field strength, M_A

Can we do better in analysing type II bursts?

Modelling of shocks in realistic coronal models

- Modelling of Moreton waves and type II in symmetrical corona (Uchida et al., 1973)
- Modelling of EUV wave, PFSS (Wang, 2000)
- Modelling of fast mode wave in realistic corona (Koukras et al., 2020)
- Modelling of pressure shock wave in realistic corona (Kouloumvakos et al. 2021)
- Together with Lukas, work of Alexandros is expanded

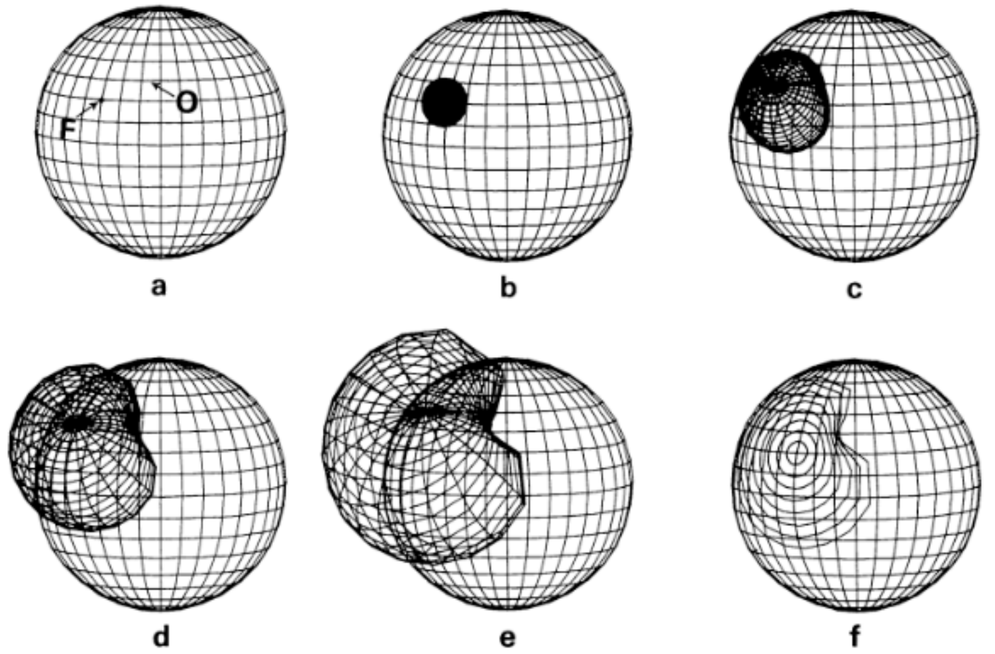

Fig. 9. The same for a simple model corona with a structure having the same shape but with a of region decreased Alfvén velocity. Parameters for the model are given in Table II.

Uchida et al. 1973

Koukras et al. EUV wave connection with type II burst
Event 1 - movie 2

Research Foundation Flanders
Opening new horizons

Royal Observatory of Belgium

Koukras et al. EUV wave connection with type II burst
Event 1 - movie 2

Research Foundation Flanders
Opening new horizons

Royal Observatory of Belgium

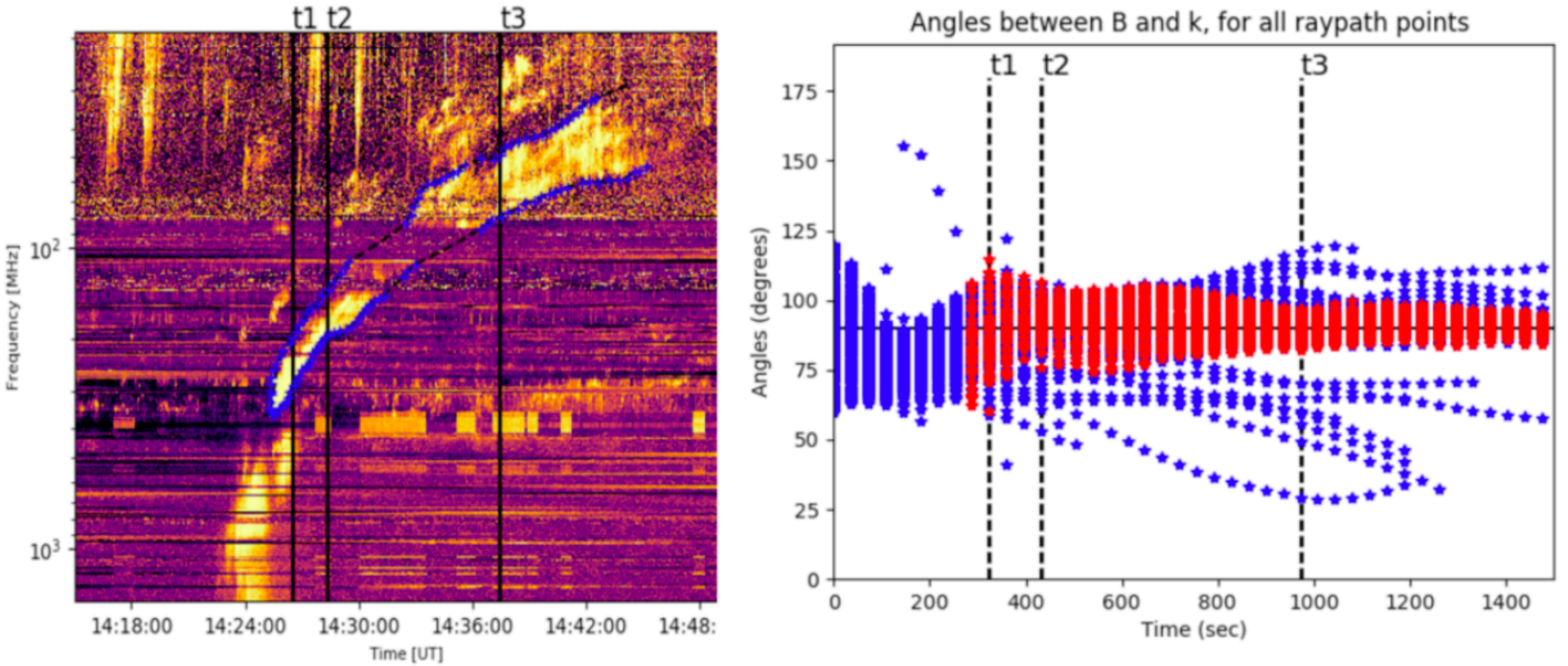

Fig. 4. *Left*: dynamic radio spectrum from the Humain station, showing the signature of the type II radio burst during Event 1. The three vertical lines correspond to the time of the snapshots in Fig. 3. Blue crosses represent manually selected points and the dashed black lines the fitting curves. *Right*: angles between the magnetic field and the wave vector for every ray-path point. Red indicates the ray-path points that are identified as the potential source of the type II radio burst emission based on the local electron density matching the plasma frequency.

Type II

How good are they for shock information?

- About half of metric type II bursts continue in low IP (~ 10 Rs)
- When both corona and IP type II are observed: likely different shocks from same driver event
- ~ 35 % of IP shocks have no IP type II (Gopalswamy et al., 2009)
- Using IP type II information for simple predictive arrival shock (Cremades et al, 2015)

Type II bursts

Are they useful for SEPs?

- Most (90%) IP type II bursts (f<10 MHz) are associated with SEPs. Much lower rate with metric type II alone (Cane & Stone, 1984; Gopalswamy et al., 2002)
- 90 % of SEPs are associated with type II bursts (irrespective of frequency; Cliver et al. 2004)
- Weak SEP events are less likely to be associated with these radio emissions

Type III bursts

- Flaring events of all magnitudes
- Beams of electrons propagating along open magnetic field lines
- Isolated or in groups
- 1/3 c
- Span a large frequency range (GHz to kHz ii.e. interplanetary medium)

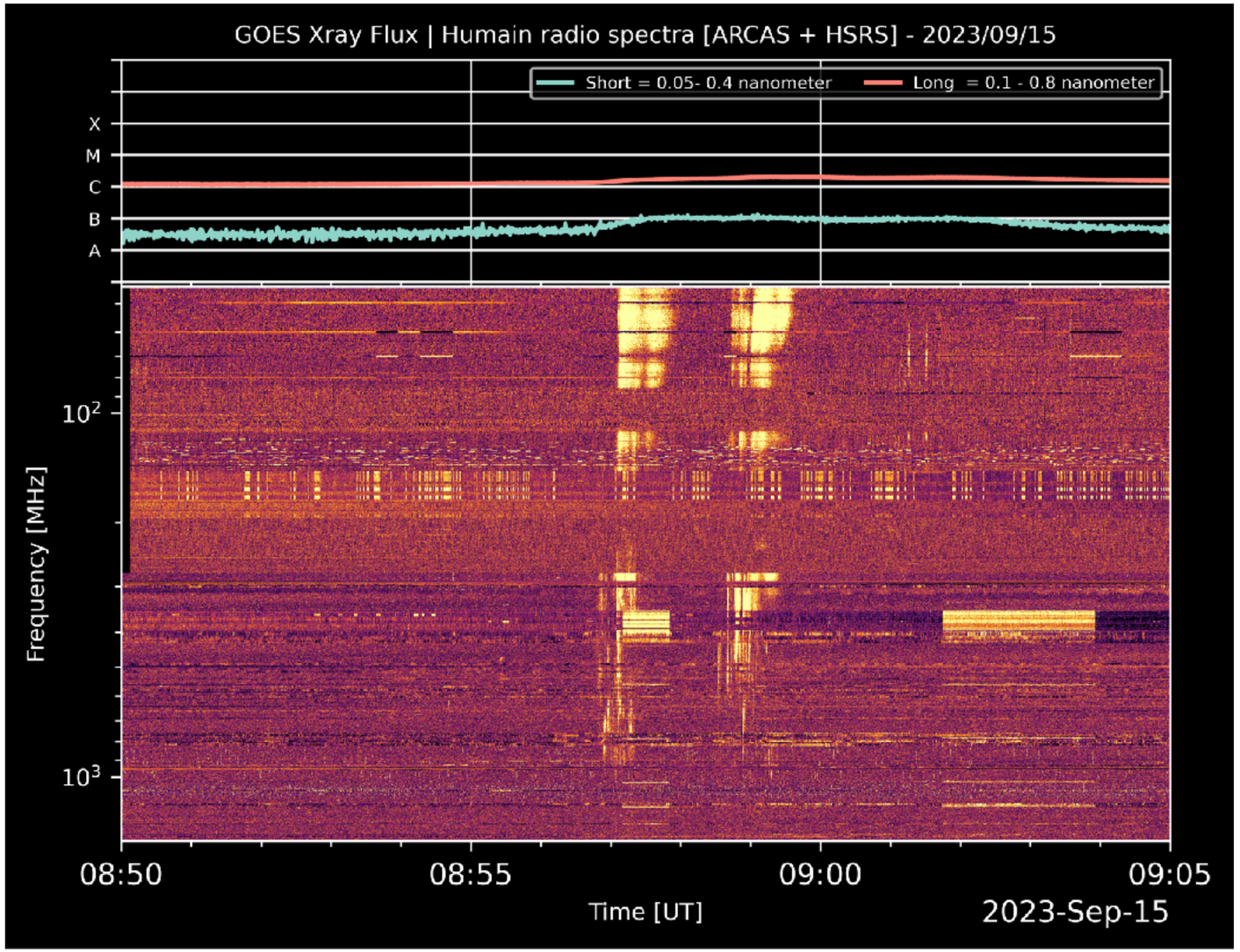

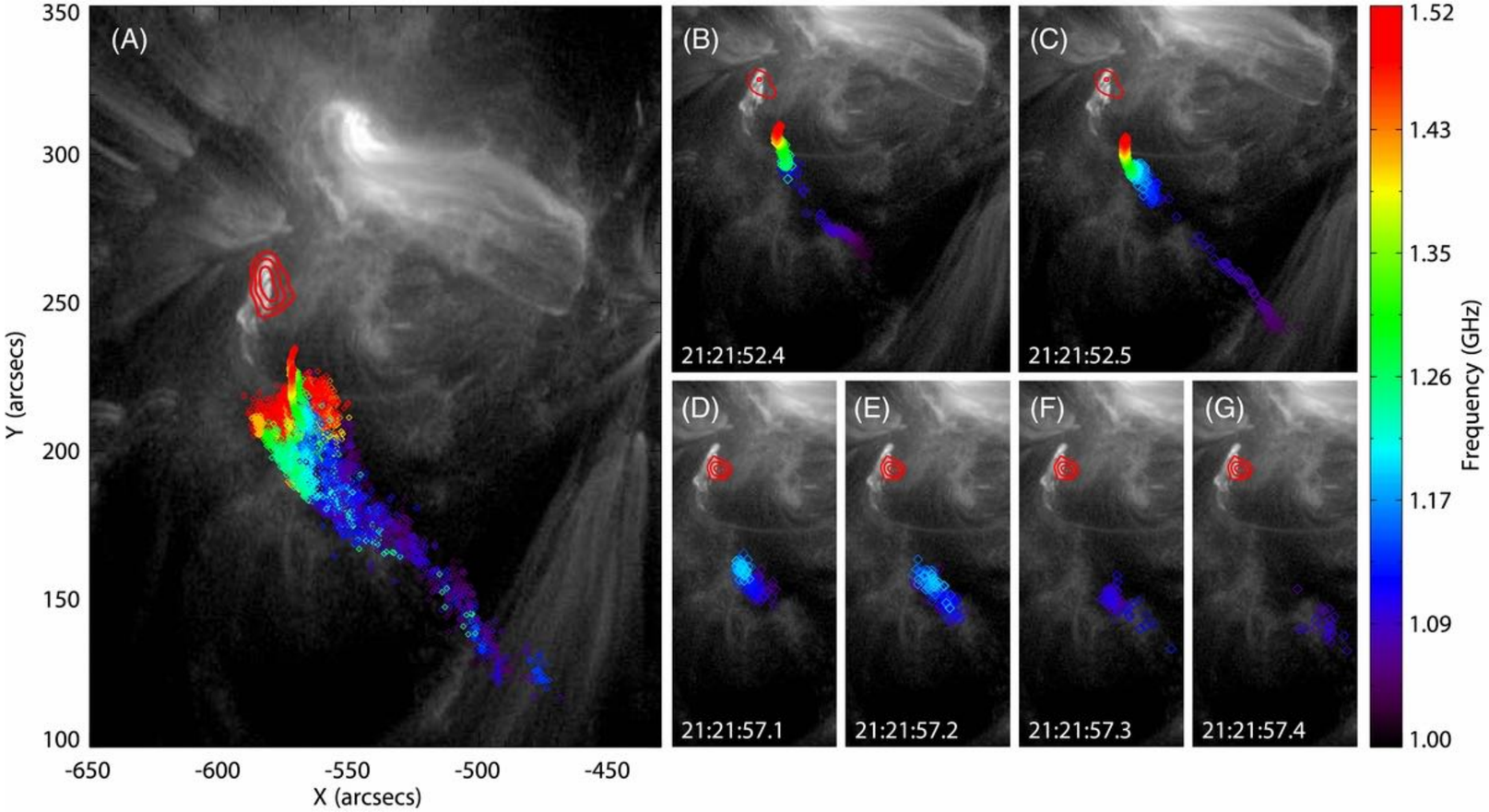

Chen et al., 2013

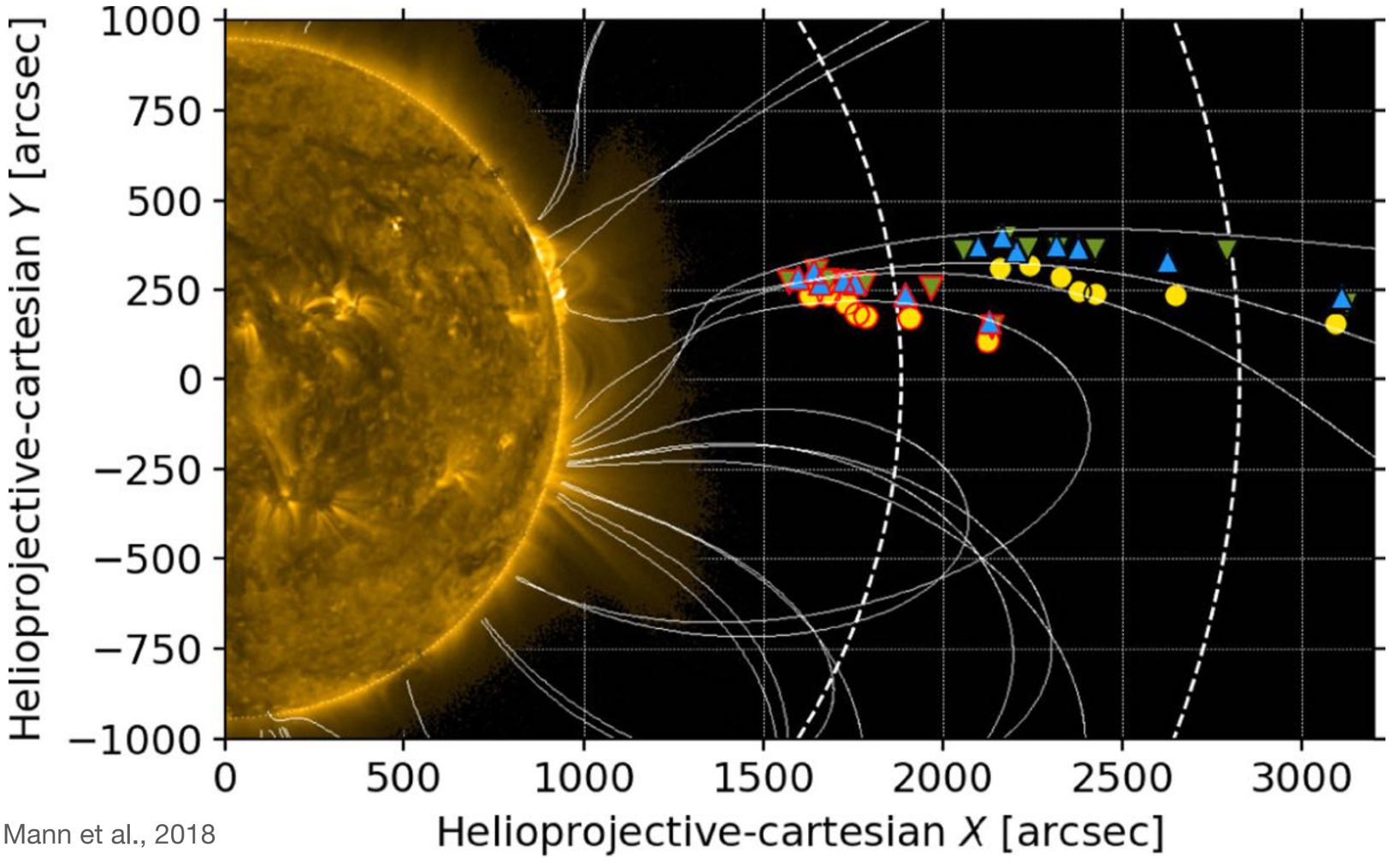

Mann et al., 2018

Type III bursts

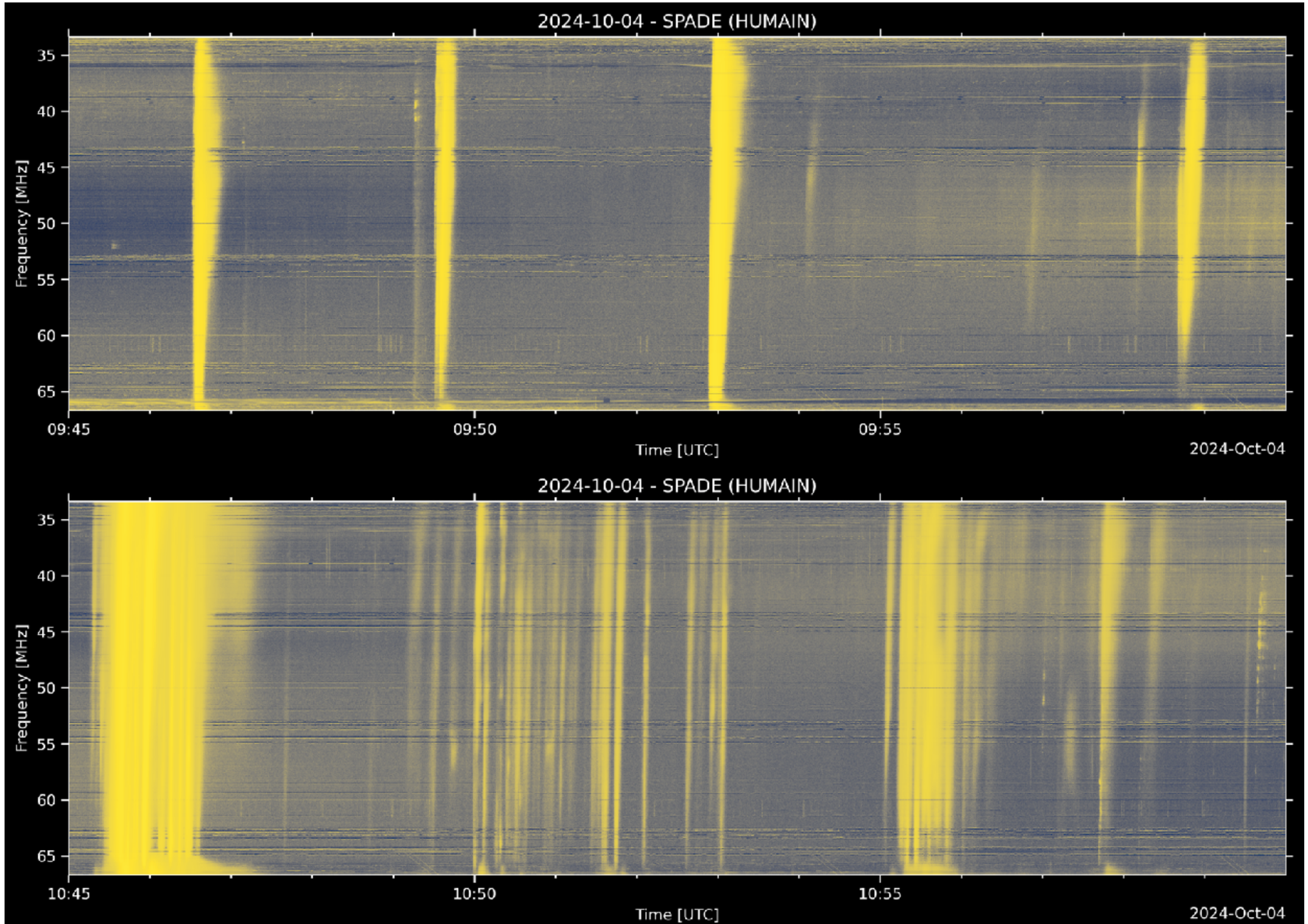

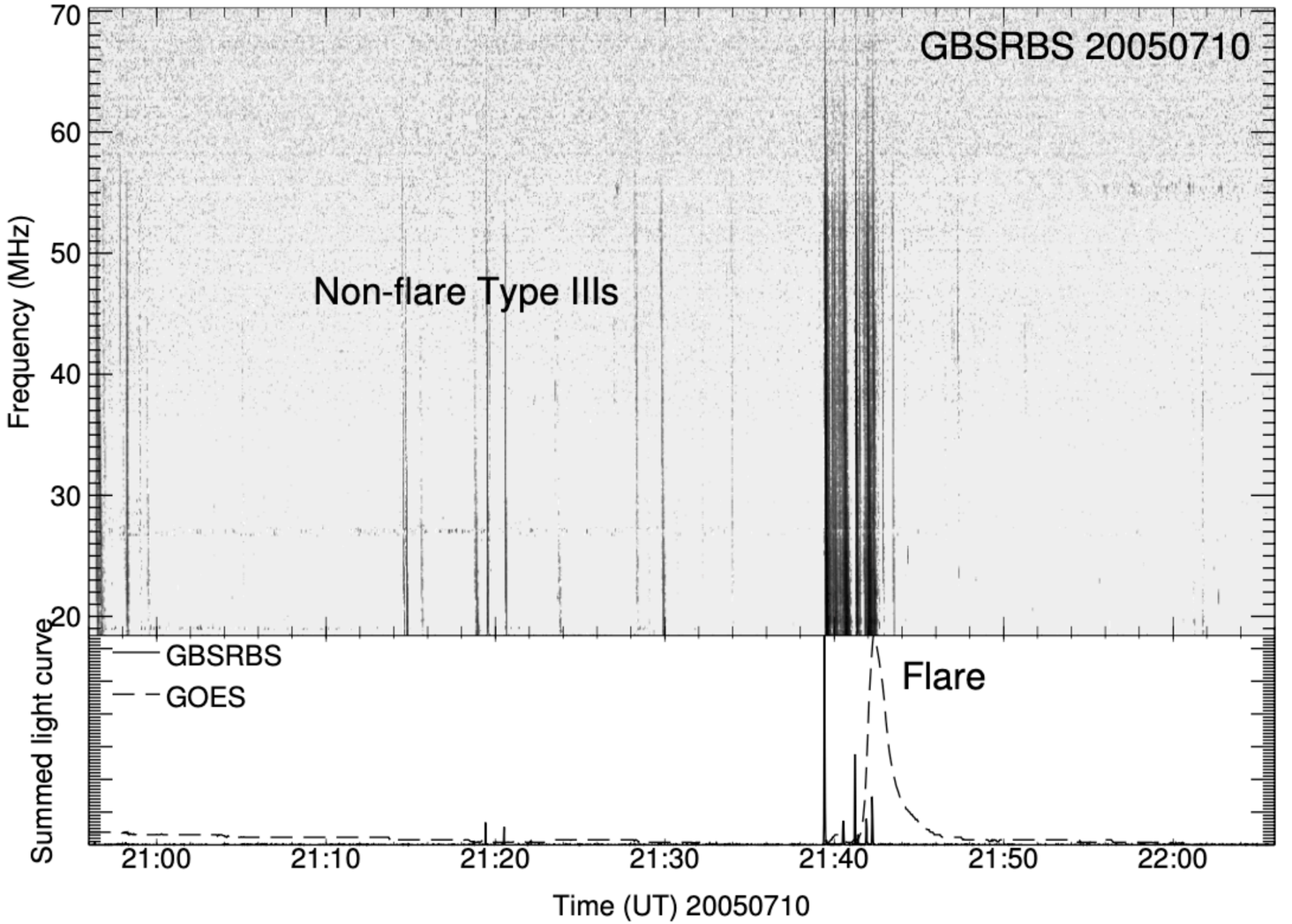

Figure 4. Dynamic spectrum of over an hour on a day of activity, showing Type III events occurring both in conjunction with a solar flare (at 21:40 UT) and in the absence of flare activity (between 21:10 and 21:35 UT).

White, 2024

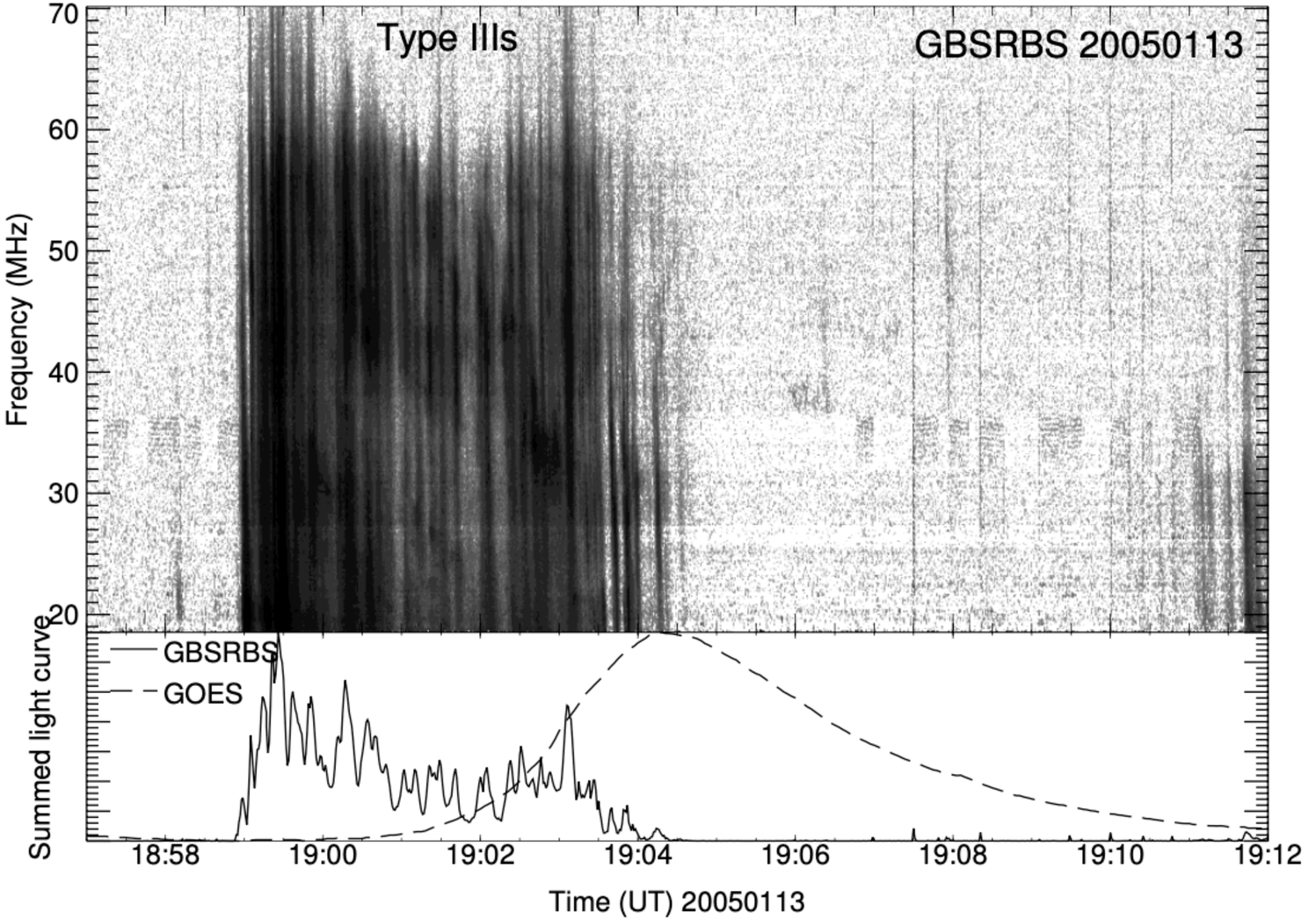

Figure 5. A large group of Type III bursts in the rise phase of a solar flare. The Type IIIs cease almost exactly at the time of the soft X–ray peak, regarded as the time at which energy release in the flare ends.

White, 2024

Type III storms

Linked with noise storms

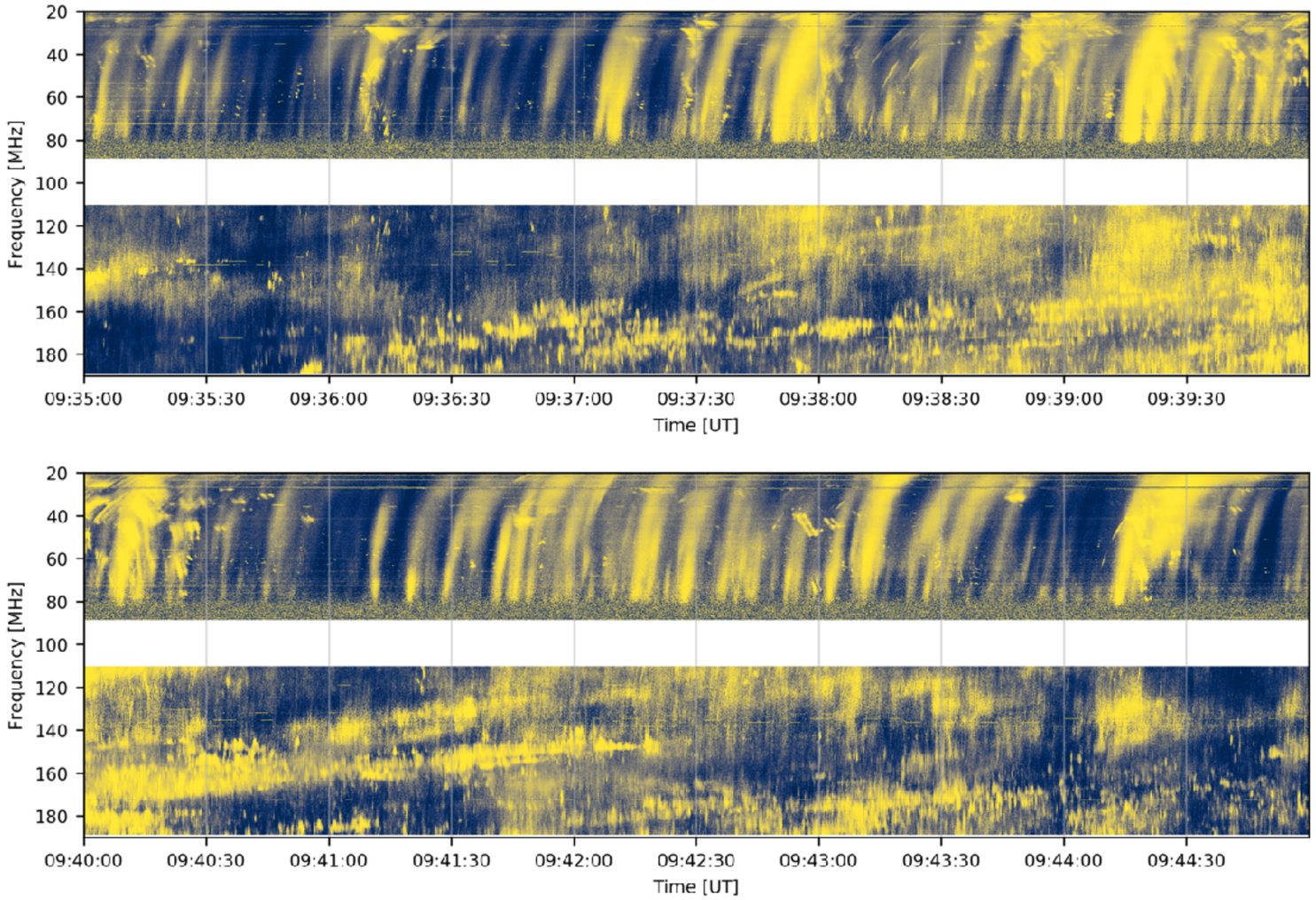

Marqué ????

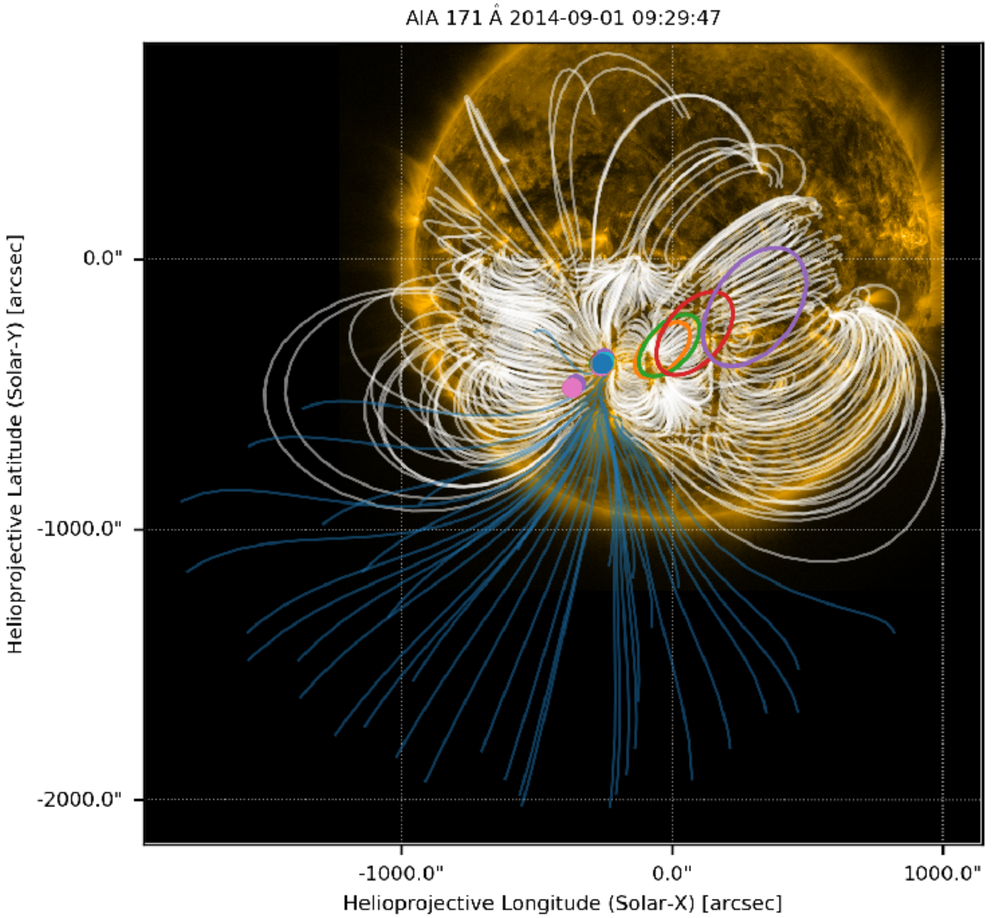

Type IV bursts

- Flare and CME related
- Energetic electrons trapped in post flare loops
- Broadband (few MHz - few GHz)
- Fine temporal structures (pulsations, zebra...)
- Can be extremely intense
- Plasma emission, gyro emissions, gyro synchrotron?

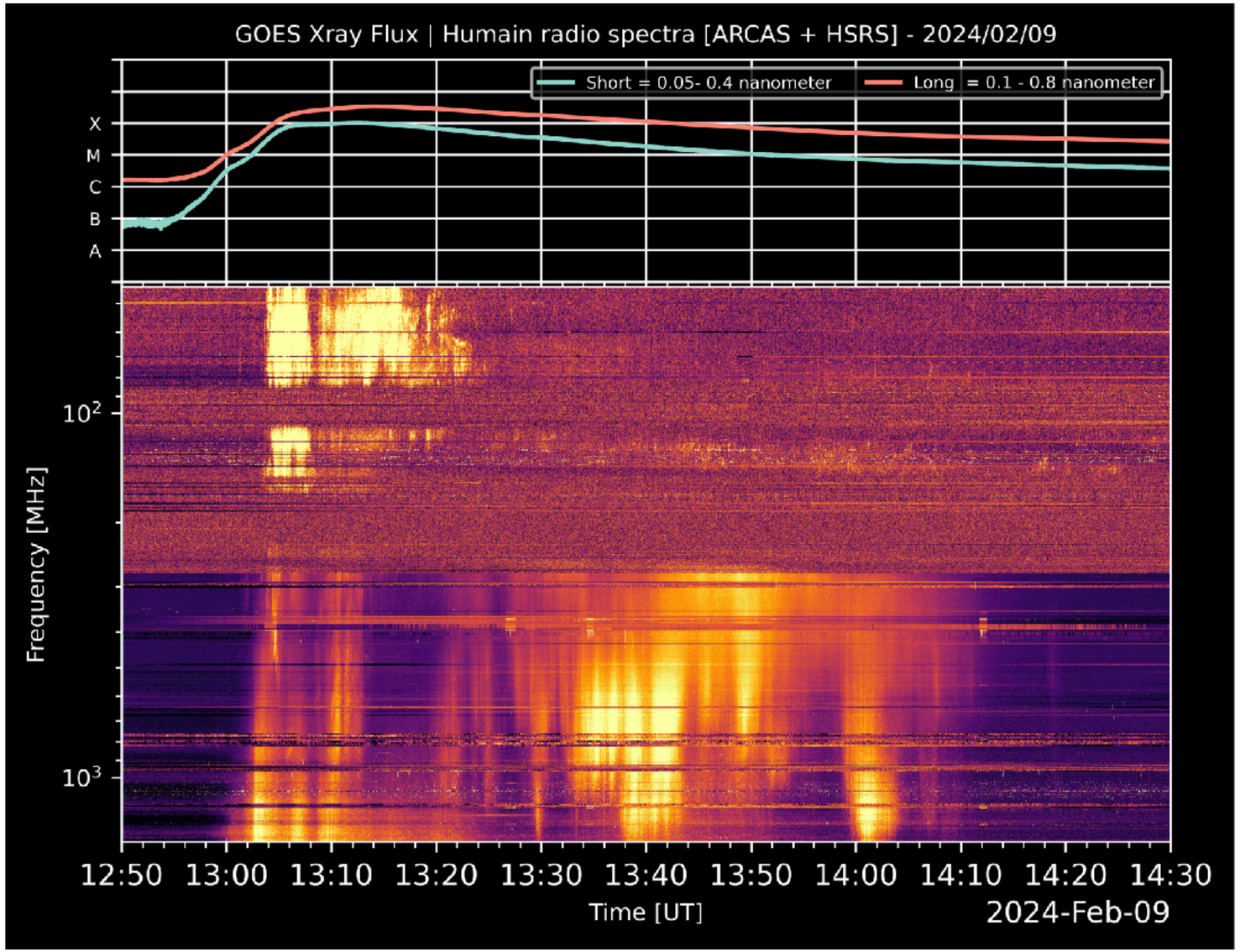

Type IV bursts

- Energetic electrons trapped in newly formed magnetic structures:
  - Post flare loops
  - Flux rope
  - Stationary (but can drift)
  - "Moving"

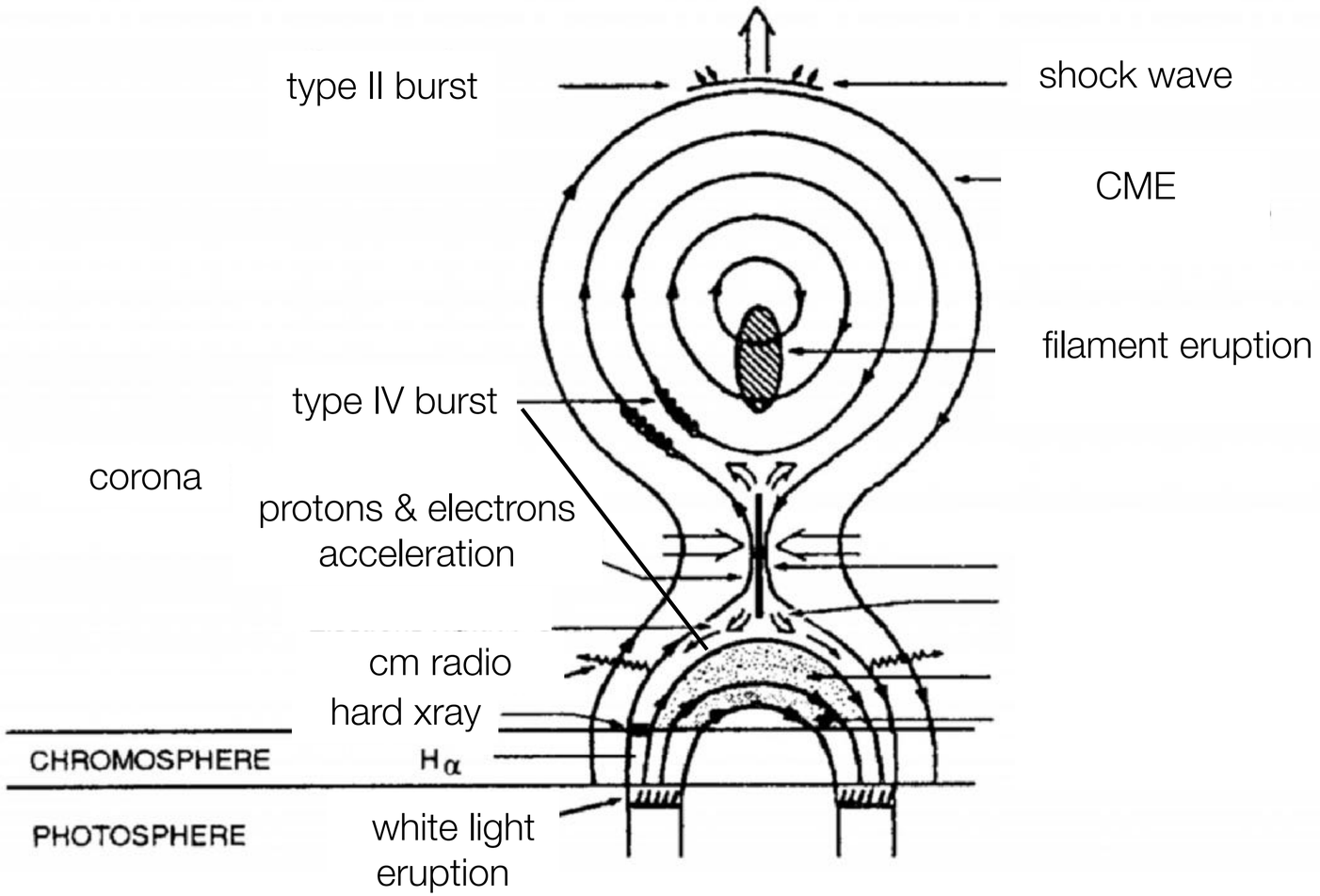

Type IV burst Stationary

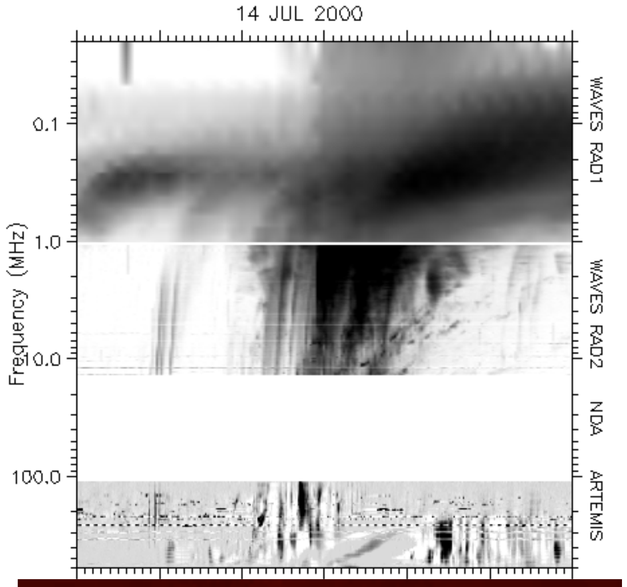

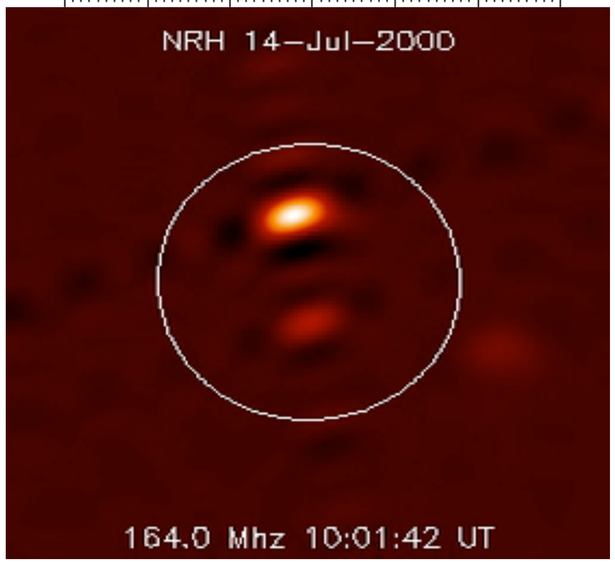

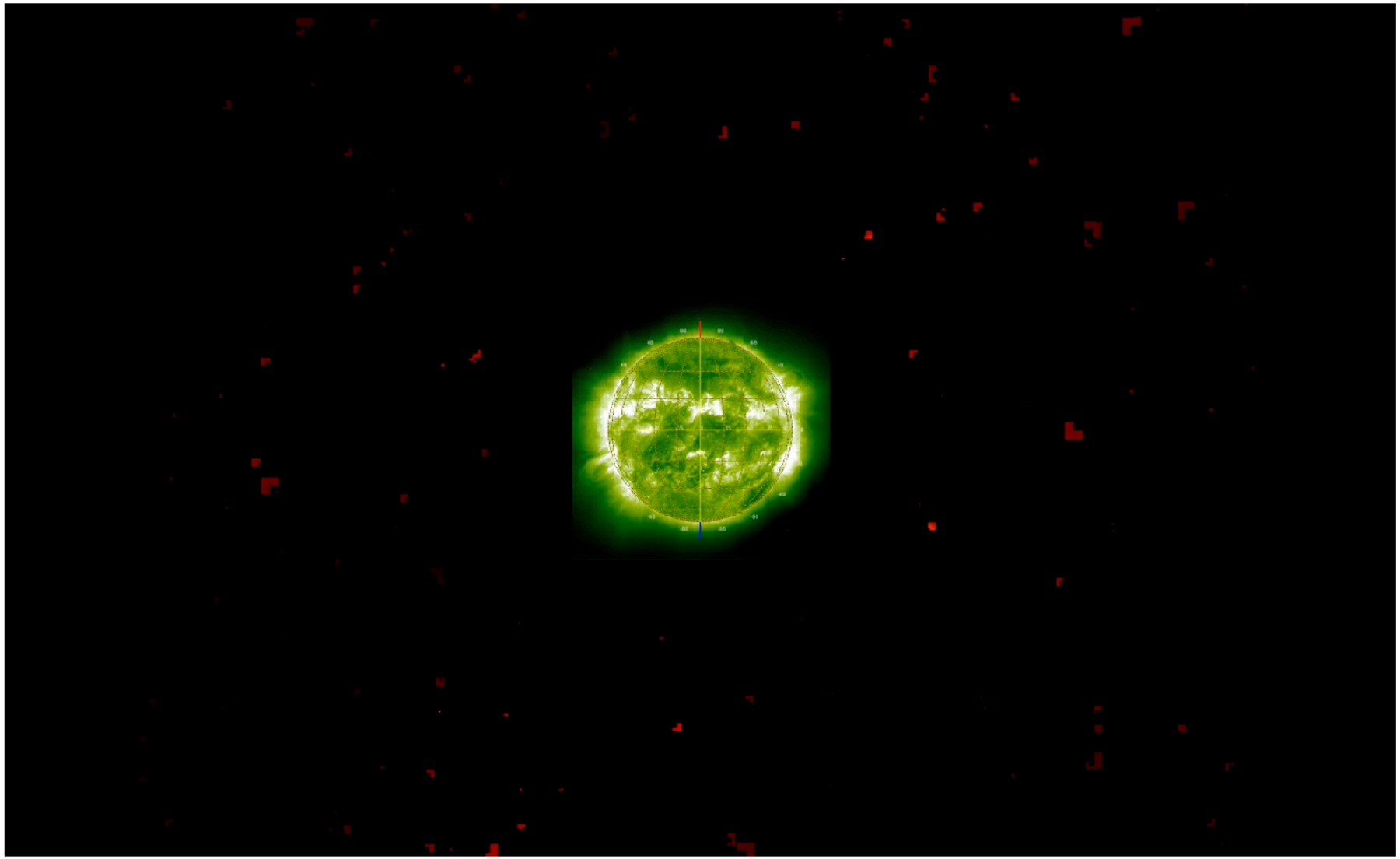

Type IV burst Stationary

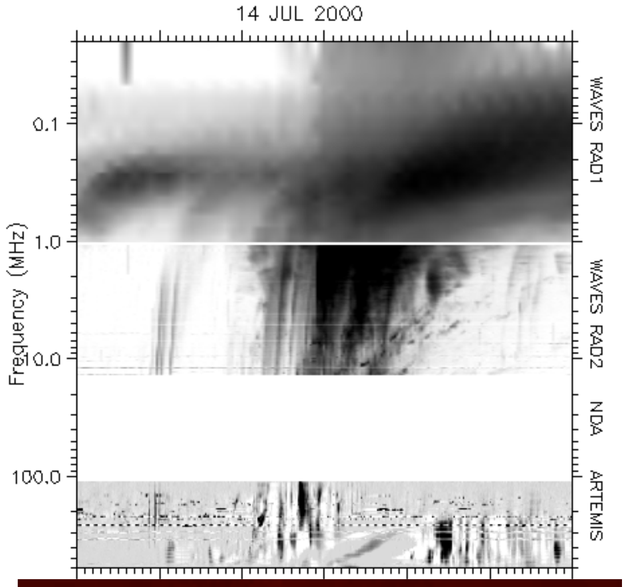

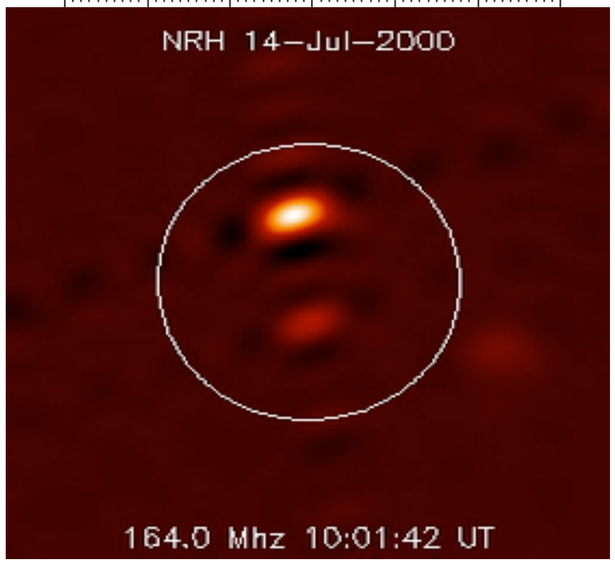

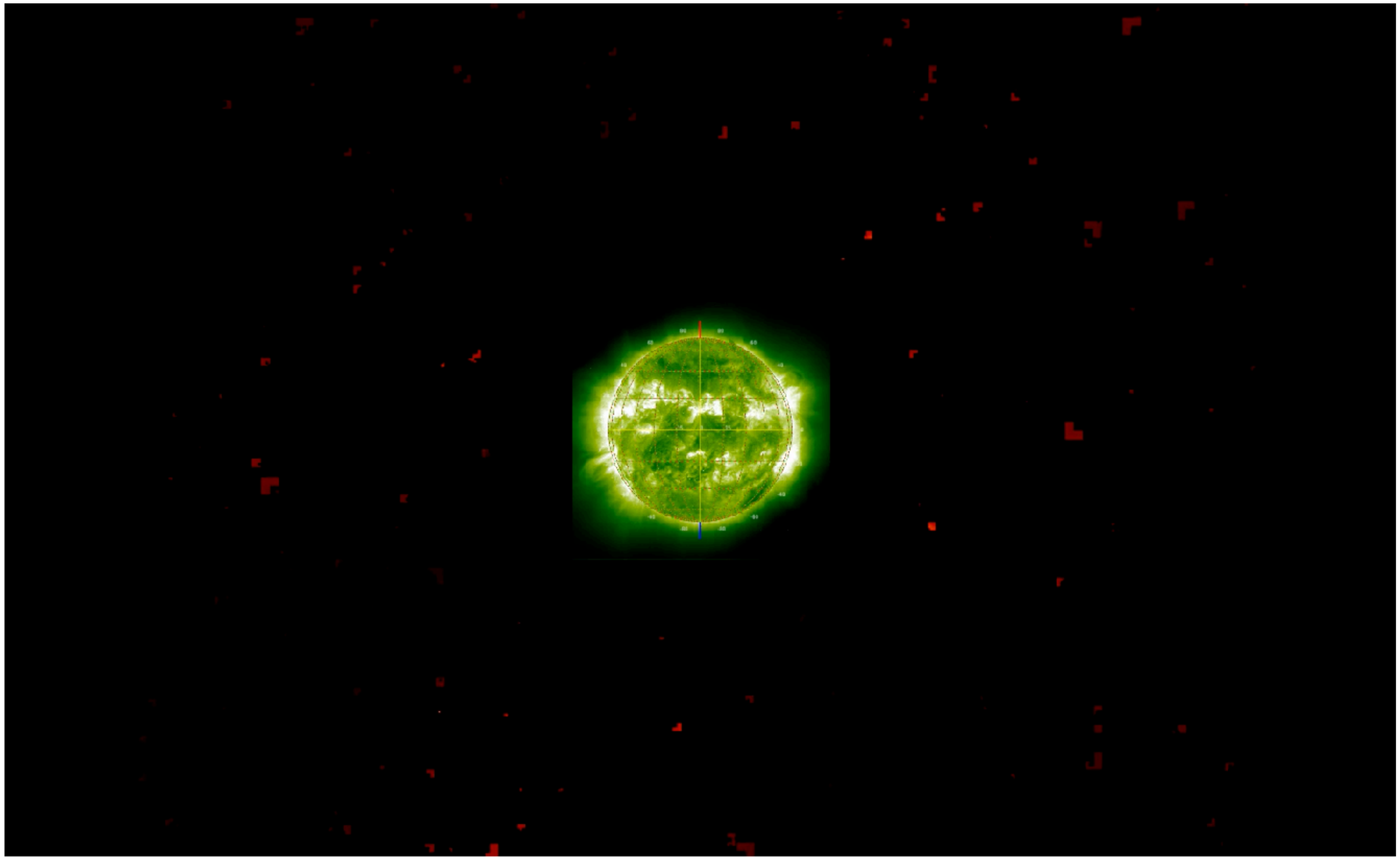

Type IV

moving type IV

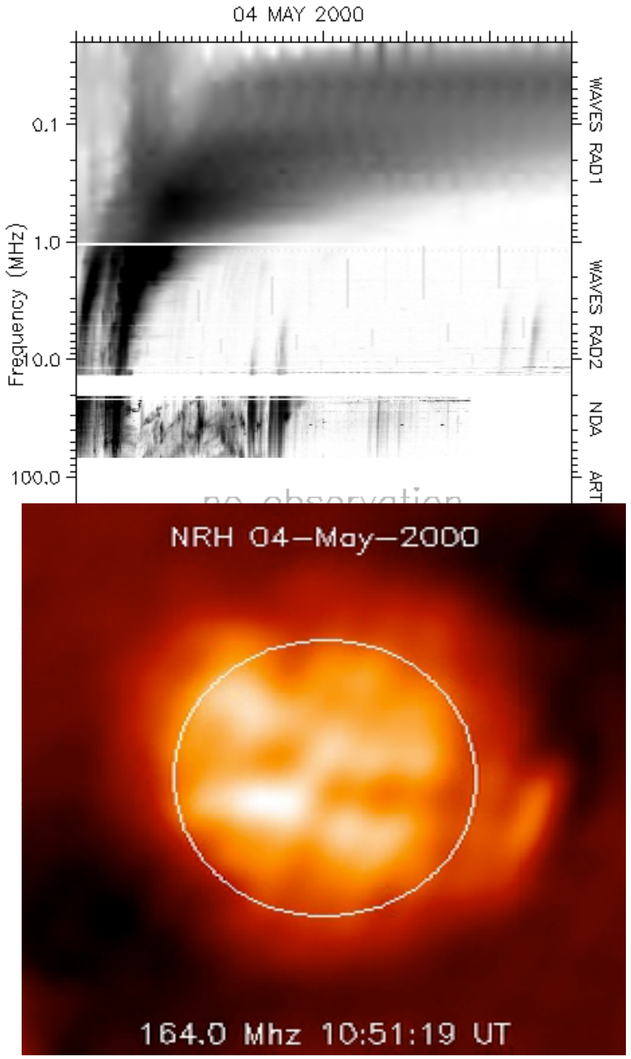

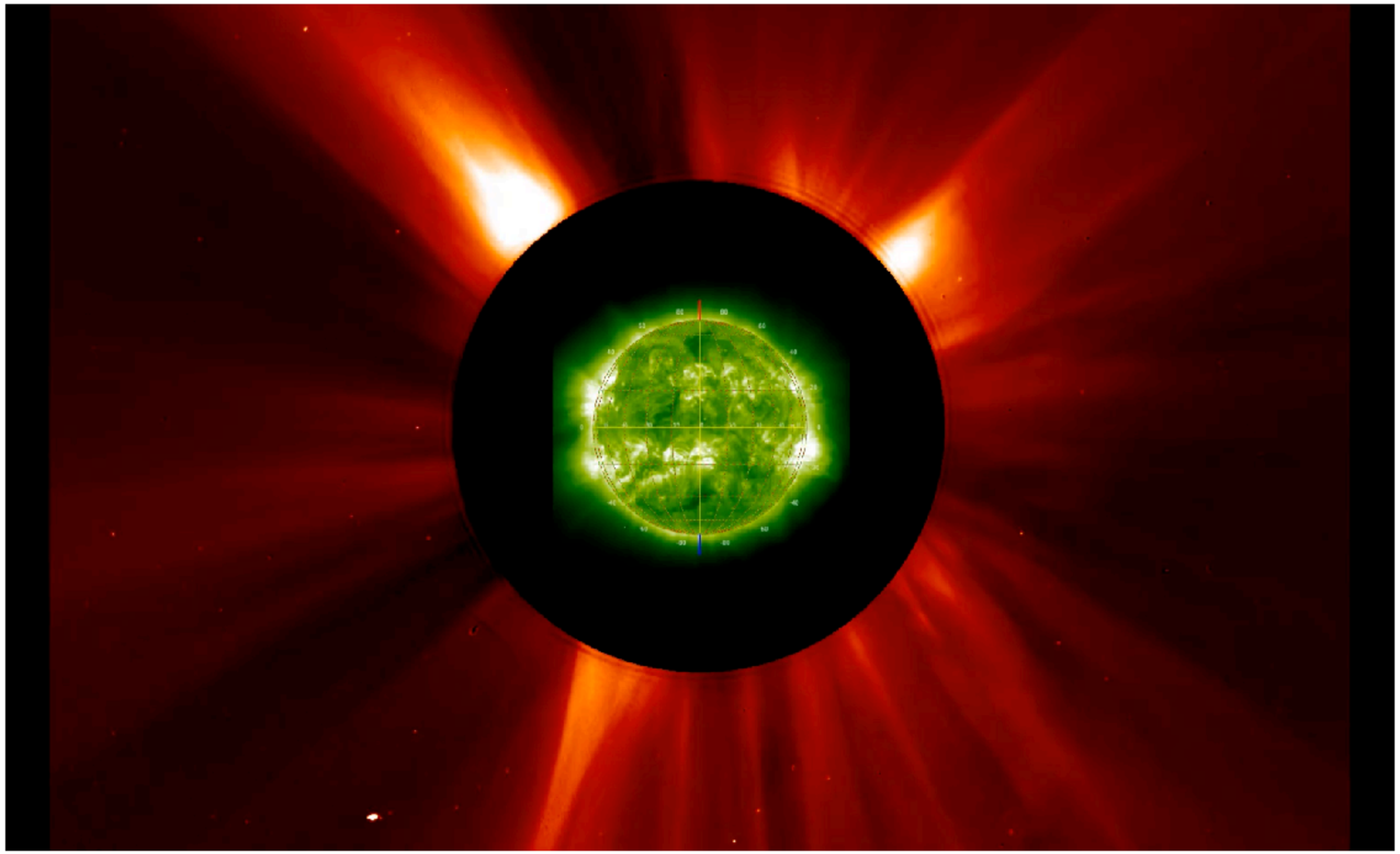

Type IV

moving type IV

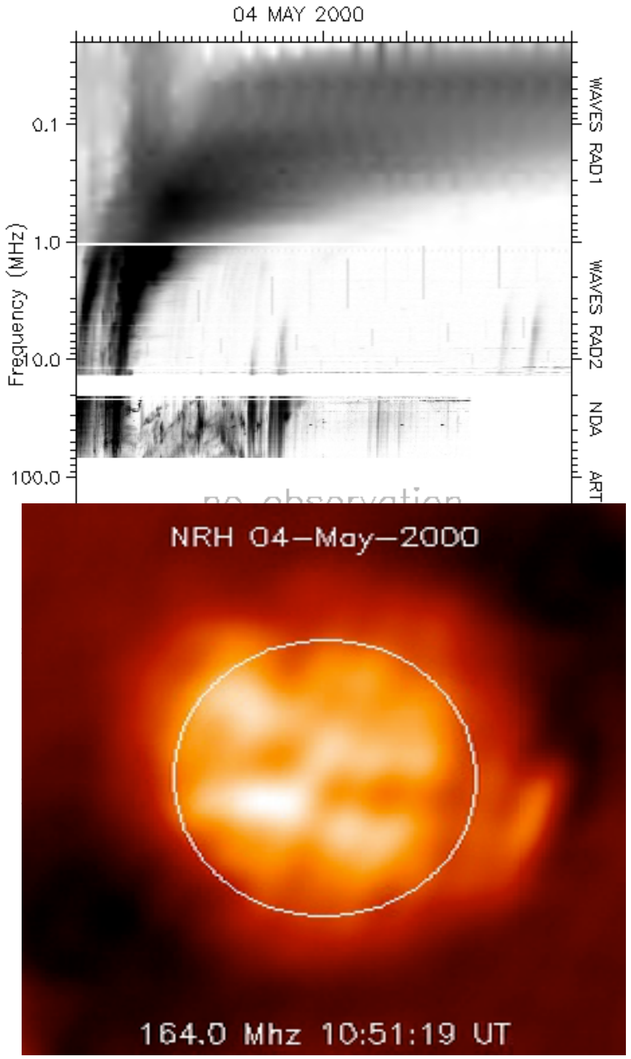

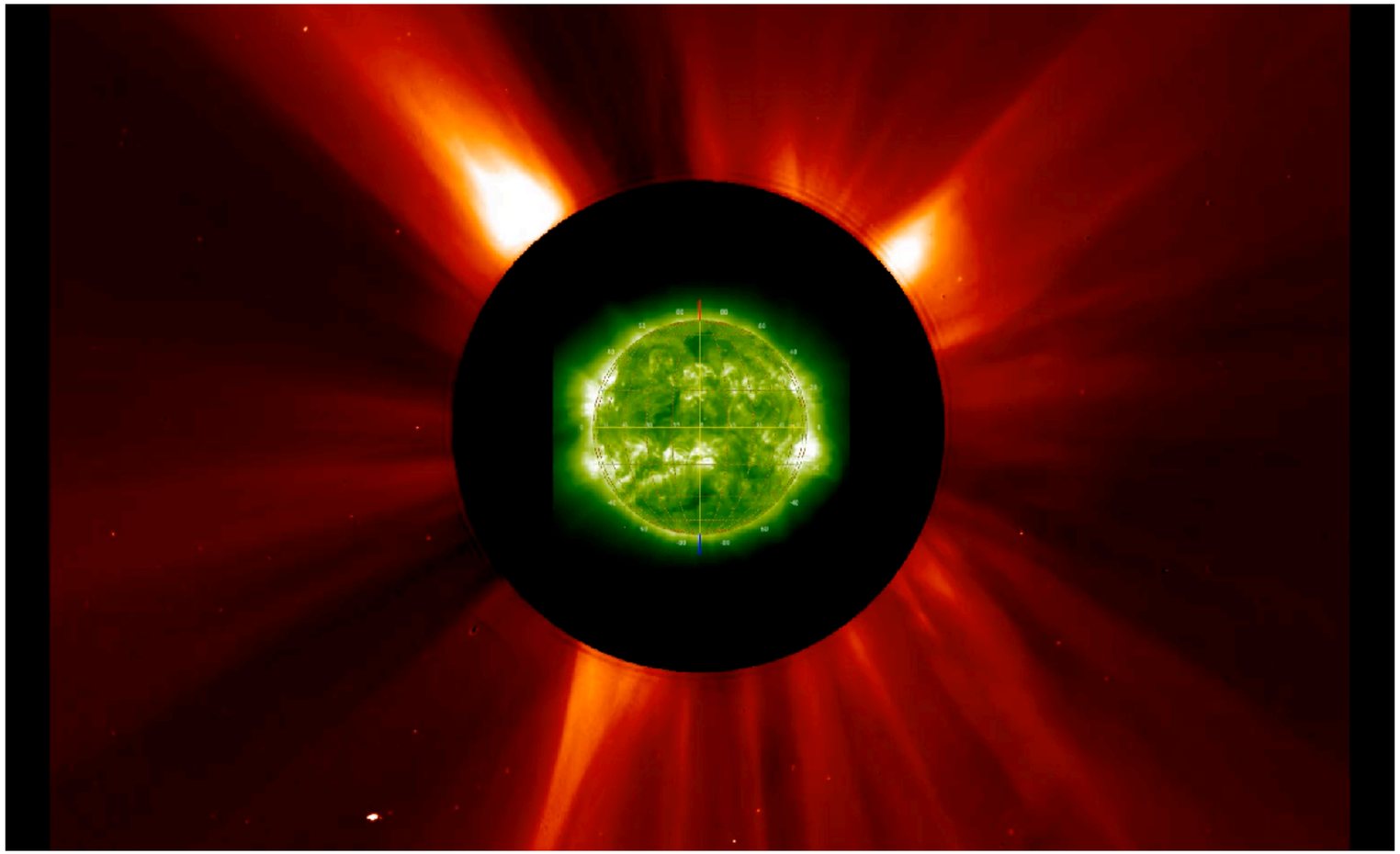

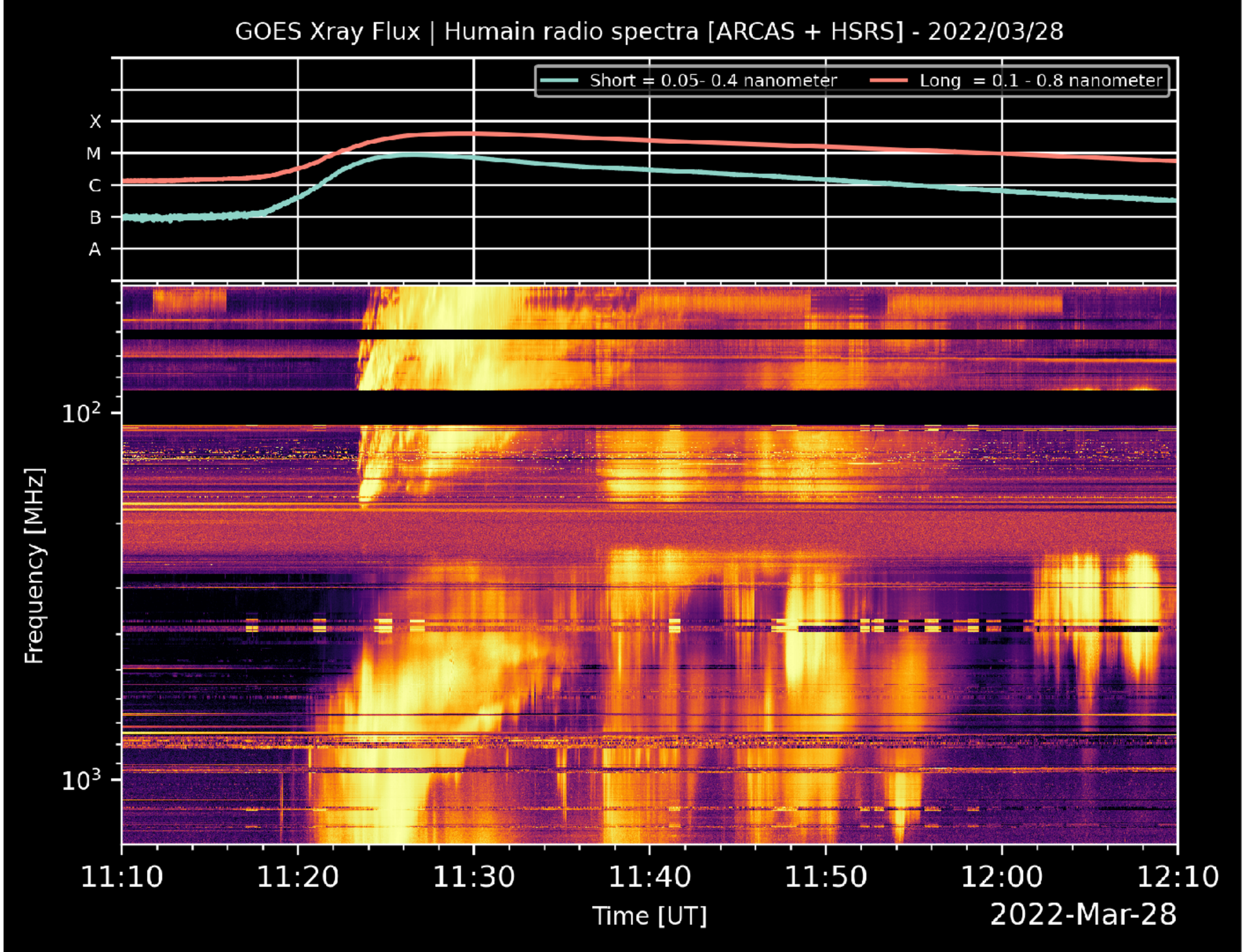
GOES Xray Flux | Humain radio spectra [ARCAS + HSRS] - 2022/03/28
Short = 0.05- 0.4 nanometer
Long = 0.1 - 0.8 nanometer
X
M
C
B
A
Frequency [MHz]
10^2
10^3
11:10
11:20
11:30
11:40
11:50
12:00
12:10
Time [UT]
2022-Mar-28

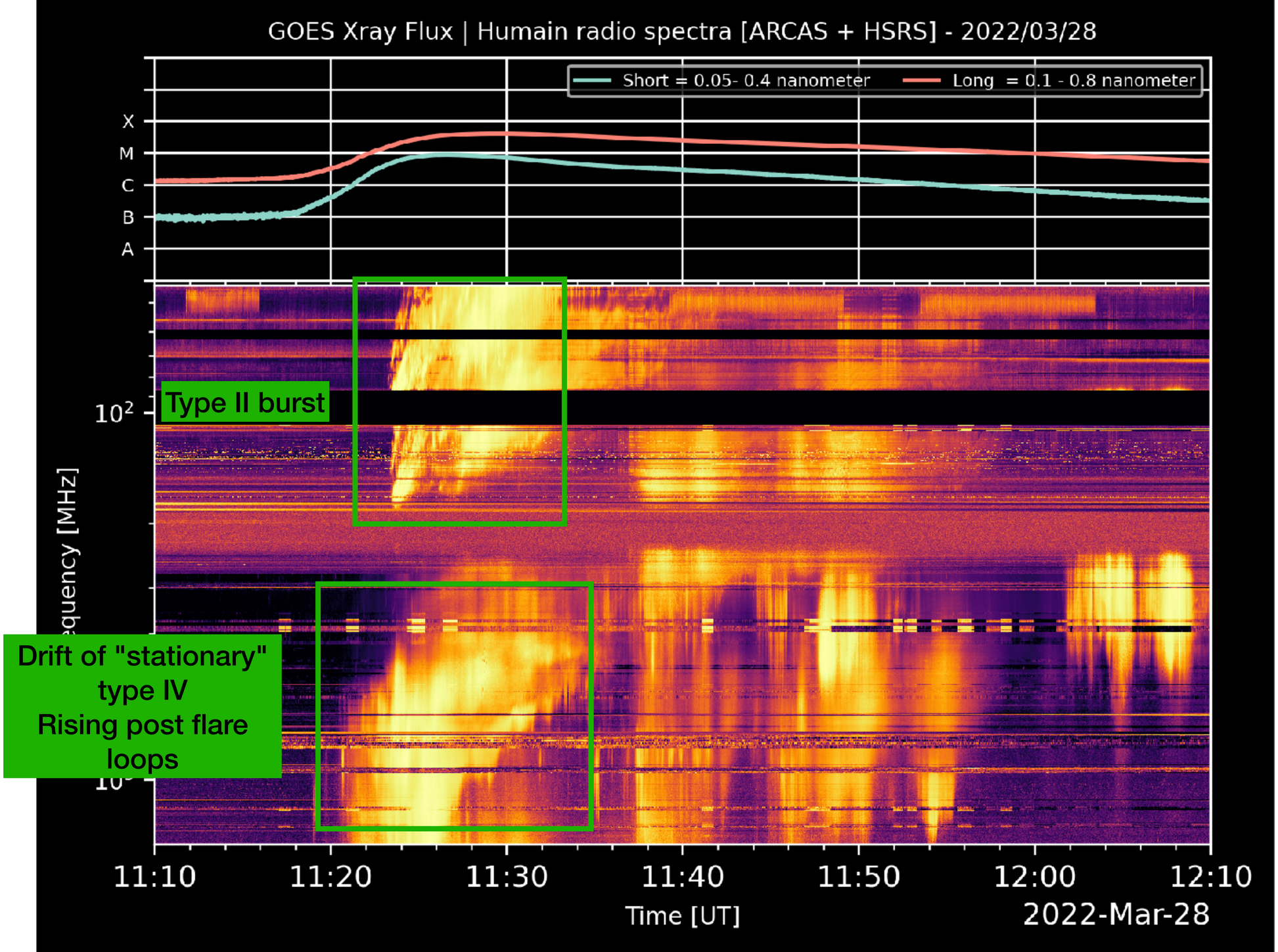
GOES Xray Flux | Humain radio spectra [ARCAS + HSRS] - 2022/03/28
Short = 0.05- 0.4 nanometer
Long = 0.1 - 0.8 nanometer
X
M
C
B
A
Type II burst
Drift of "stationary" type IV
Rising post flare loops
10^2
11:10
11:20
11:30
11:40
11:50
12:00
12:10
Time [UT]
2022-Mar-28

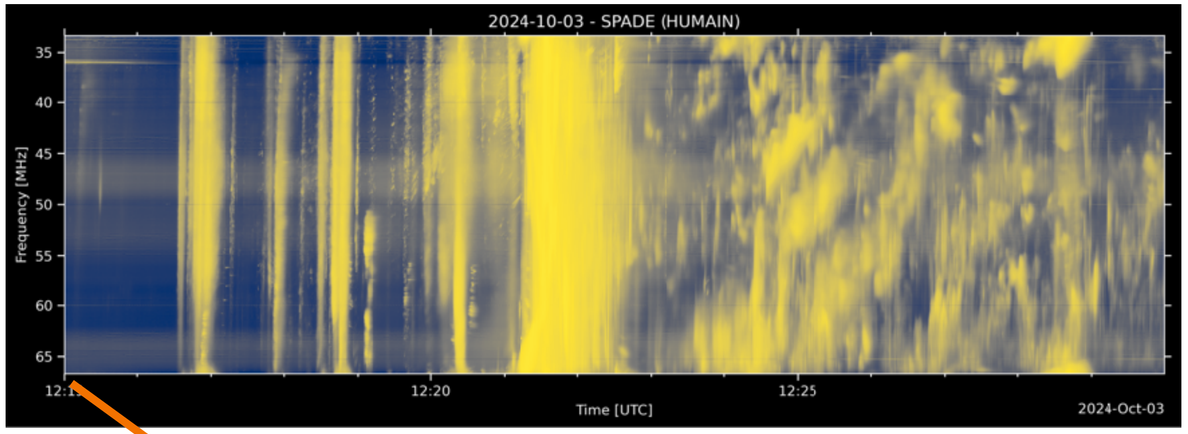
2024-10-03 - SPADE (HUMAIN)
Frequency [MHz]
35
40
45
50
55
60
65
12:20
12:25
Time [UTC]
2024-Oct-03

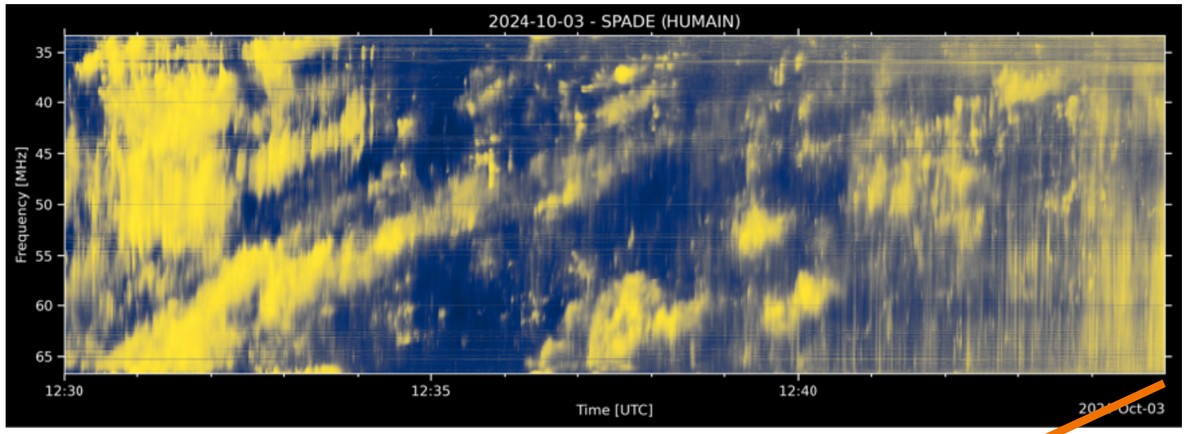
2024-10-03 - SPADE (HUMAIN)
Frequency [MHz]
35
40
45
50
55
60
65
12:30
12:35
12:40
Time [UTC]
2024-Oct-03

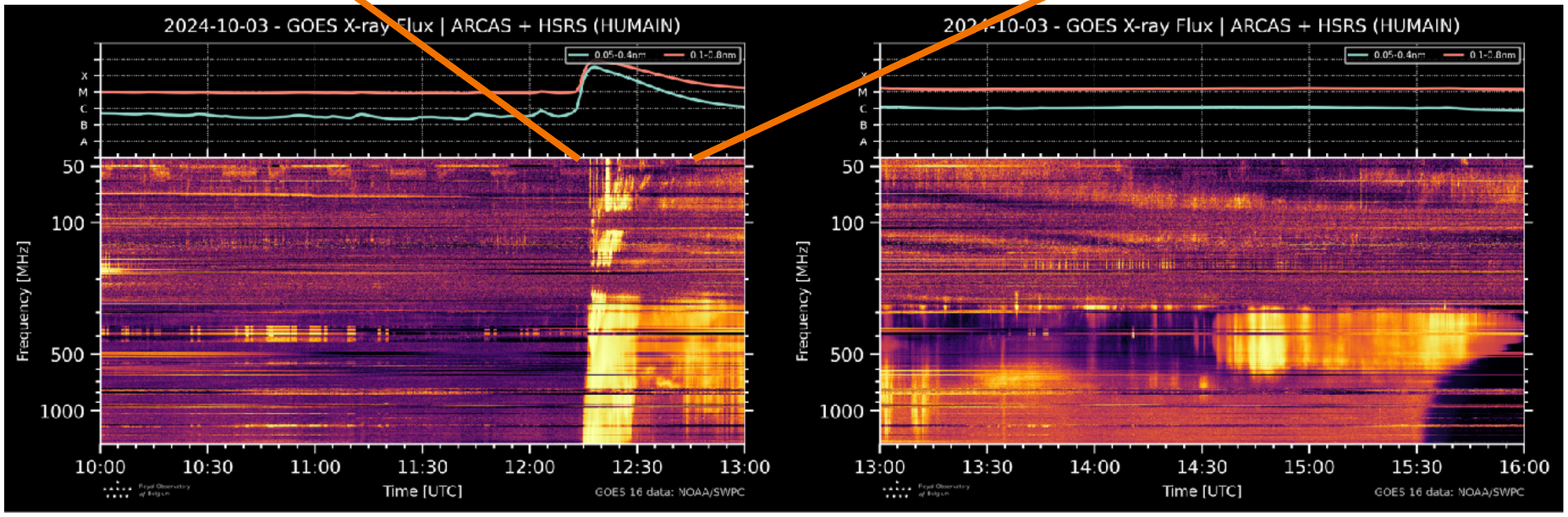
2024-10-03 - GOES X-ray Flux | ARCAS + HSRS (HUMAIN)
0.05-0.4nm
0.1-0.8nm
X
M
C
B
A
Frequency [MHz]
50
100
500
1000
10:00
10:30
11:00
11:30
12:00
12:30
13:00
Time [UTC]
GOES 16 data: NOAA/SWPC
2024-10-03 - GOES X-ray Flux | ARCAS + HSRS (HUMAIN)
0.05-0.4nm
0.1-0.8nm
X
M
C
B
A
Frequency [MHz]
50
100
500
1000
13:00
13:30
14:00
14:30
15:00
15:30
16:00
Time [UTC]
GOES 16 data: NOAA/SWPC

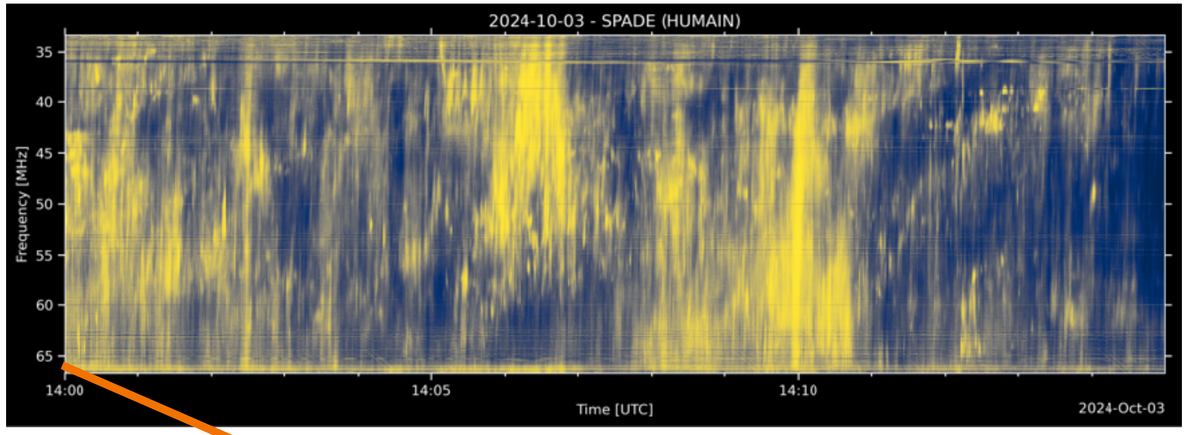
2024-10-03 - SPADE (HUMAIN)
Frequency [MHz]
35
40
45
50
55
60
65
14:00
14:05
14:10
Time [UTC]
2024-Oct-03

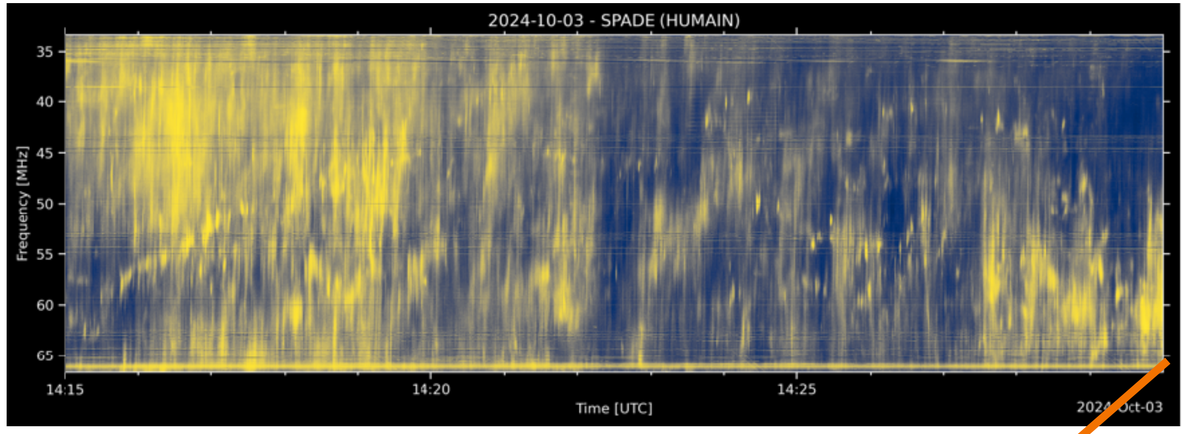
2024-10-03 - SPADE (HUMAIN)
Frequency [MHz]
35
40
45
50
55
60
65
14:15
14:20
14:25
Time [UTC]
2024-Oct-03

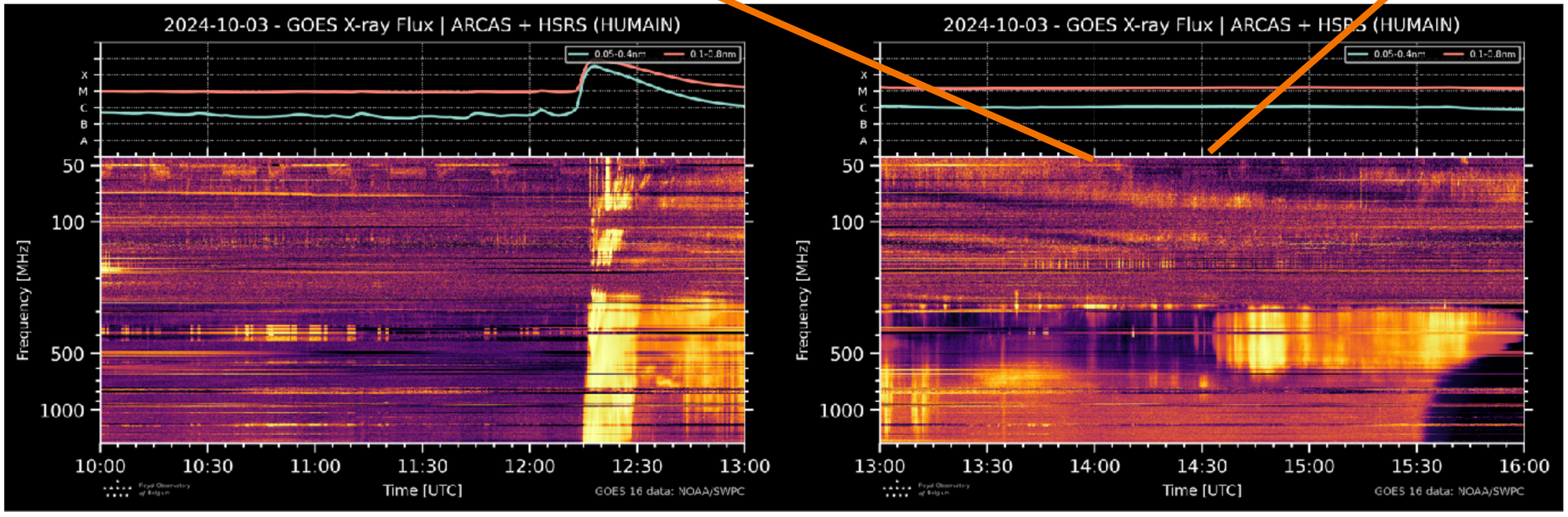
2024-10-03 - GOES X-ray Flux | ARCAS + HSRS (HUMAIN)
0.05-0.4nm
0.1-0.8nm
X
M
C
B
A
Frequency [MHz]
50
100
500
1000
10:00
10:30
11:00
11:30
12:00
12:30
13:00
Time [UTC]
GOES 16 data: NOAA/SWPC
2024-10-03 - GOES X-ray Flux | ARCAS + HSRS (HUMAIN)
0.05-0.4nm
0.1-0.8nm
X
M
C
B
A
Frequency [MHz]
50
100
500
1000
13:00
13:30
14:00
14:30
15:00
15:30
16:00
Time [UTC]
GOES 16 data: NOAA/SWPC

Type IV bursts

Intensity - time profile

- Can reach 1 MSFU (december 2006) in L band ... or at low frequencies
- Peak time can be up to hour and half after peak of the flare
- Magnitude is challenging for plasma emission, ECM?

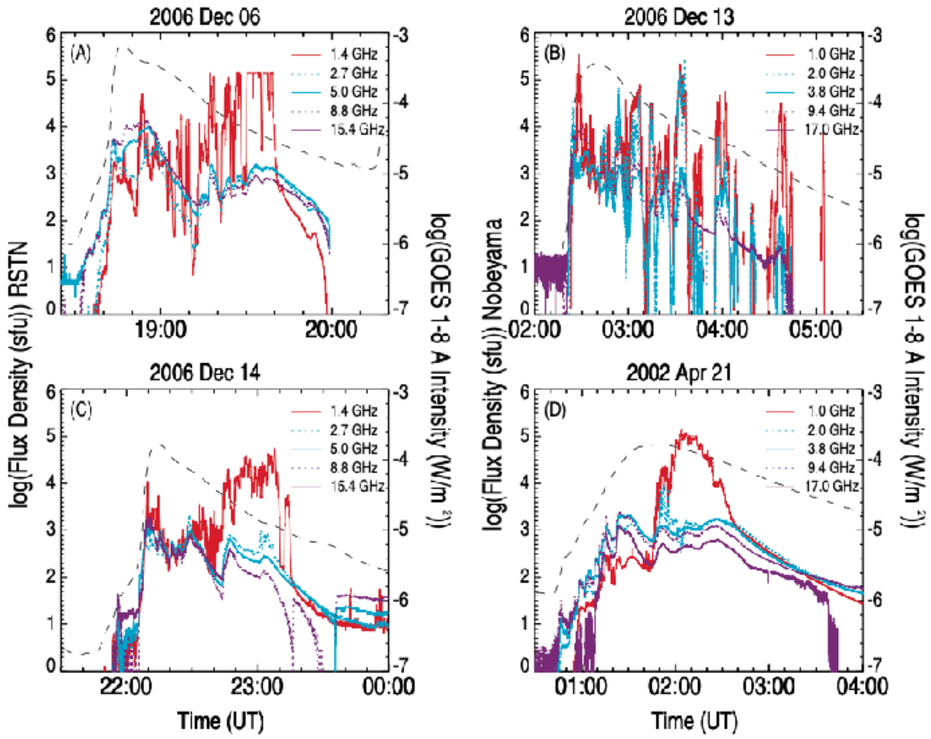

Figure 2. Great ($>10^5$ sfu) decimetric radio bursts on (a) 2006 December 6; (b) 2006 December 13; (c) 2006 December 14; and (d) 2002 April 21. The data are plotted at 1 s time resolution. For the event on December 14, OVSA recorded a burst at 1.6 GHz (not shown) with a peak intensity of $\sim 1.5 \times 10^5$ sfu at 1.6 GHz. The dashed gray line in each of the panels is the time-intensity profile of the associated *GOES* 1–8 Å burst.

Cliver, 2011

Type IV bursts

How useful are they for forecasting?

- Was a proxy for CMEs before CMEs were discovered (Work by M. Pick), linked with geomagnetic storms
- Link with SEP events (gradual) when favourable position of source regions
- Studies linking Type II bursts and SEPs may be biased because in most cases there are also type IV bursts (metric or IP)

Microwave bursts and SEPs

Can be used as proxies for impulsive SEPs

- **SEP events: Chertok et al. 2009**

"Proton fluxes with hard (flat) energy spectra (δ ≤ 1.5) correspond to hard microwave frequency spectra (S9/S15 ≤ 1 and fm ≥ 15 GHz), while flares with soft radio spectra (S9/S15 ≥ 1.5 and fm ≤ 5 GHz) result in proton fluxes with soft (steep) energy spectra (δ ≥ 1.5–2)."

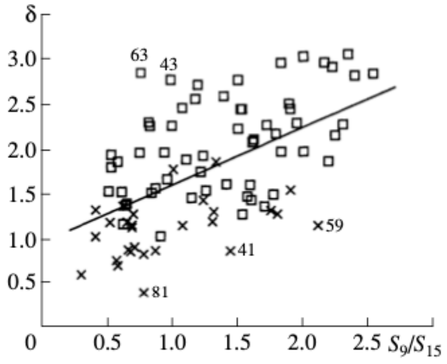

All events

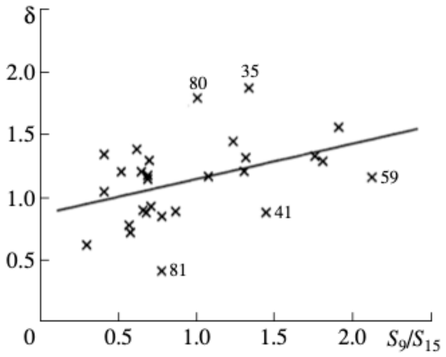

GLEs

Exploring the potential of microwave diagnostics in SEP forecasting: The occurrence of SEP events

Pietro Zucca[1], Marlon Núñez[2] and Karl-Ludwig Klein[1]*

[1] LESIA-UMR 8109 – Observatoire de Paris, PSL Research University, CNRS, Université P & M Curie and Paris-Diderot, 92190 Meudon, France

[2] Departamento de Lenguajes y Ciencias de la Computación, Universidad de Málaga, Campus de Teatinos, 29071 Málaga, Spain

* Corresponding author: ludwig.klein@obspm.fr

Received: 17 January 2017 | **Accepted:** 13 April 2017

Abstract

Solar energetic particles (SEPs), especially protons and heavy ions, may be a space-weather hazard when they impact spacecraft and the terrestrial atmosphere. Forecasting schemes have been developed, which use earlier signatures of particle acceleration to predict the arrival of solar protons and ions in the space environment of the Earth. The UMASEP (University of MAlaga Solar particle Event Predictor) scheme forecasts the occurrence and the importance of an SEP event based on combined observations of soft X-rays, their time derivative and protons above 10 MeV at geosynchronous orbit. We explore the possibility to replace the derivative of the soft X-ray time history with the microwave time history in the UMASEP scheme. To this end we construct a continuous time series of observations for a 13-month period from December 2011 to December 2012 at two microwave frequencies, 4.995 and 8.8 GHz, using data from the four *Radio Solar Telescope Network* (RSTN) patrol stations of the US Air Force, and feed this time series to the UMASEP prediction scheme. During the selected period the *Geostationary Operational Environmental Satellites* (GOES) detected nine SEP events related to activity in the western solar hemisphere. We show that the SEP forecasting using microwaves has the same probability of detection as the method using soft X-rays, but no false alarm in the considered period, and a slightly increased warning time. A detailed analysis of the missed events is presented. We conclude that microwave patrol observations improve SEP forecasting schemes that employ soft X-rays. High-quality microwave data available in real time appear as a significant addition to our ability to predict SEP occurrence.

Impact of SRBs

Noise in radio systems

"A time-varying electromagnetic phenomenon having components in the radio-frequency range, apparently not conveying information and which may be superimposed on, or combined with, a wanted signal."

ITU REC 573

Minimum noise level in systems

$$P_m = kT\Delta_\nu$$

$$P_m \approx -174\ dBm$$

$$T = 290\ K; \Delta_\nu = 1\ Hz; k = 1.38 \times 10^{-23} J\,.\,K^{-1}$$

Noise received by antenna

$$P_R = \frac{1}{2}\frac{G\lambda^2}{4\pi}\Delta_\nu F$$

Antenna, with gain G,
pointed at a source
with flux density F

Simple interference threshold

$$P_m = kT\Delta_\nu \equiv P_R = \frac{1}{2}\frac{G\lambda^2}{4\pi}\Delta_\nu F$$

Double the noise that enters the system

S/N decreases by 3 dB

Cell phones



Interference of cell phone towers

Only published report on proven effects of SRBs on cell phones

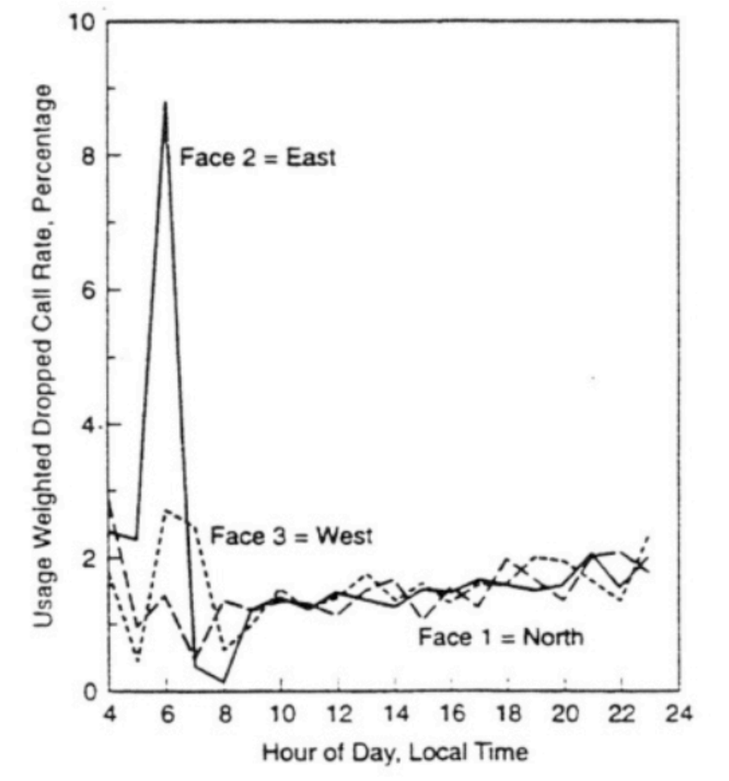

Figure 1. Usage-weighted dropped call rate for a wireless system base station, showing an enhanced level of dropped calls on the east-facing receivers near local sunrise. From Lanzerotti et al. (1999).

Gary et al. 2001

Surveillance radars

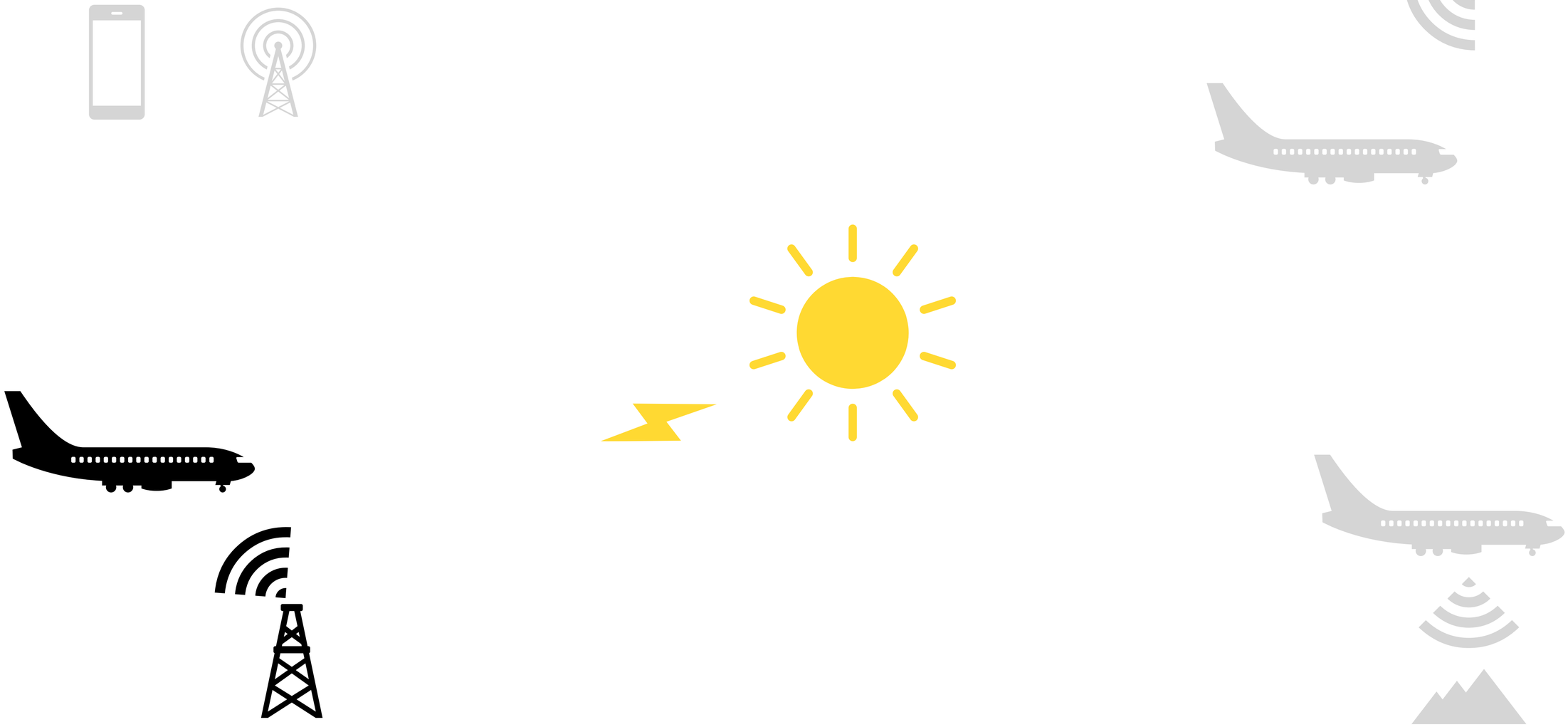

Impact on radars

Military devices - UK, World War II

110 m

Transmission steel towers (4)

Receiving wooden towers

73 m

One of the Chain Home radar stations, in the UK

from the collections of the Imperial War Museums, Public domain

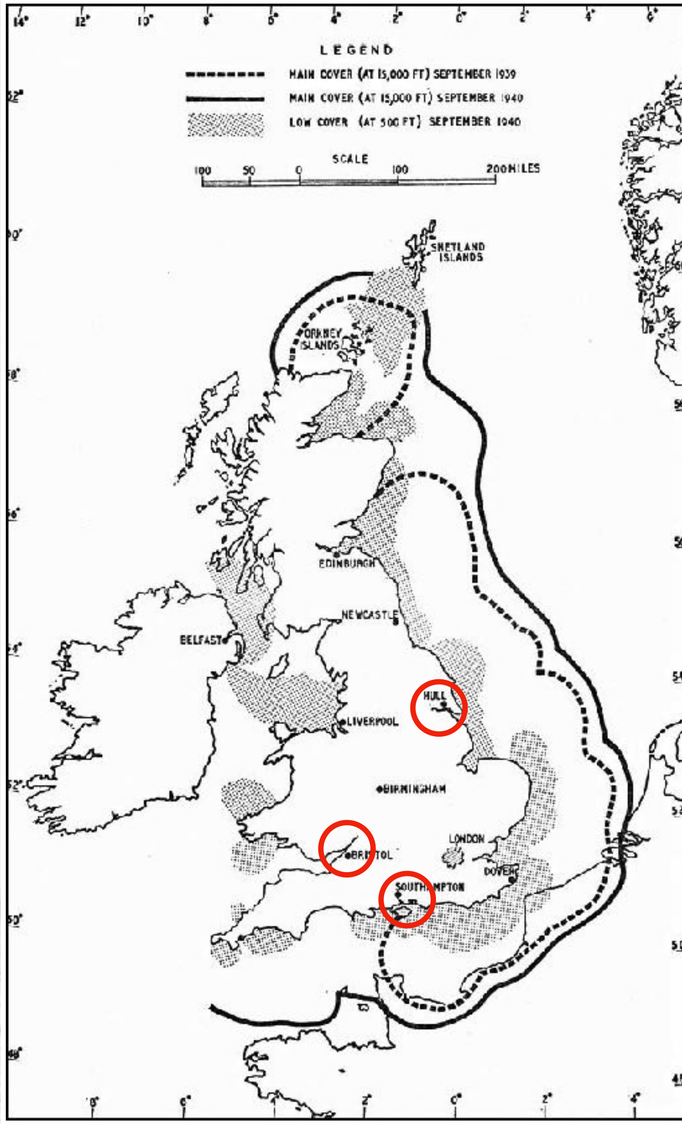

WIKIPEDIA

Impact on radars

Military devices - UK, World War II

Solar Radiations in the 4–6 Metre Radio Wave-Length Band

THE solar radiation spectrum does not normally extend into the 5-metre wave-length region with sufficient intensity to be detectable on radio receiving equipments in commercial or Service use. It is now possible to disclose that, on one occasion during the War, Army equipments observed solar radiations of the order of 10^5 times the power expected from the sun, assuming that the sun behaves as a perfect black-body radiator at a temperature of 6,000° K.

This abnormally high intensity of solar radiation occurred on February 27 and 28, 1942, when Army radar receiving equipments, working at various wave-lengths in the 4–6 metre band, noticed strong directional radiations similar in character to the random fluctuations of internal receiver noise (thermal and valve noise). The radiation was first detected in the afternoon on February 26, 1942, and was almost

Hey, 1946

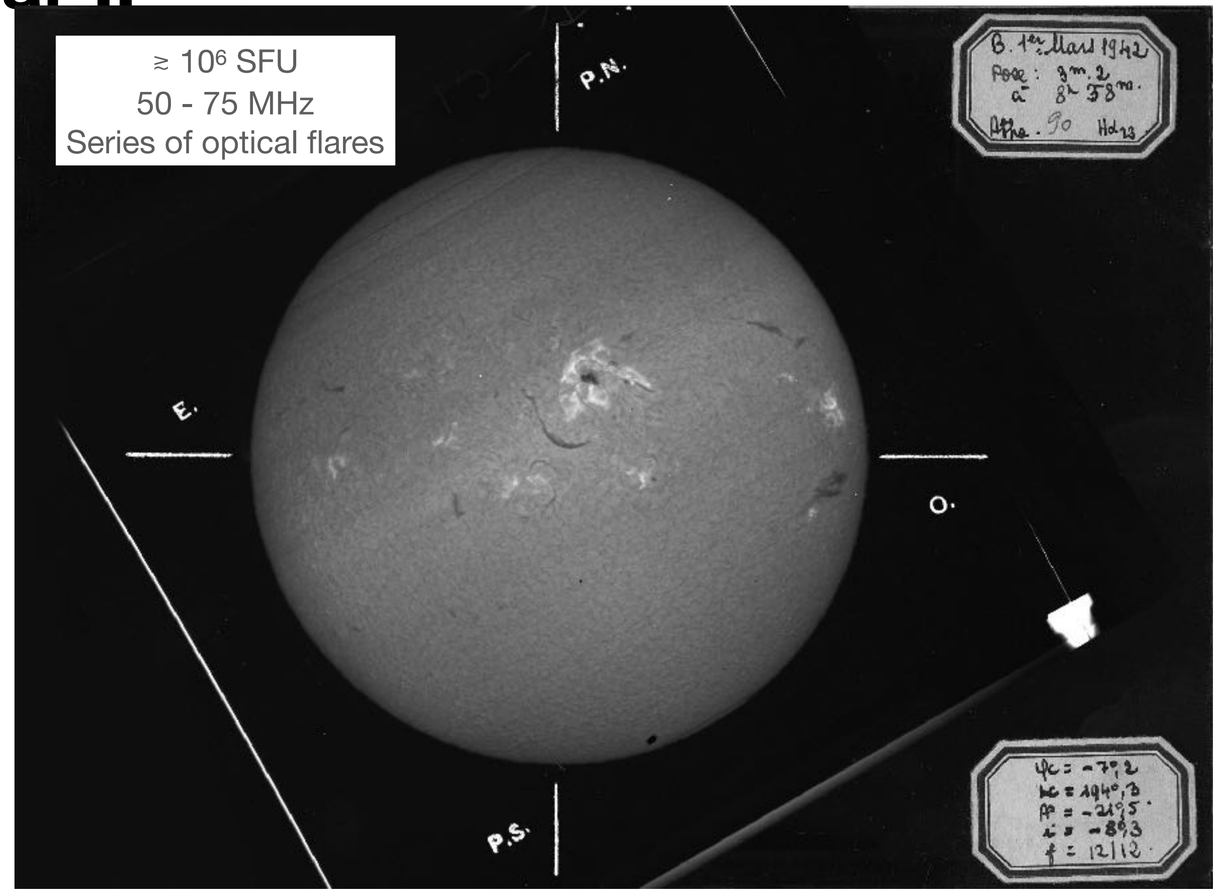

source: https://observations-solaires.obspm.fr/

Impact on radars

Military radars - NZ, World War II

- In March - April1945, Royal New Zealand Air Force radar station on the Norfolk Island picked up increase level of noise at Sun rise and Sun set at 200 MHz
- The head of the ORS of Radio Development Lab., Elisabeth Alexander investigated it, with new measurements and linked it to the Sun itself

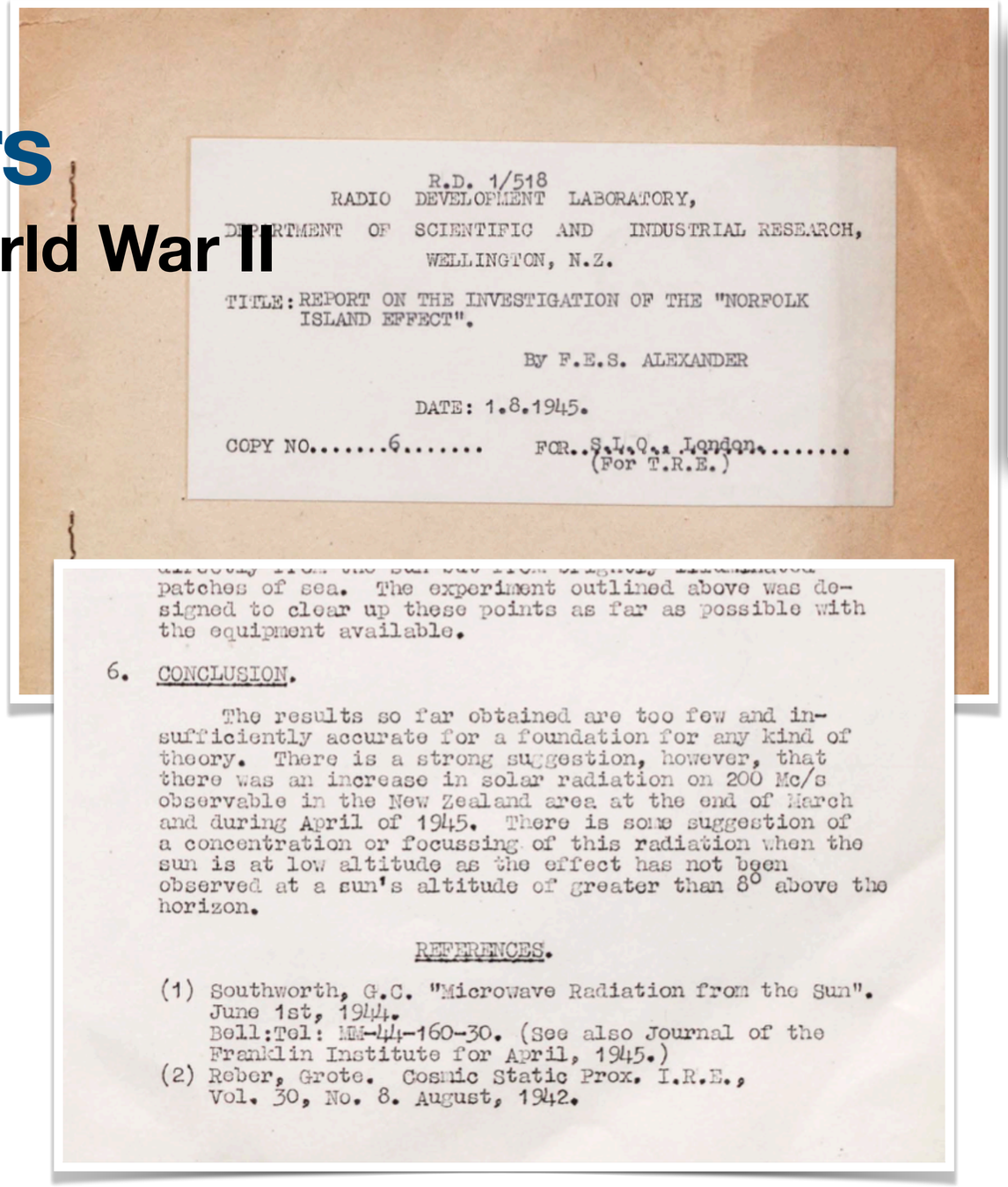

R.D. 1/518
RADIO DEVELOPMENT LABORATORY,
DEPARTMENT OF SCIENTIFIC AND INDUSTRIAL RESEARCH,
WELLINGTON, N.Z.

TITLE: REPORT ON THE INVESTIGATION OF THE "NORFOLK ISLAND EFFECT".

By F.E.S. ALEXANDER

DATE: 1.8.1945.

COPY NO.....6..... FOR..S.L.O., London.....
(For T.R.E.)

patches of sea. The experiment outlined above was designed to clear up these points as far as possible with the equipment available.

6. CONCLUSION.

The results so far obtained are too few and insufficiently accurate for a foundation for any kind of theory. There is a strong suggestion, however, that there was an increase in solar radiation on 200 Mc/s observable in the New Zealand area at the end of March and during April of 1945. There is some suggestion of a concentration or focussing of this radiation when the sun is at low altitude as the effect has not been observed at a sun's altitude of greater than 8° above the horizon.

REFERENCES.

(1) Southworth, G.C. "Microwave Radiation from the Sun". June 1st, 1944. Bell:Tel: MM-44-160-30. (See also Journal of the Franklin Institute for April, 1945.)
(2) Reber, Grote. Cosmic Static Prox. I.R.E., Vol. 30, No. 8. August, 1942.

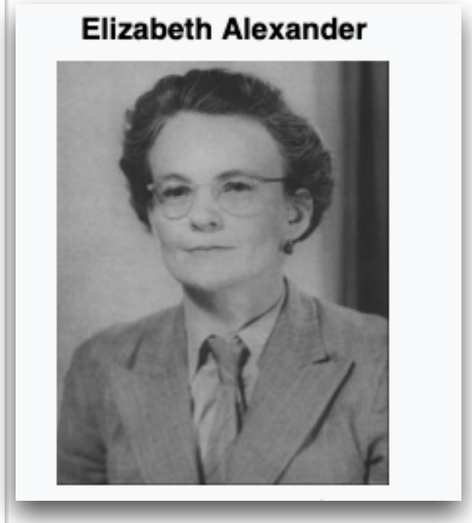

Likely the radar picked up intense noise storm emission from sunspot groups

Impact on radars

"Cold War military commanders viewed full scale jamming of surveillance sensors as a potential act of war. (...) the online memorial tributes to Col C. K. Anderson, (...) clearly credit him and his NORAD solar forecasting staff (...) with providing the information that eventually calmed nerves and allowed aircraft engines to cool as they returned to normal alert stance."

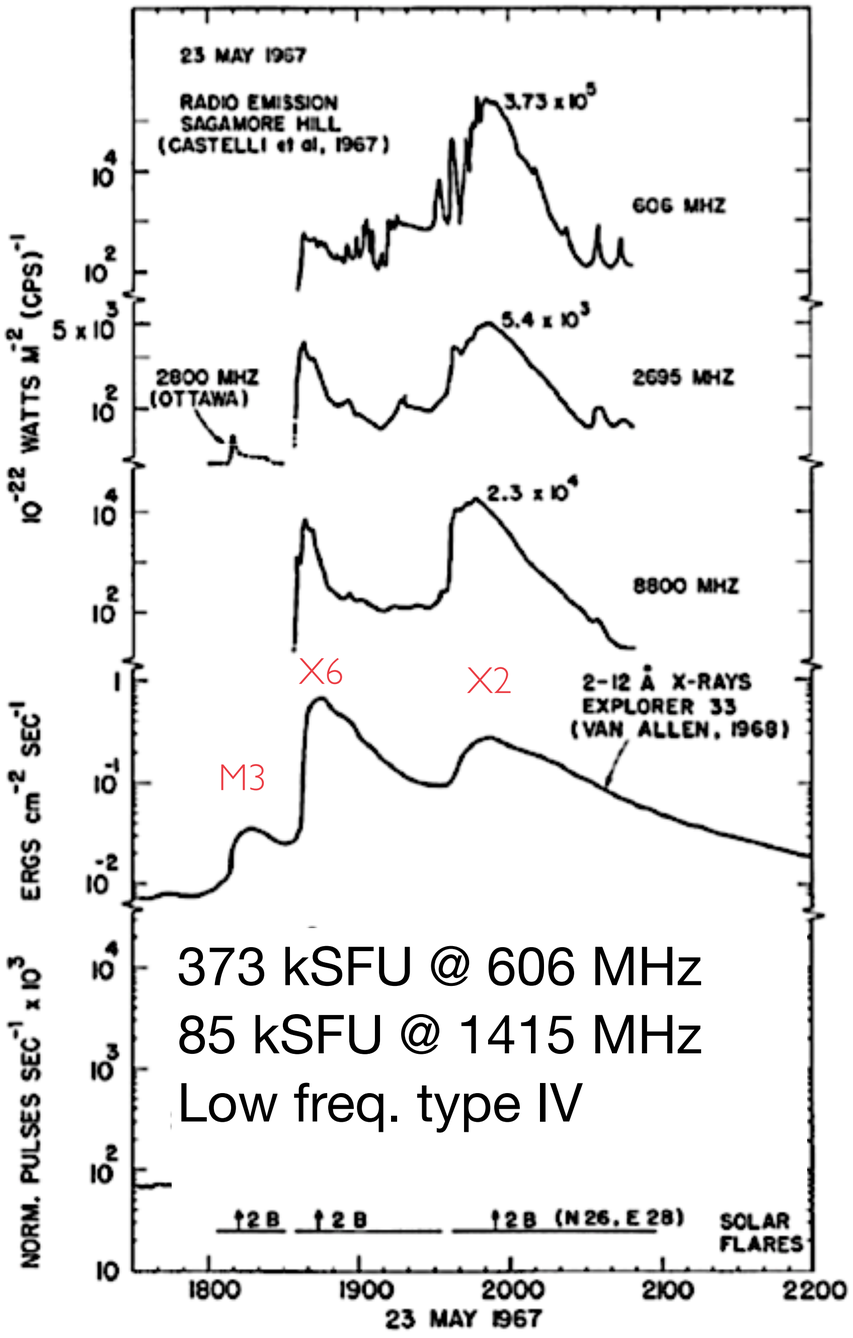

Knipp et al. 2016

MAY 27, 1967 (P=-17.51, B_o=-1.29, L_o=207.53)

SACRAMENTO PEAK Hα

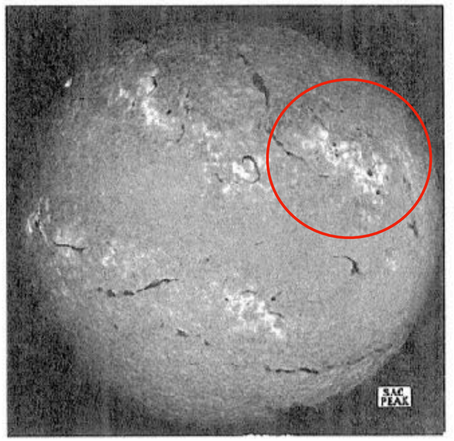

1516 UT

ESSA-BOULDER SUNSPOTS

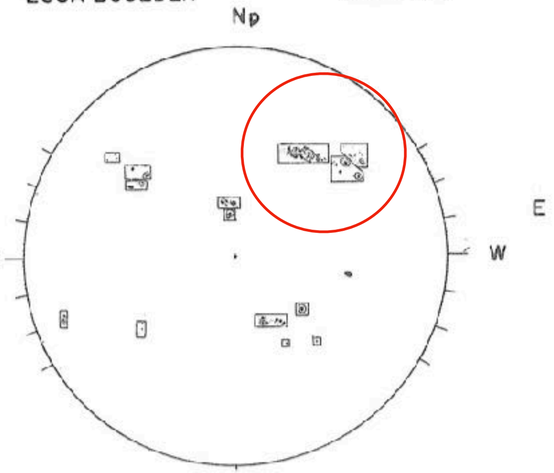

1400 UT SAC PEAK

MT. WILSON MAGNETOGRAM

Np

Solid

Dotte

NO DATA

Sp

1300 UT

STANFORD 9.1 cm.

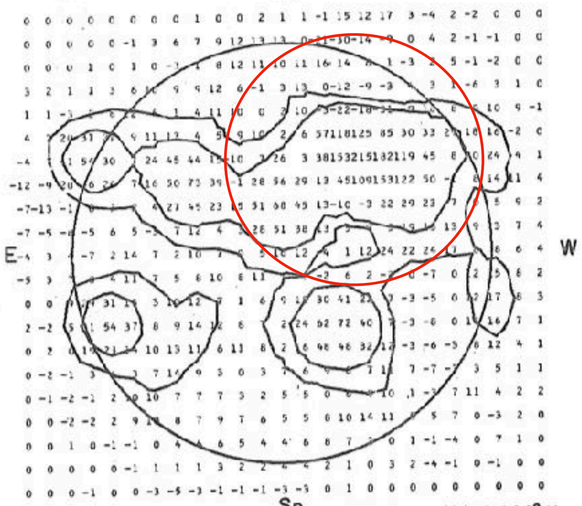

20-21 UT Brightness Unit 5,000° K

FLEURS, AUSTRALIA 21 cm.

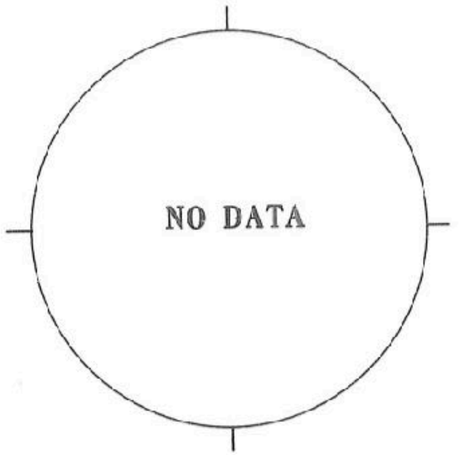

Resolution 3 Minutes of Arc

02-03 UT Brightness Unit 1,700° K

McMATH-HULBERT CALCIUM REPOR

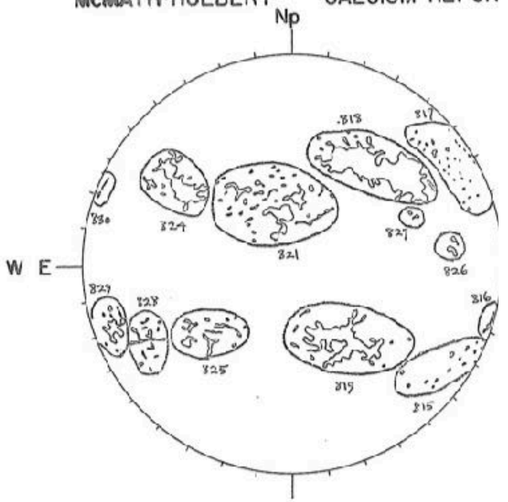

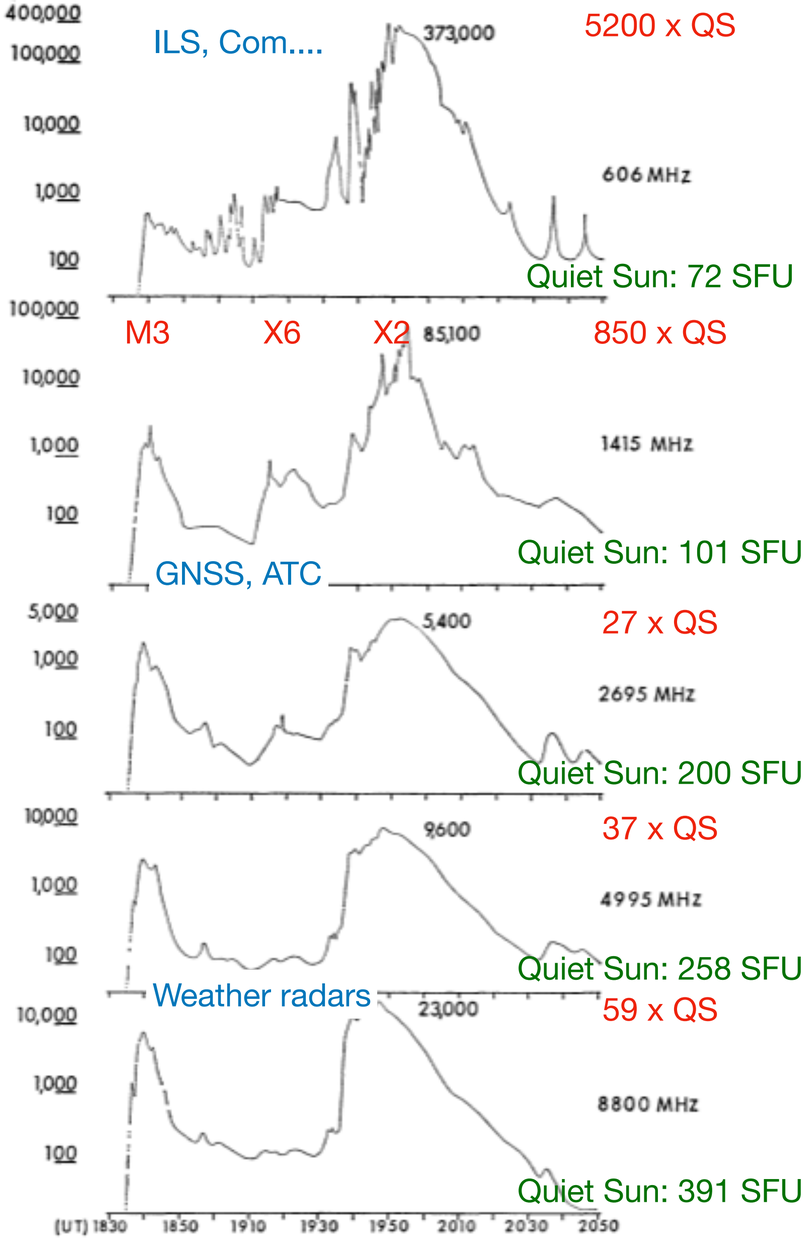

Air traffic radars

Civil aviation

Primary radars : 2800 MHz

Secondary radars: 1030 & 1090 MHz

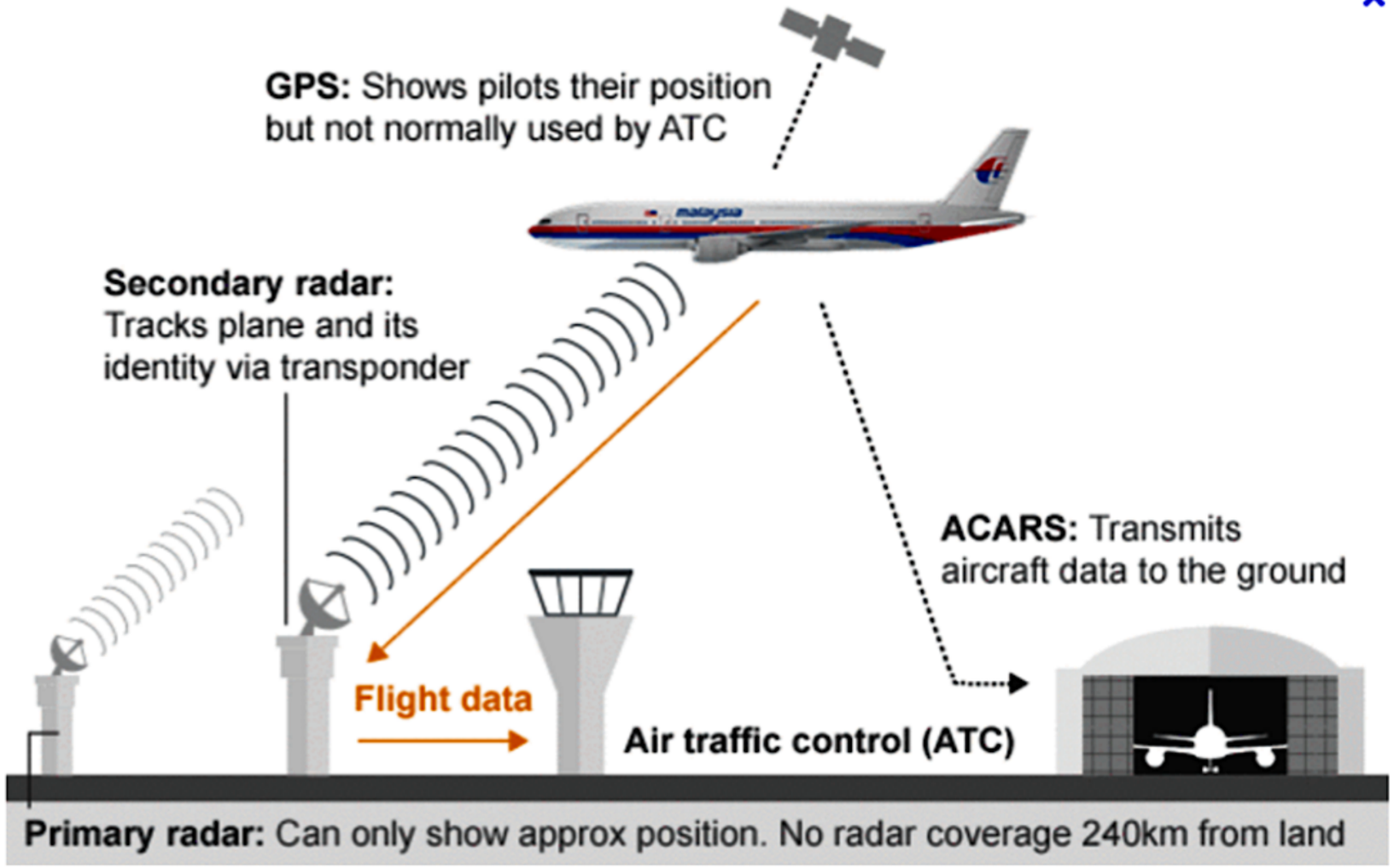

Source: BBC

November 4 2015

A media storm

- ATC radars in Sweden suffered severe disturbances between 14:20 UT and 16:00 UT
- Incoming flights were deviated, no departures allowed
- Geomagnetic storm was initially considered as the source of disturbances (media)





A European wide disruption

- Sweden: ATC radars suffered severe disturbances 14:20 UT - 16:00 UT
- Sweden: Partial closure of air space for an hour
- Minor disturbances in Norway, Belgium

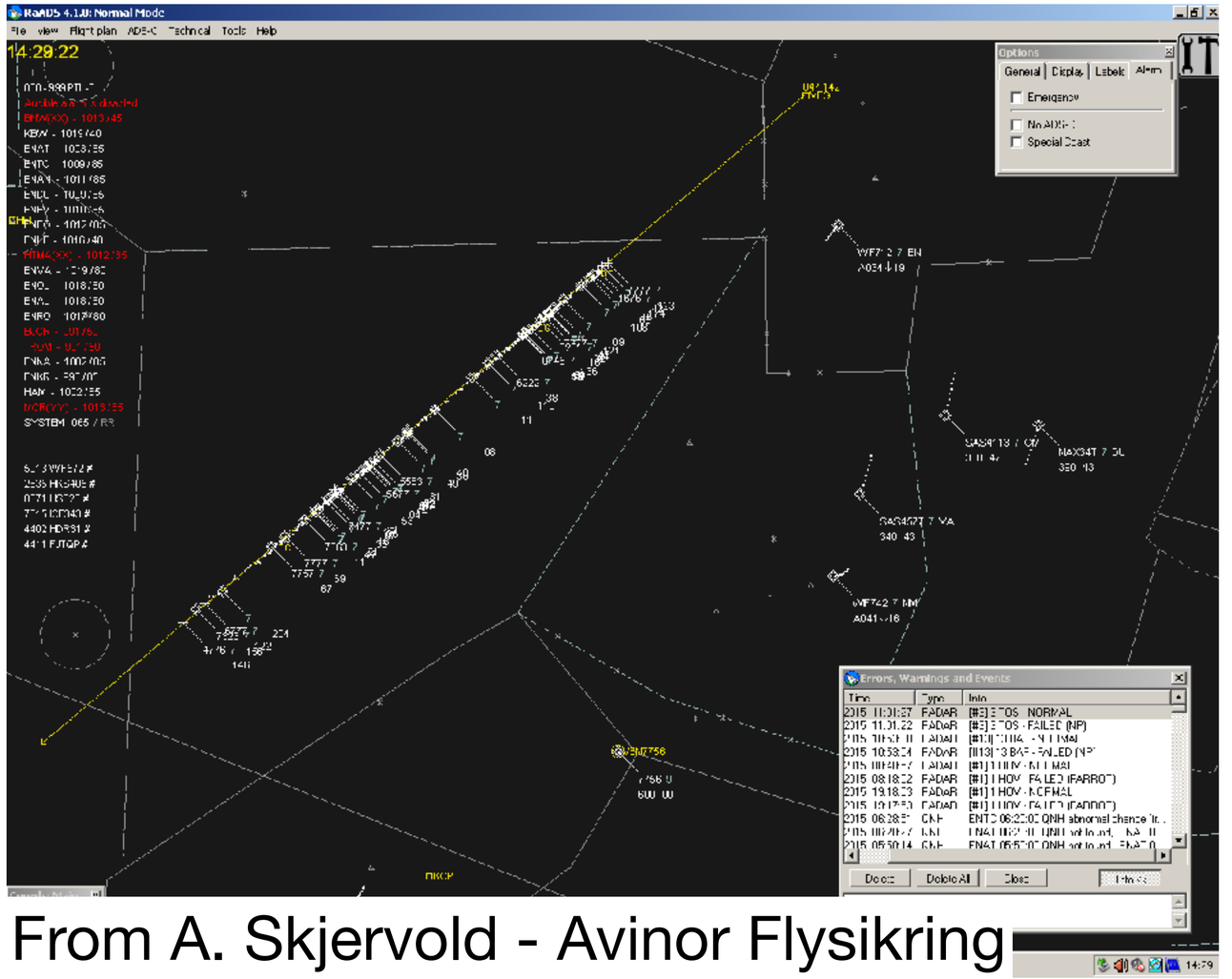

From A. Skjervold - Avinor Flysikring

A European wide disruption

- Sweden: ATC radars suffered severe disturbances 14:20 UT - 16:00 UT
- Sweden: Partial closure of air space for an hour
- Minor disturbances in Norway, Belgium

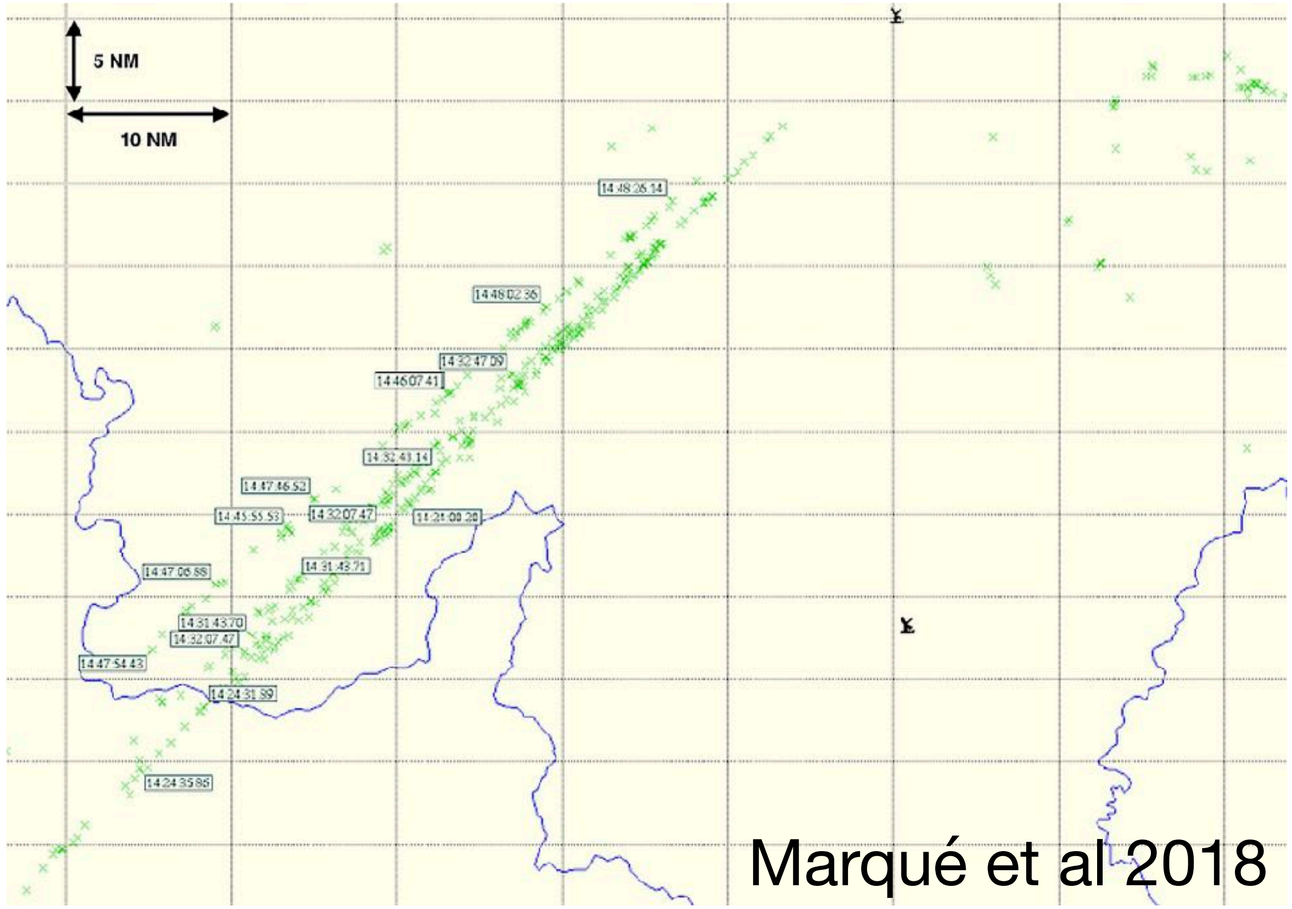

Marqué et al 2018

Solar event

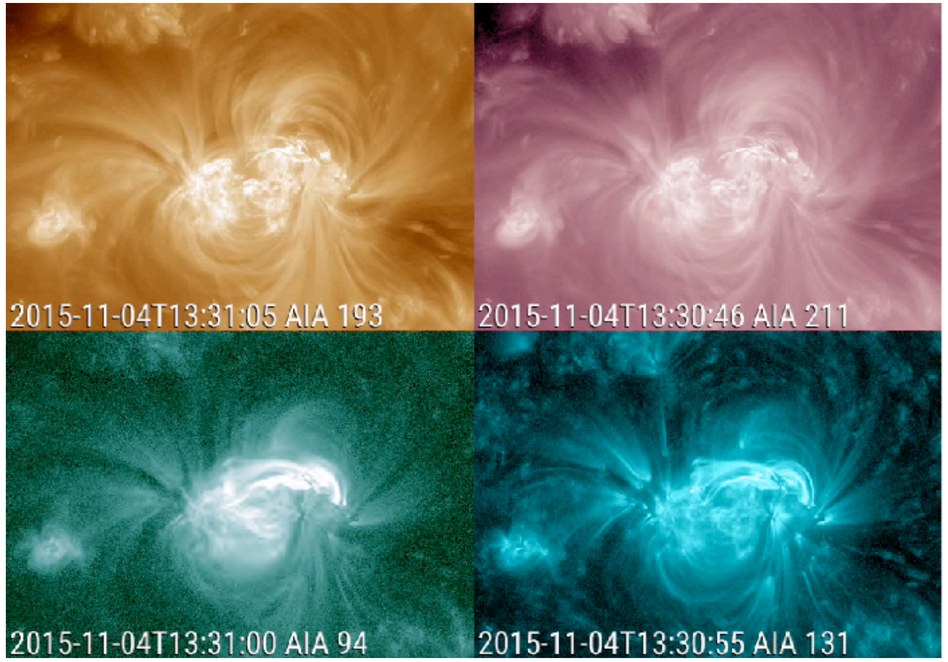

M3.7 flare peaking @1352 UT
NOAA AR 2243

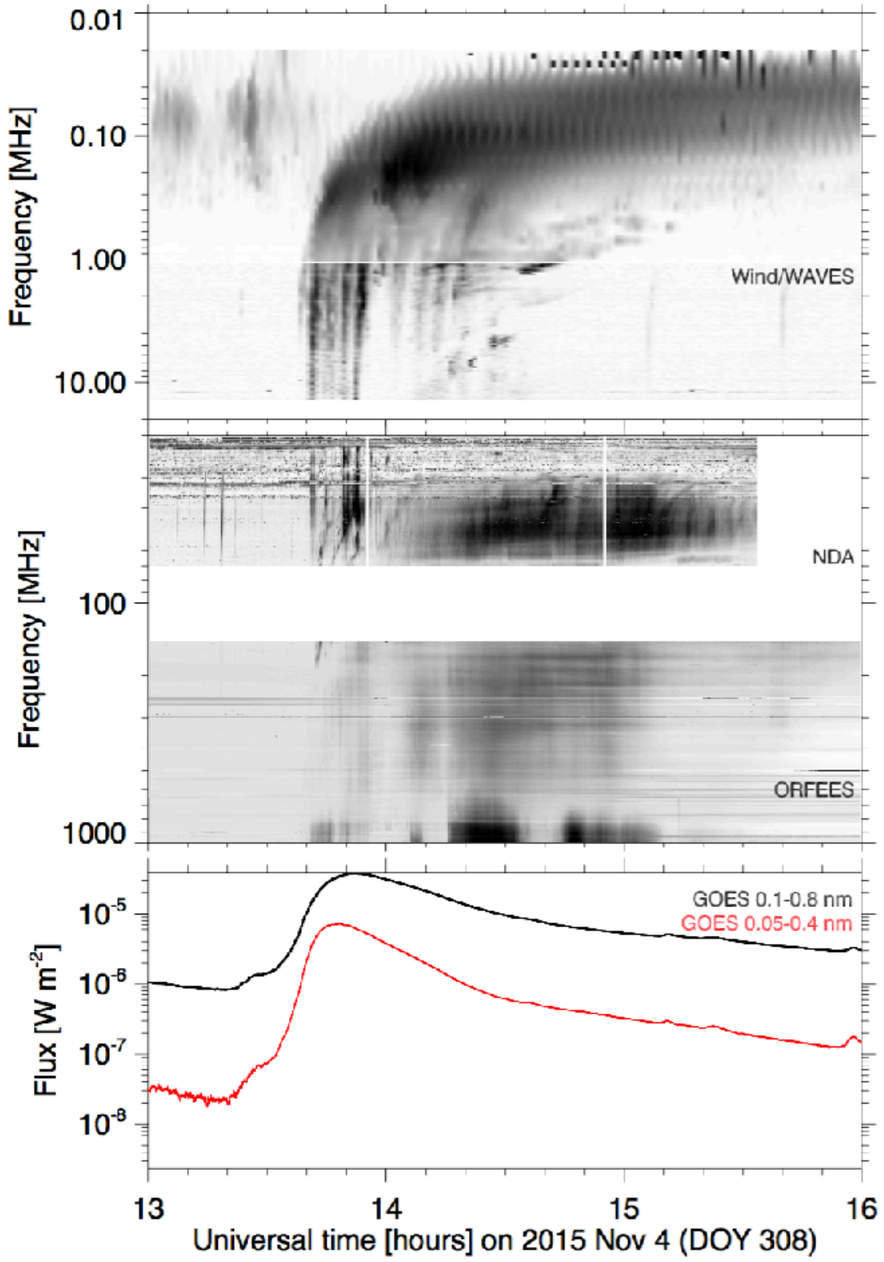

Solar event

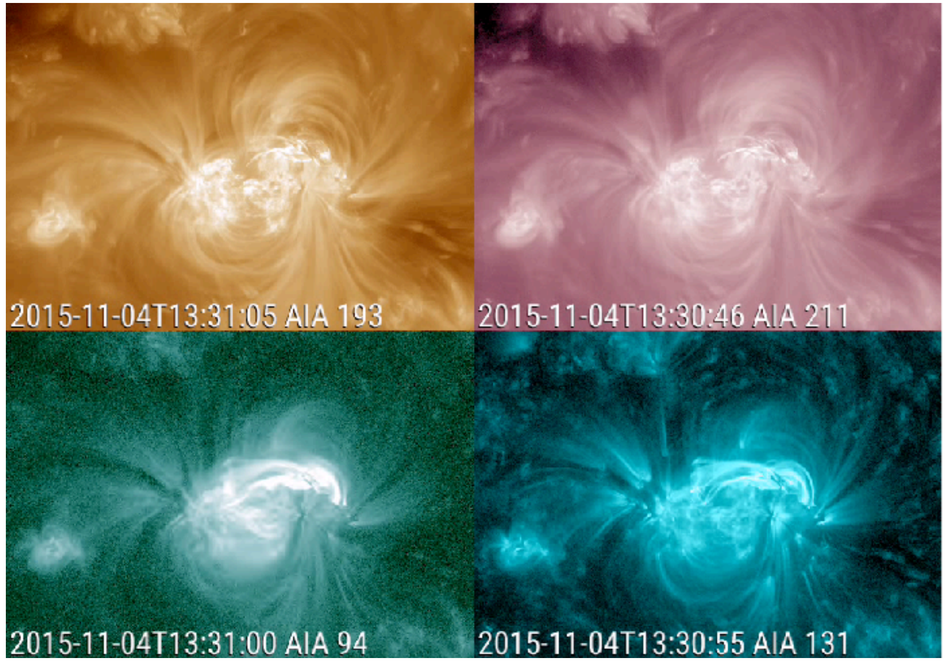

M3.7 flare peaking @1352 UT
NOAA AR 2243

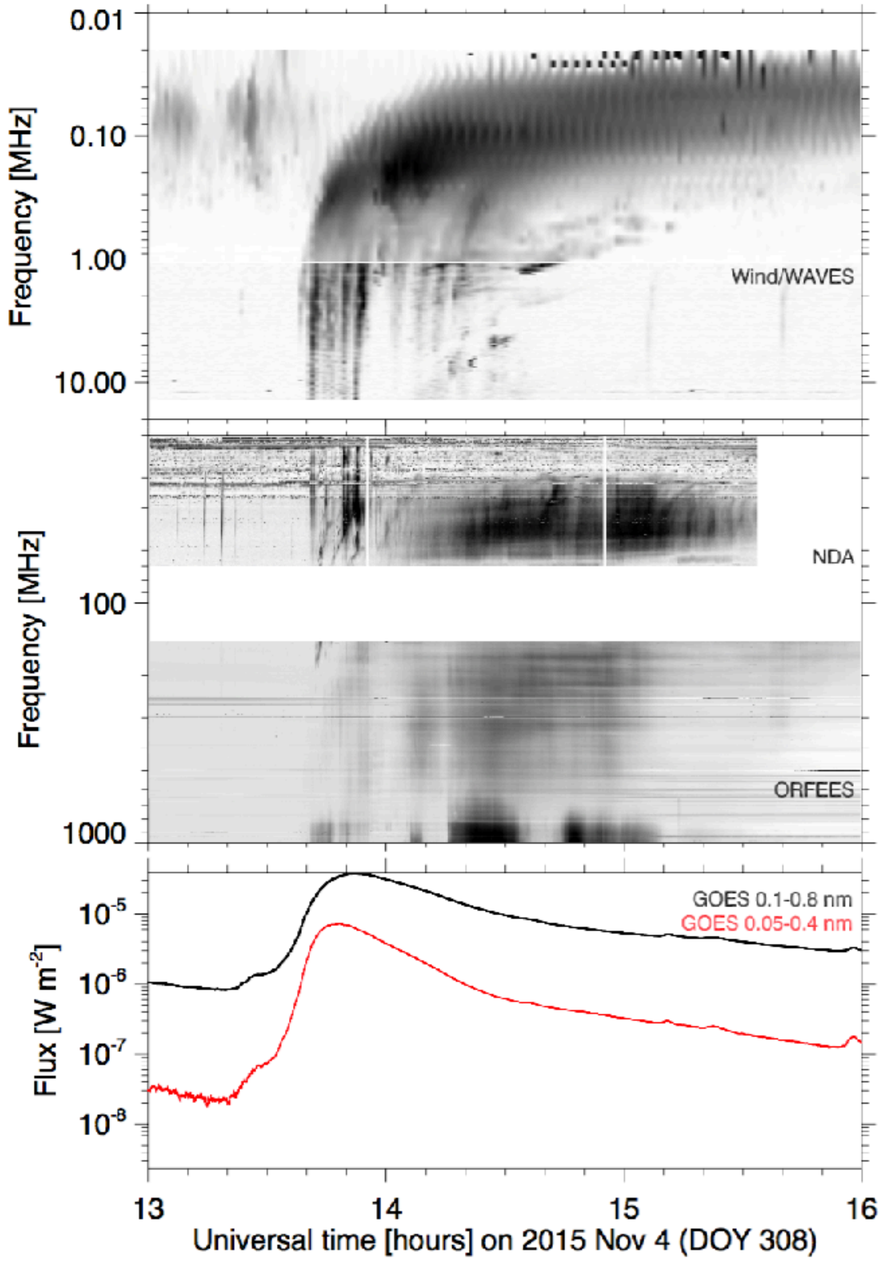

Solar event

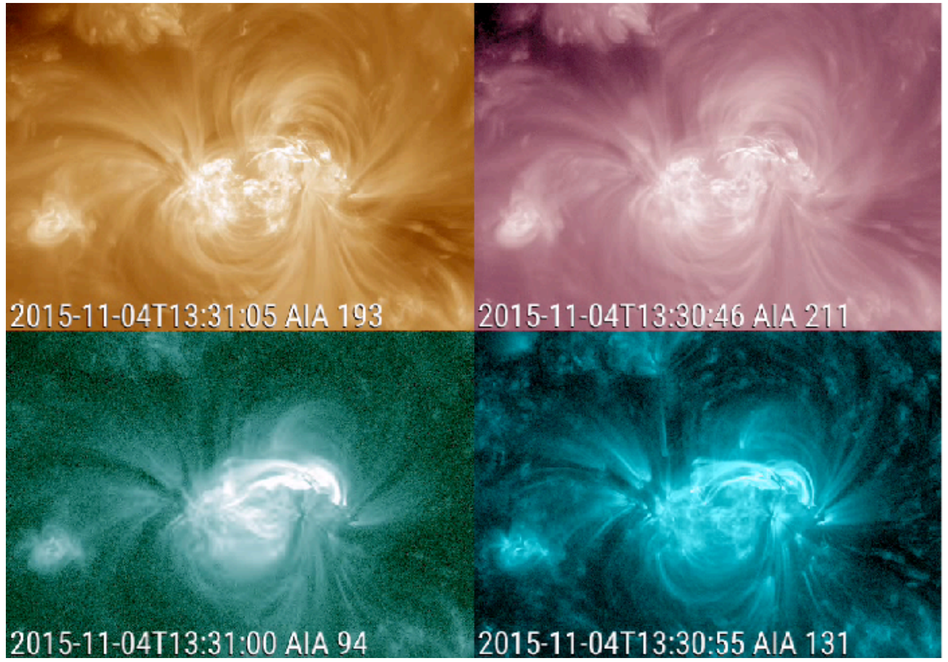

M3.7 flare peaking @1352 UT
NOAA AR 2243

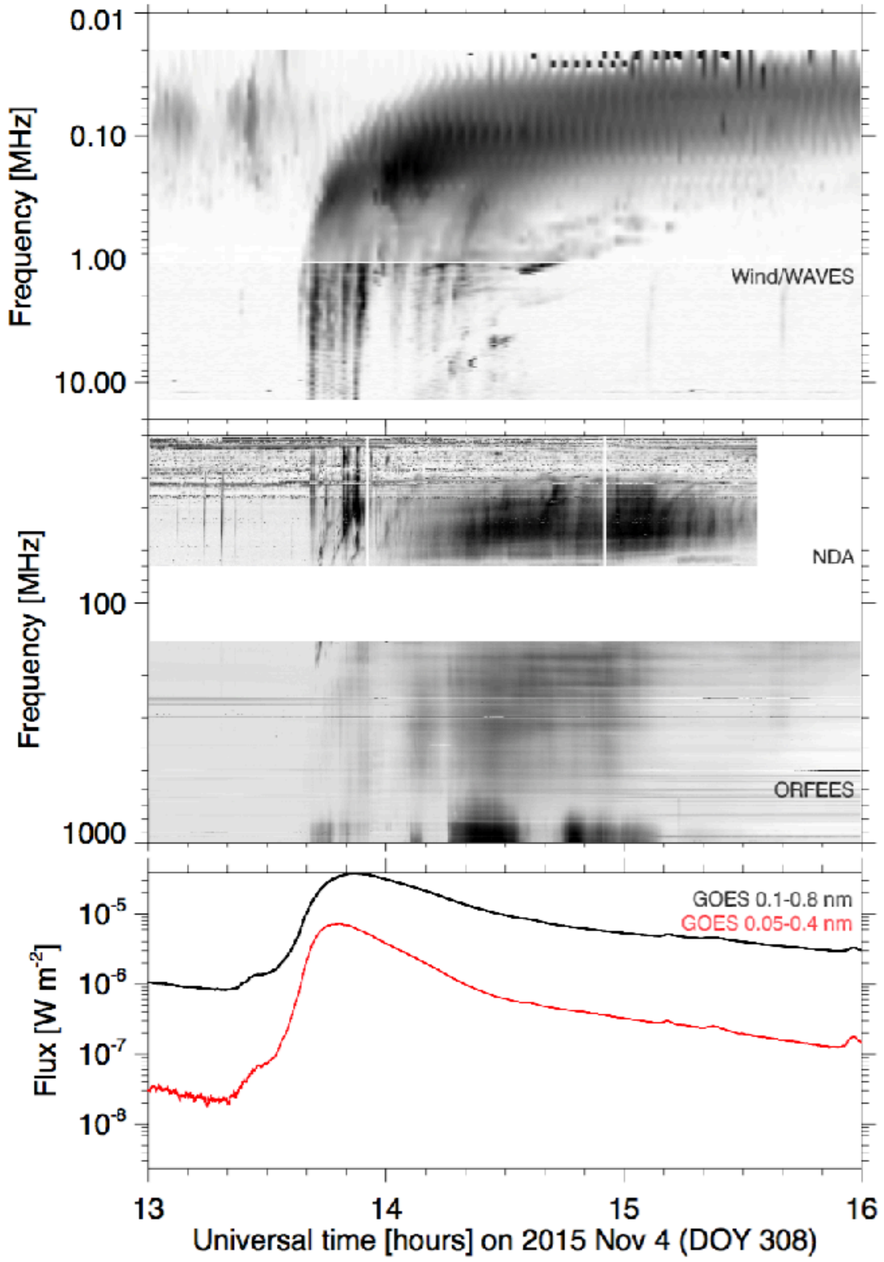

In Humain



https://www.sidc.be/humain

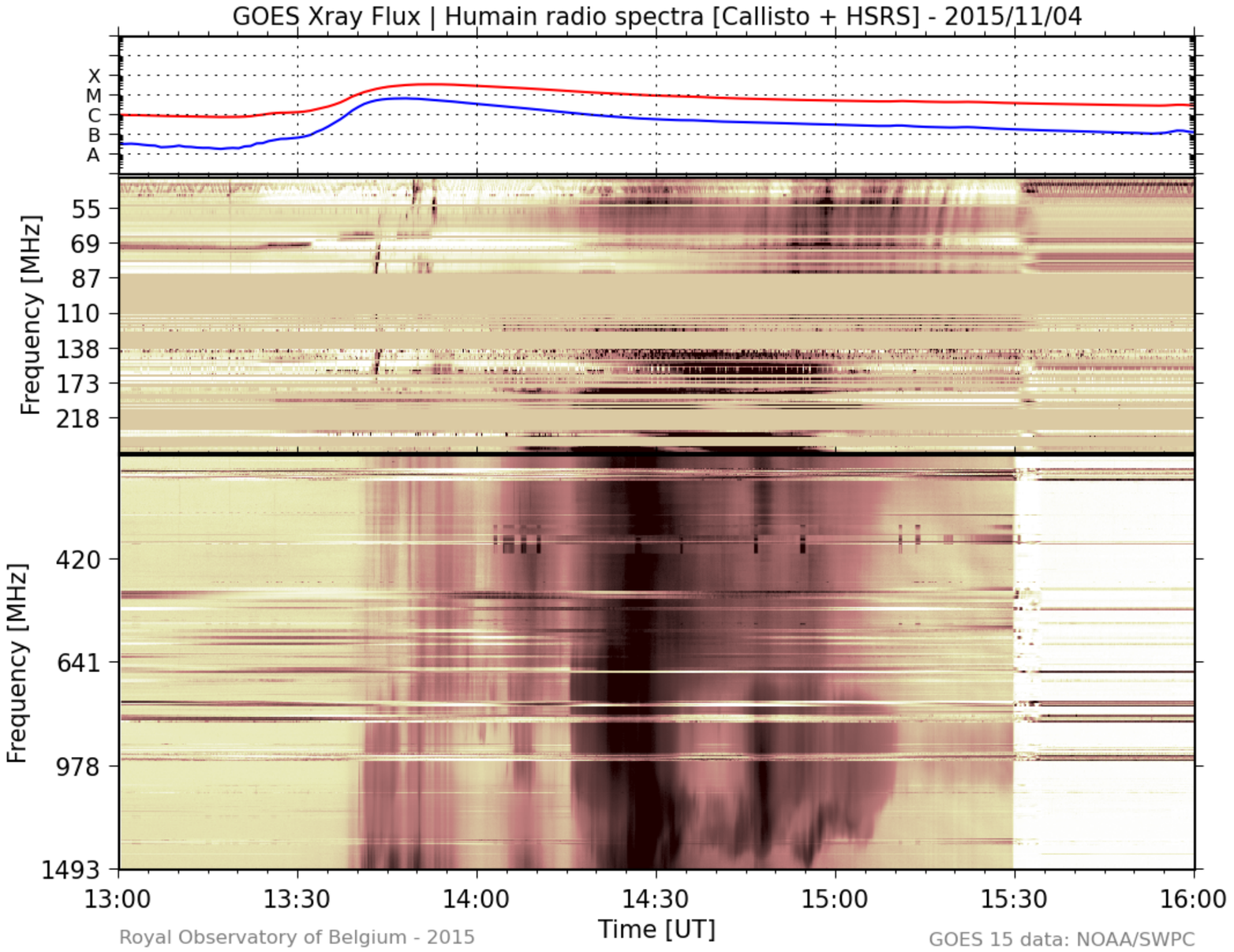

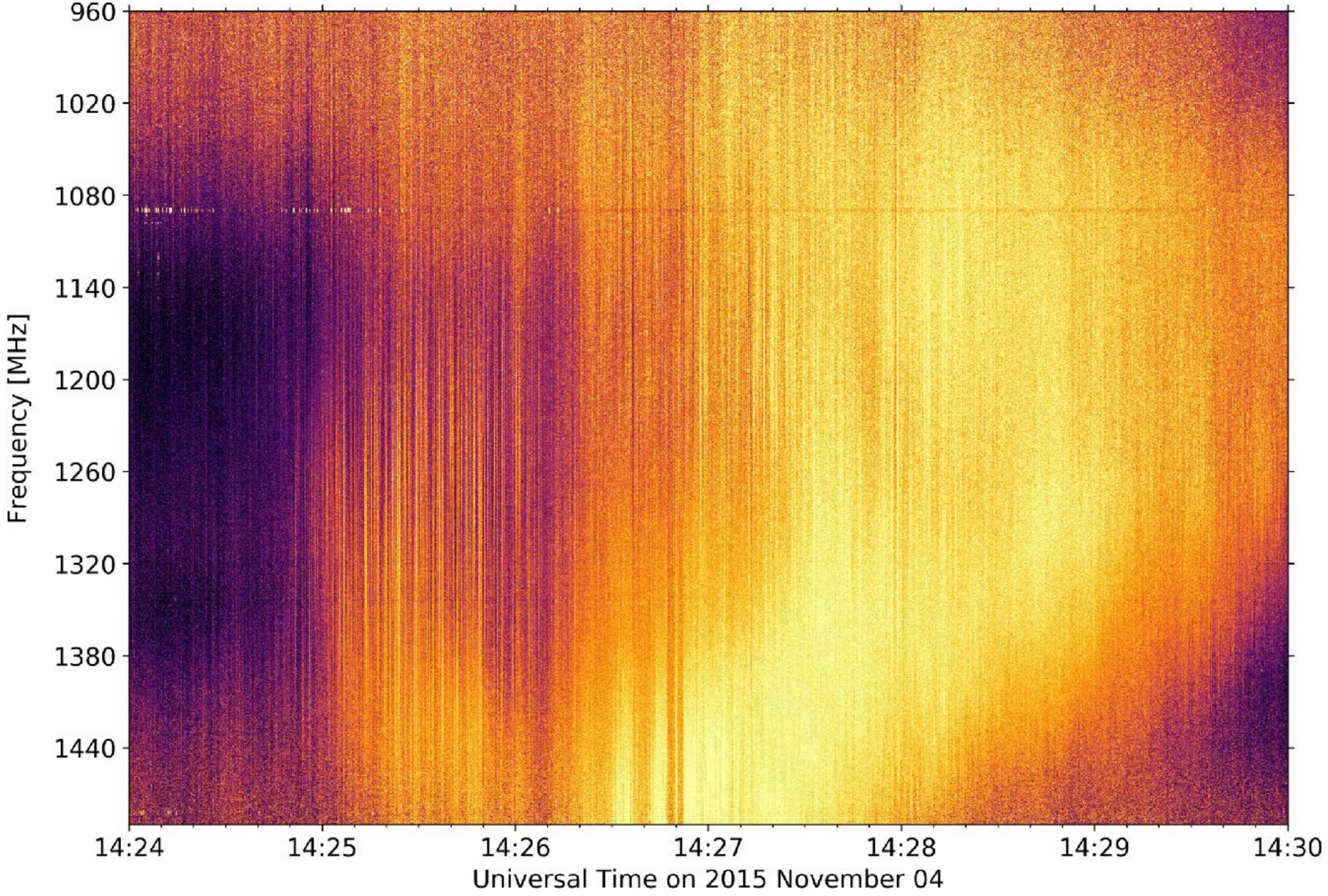
960
1020
1080
1140
1200
1260
1320
1380
1440
Frequency [MHz]
14:24
14:25
14:26
14:27
14:28
14:29
14:30
Universal Time on 2015 November 04

Radar band Saint-Hubert Air base, 21 km

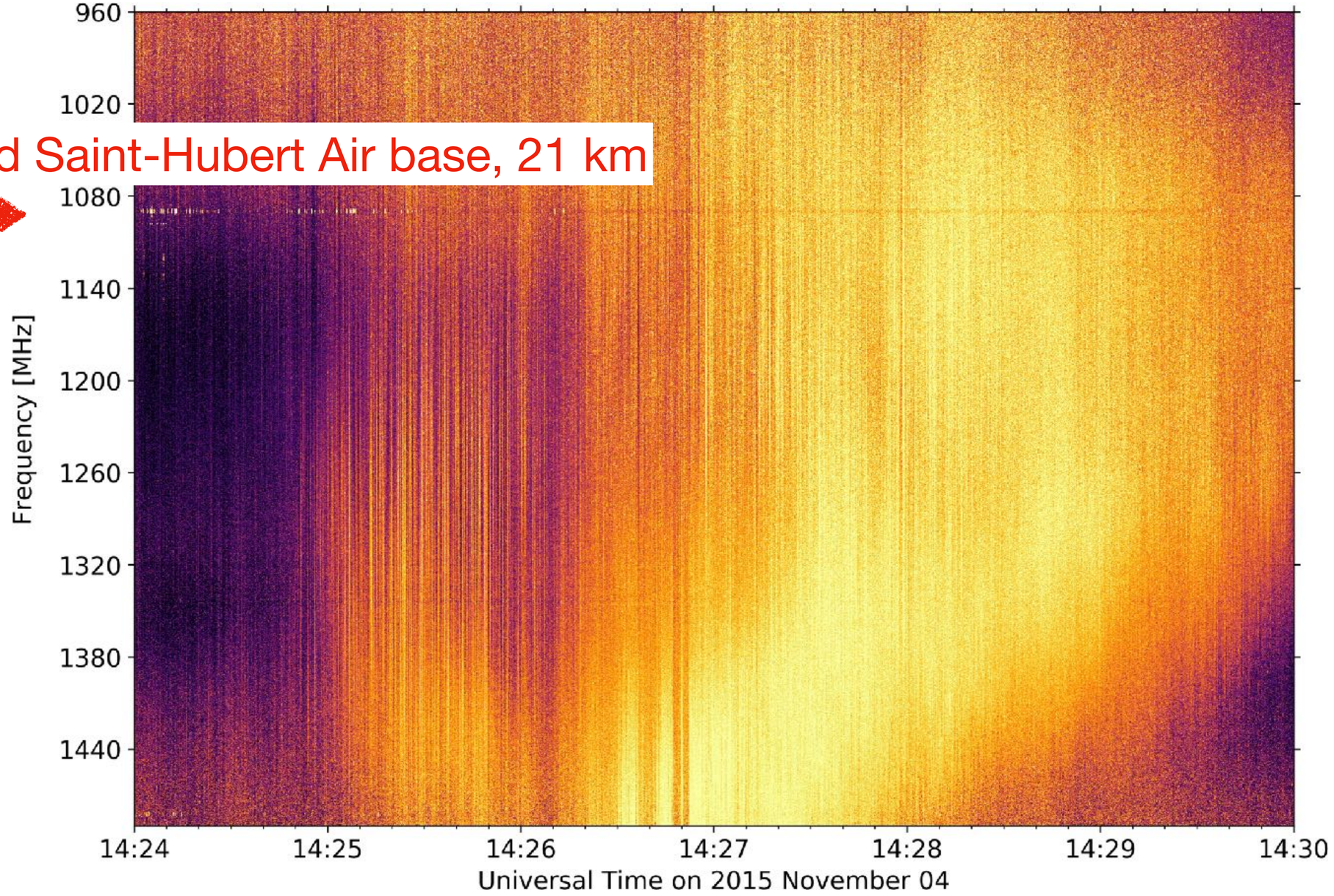

An exceptional event?

Strong magnitude

ORFEES (1000 MHz) 🇫🇷	100 kSFU
Blein (1000 – 1250 MHz) 🇨🇭	123 kSFU
Humain (1060 MHz) 🇧🇪	157 kSFU

But...

610 MHz 🇫🇷🇧🇪	820 - 1000 SFU
1415 – 1427 MHz 🇨🇭🇧🇪🇺🇸	5200 - 6300 SFU

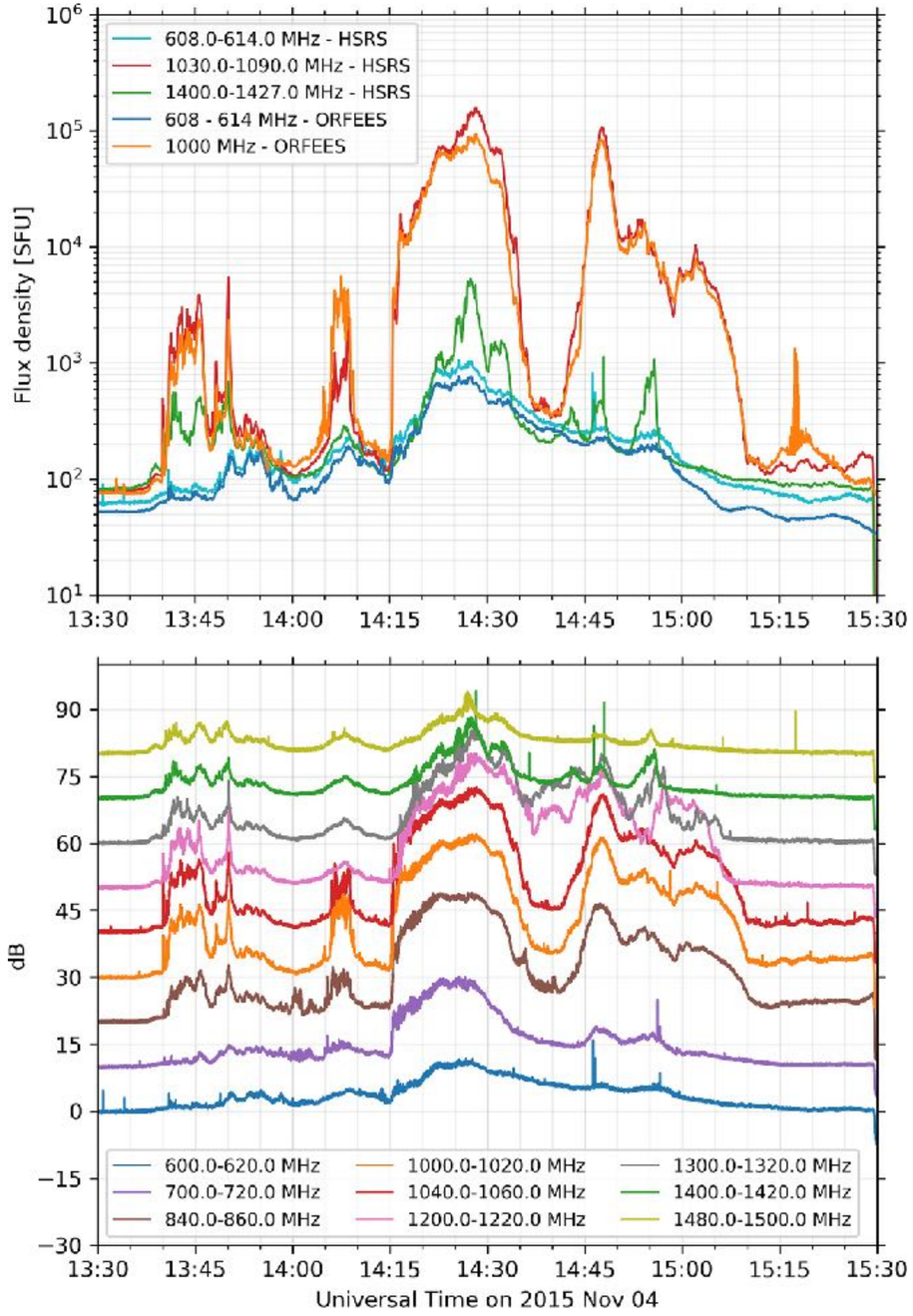

Interference threshold comparison

- The interference threshold for such radars is about **-102 dBm** (6,3 . 10^{-14} W) at receiver input.
- The quiet sun level on that day was about 75 SFU (75 . 10^{-22} $W.m^{-2}.Hz^{-1}$), which results in a power at receiver input of **-101 dBm**
- At the peak of the burst the Sun emission level was more than 100 000 SFU, which gives at least a power at receiver input of **-68 dBm**

34 dB above interference threshold (~ 2500 times that level)

So how vulnerable are we?

- Oldest radars are most at risk
  - Upgrades are planned
- Newer radars had the least disturbance
  - Better signal processing
- ARTAS tracker only partly cleaned this up
- Mode S on MSSR had minor influence
- New WAM system
  - Only small influence inside coverage area

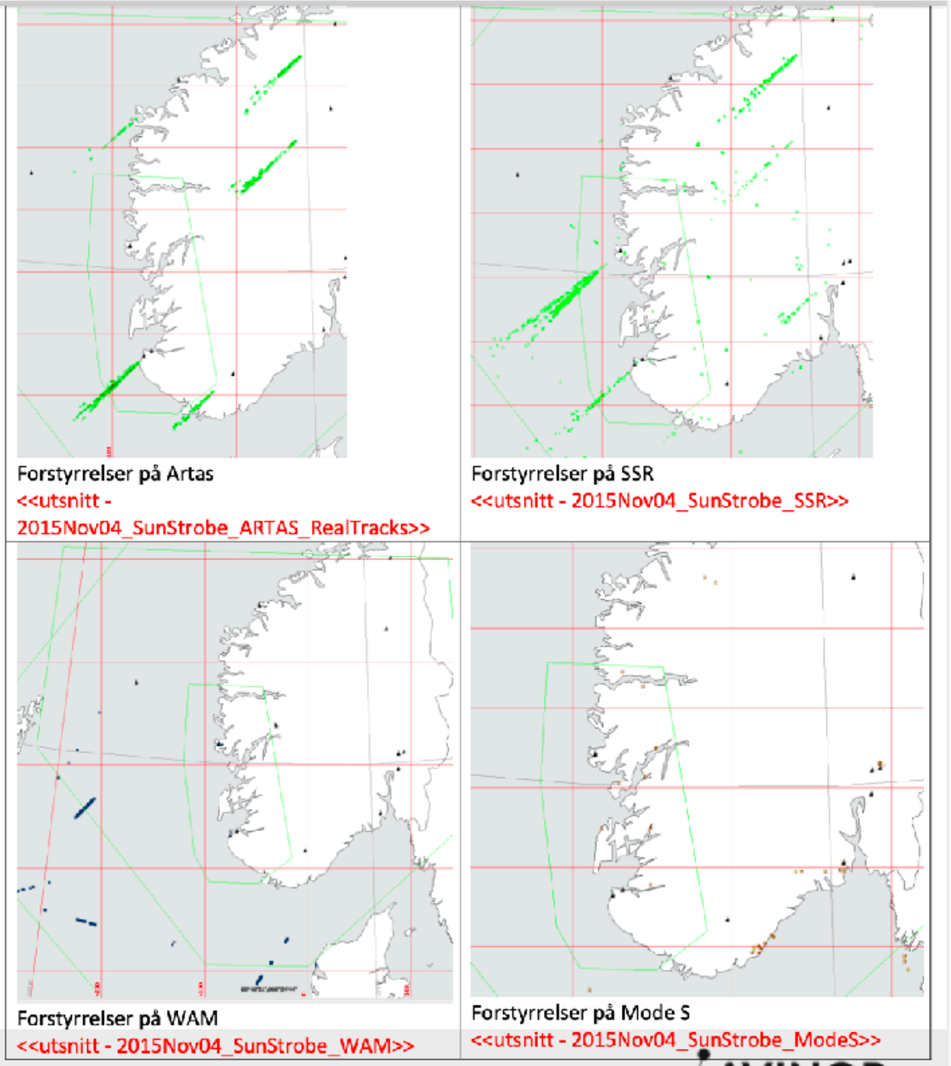

Forstyrrelser på Artas
<<utsnitt - 2015Nov04_SunStrobe_ARTAS_RealTracks>>

Forstyrrelser på SSR
<<utsnitt - 2015Nov04_SunStrobe_SSR>>

Forstyrrelser på WAM
<<utsnitt - 2015Nov04_SunStrobe_WAM>>

Forstyrrelser på Mode S
<<utsnitt - 2015Nov04_SunStrobe_ModeS>>

http://www.mn.uio.no/english/about/news-and-events/events/The%20Birkeland%20Anniversary/andreas-d-skjervold_150617.pdf

GNSS systems

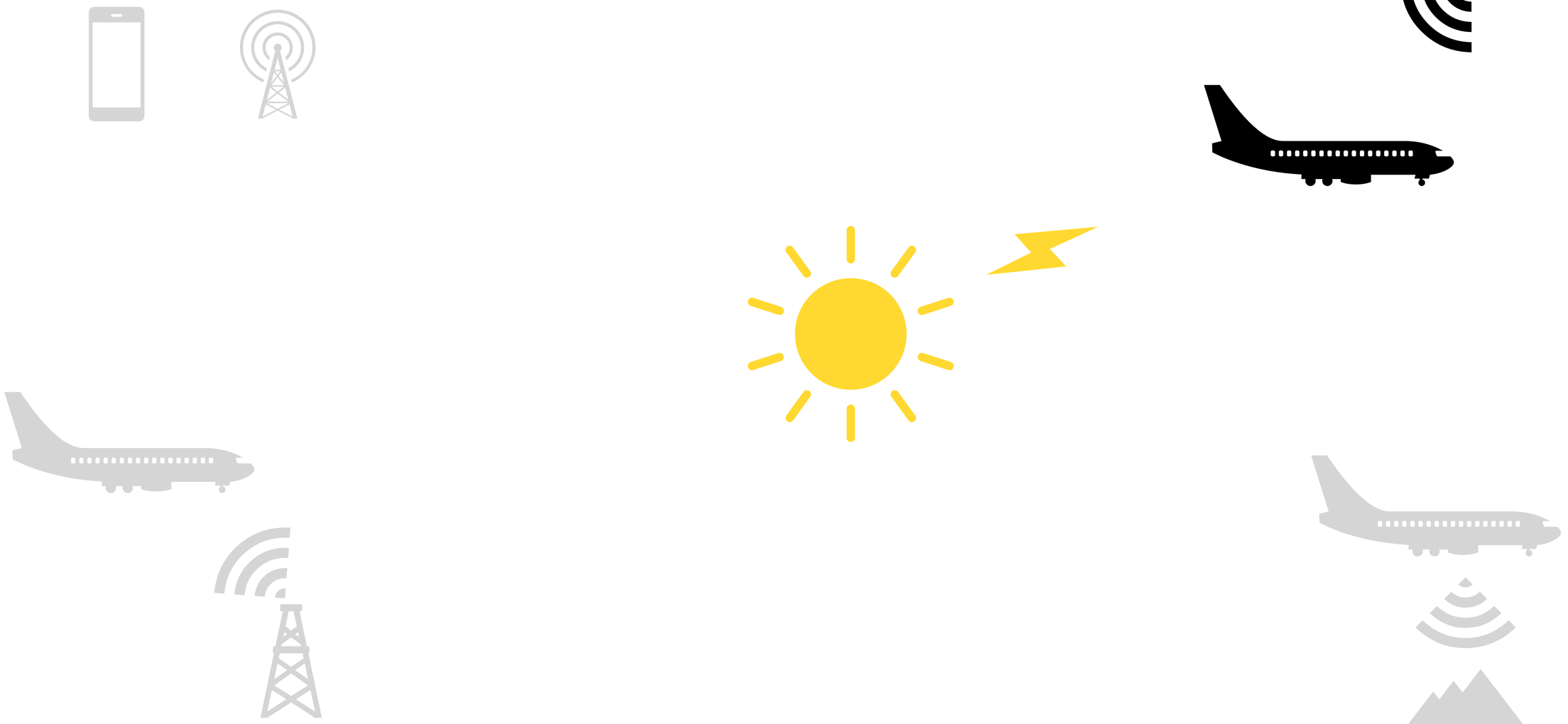

Interference Thresholds

- Change the level of noise, decrease in C/N0 ($\Delta C/N_0$)
- Decrease in C/N0 triggers loss of locks with satellites, decrease in positioning precision, etc..
- First report: September 2005 Cerruti et al., 2006
- Dec. 2006 event (Cerruti et al., 2008; Carrano et al., 2009; Demyanov et al. 2012)

Thresholds

L1 3dB	L2 3dB codeless	L1 3dB	L2 5.2 dB	L1 signal tracking fail	L2 signal tracking fail
20000 SFU	~8000 SFU	10000 SFU	10000 SFU	10000 SFU	4000 SFU
Klobuchar, 1999	Chen et al. 2005	Cerruti et al., 2006		Demyanov et al., 2012	

GNSS

24 September 2011

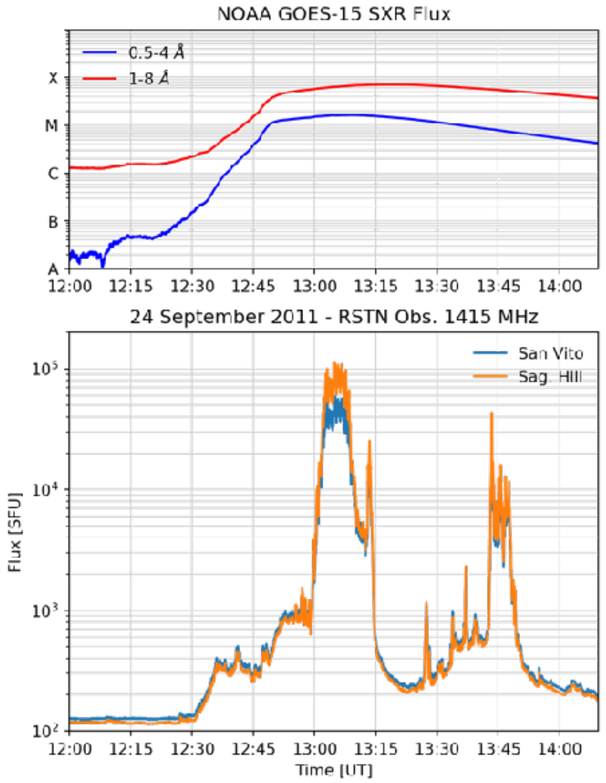

- M7.1 flare, max @ 13:20 UT
- AR 11302, Ekc, $\beta\gamma$
- ★110000 SFU @13:02 UT [Sag. Hill]
- ★60000 SFU [San Vito]
- Dm type IV burst (Bleien, Ondrejov)

C/N0 degradation

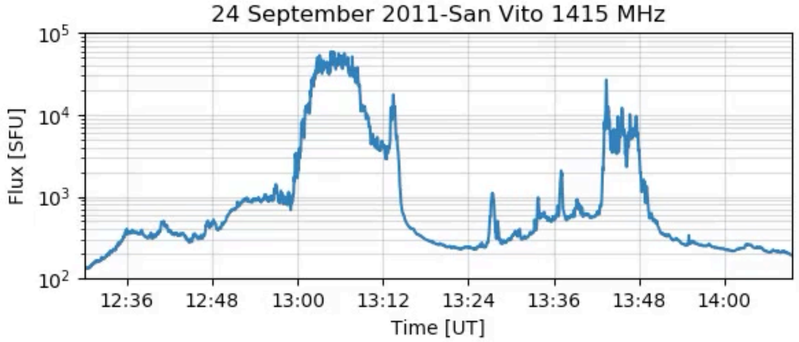

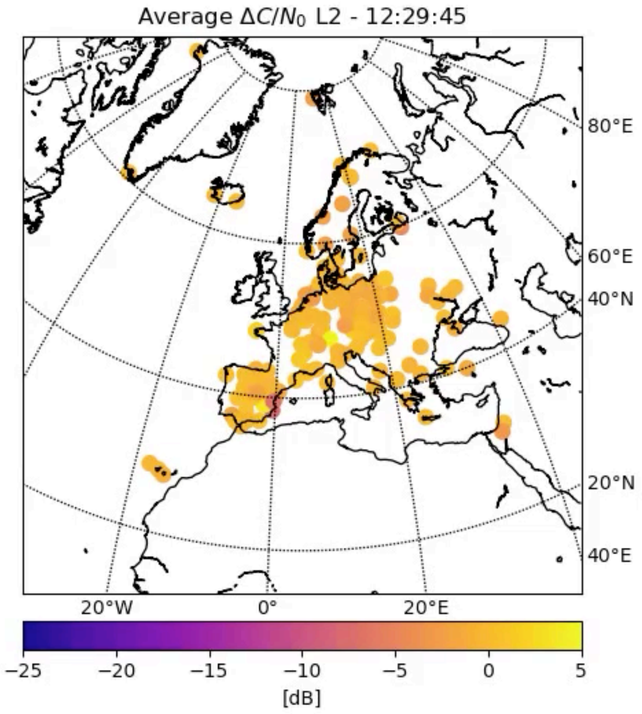

GNSS

24 September 2011

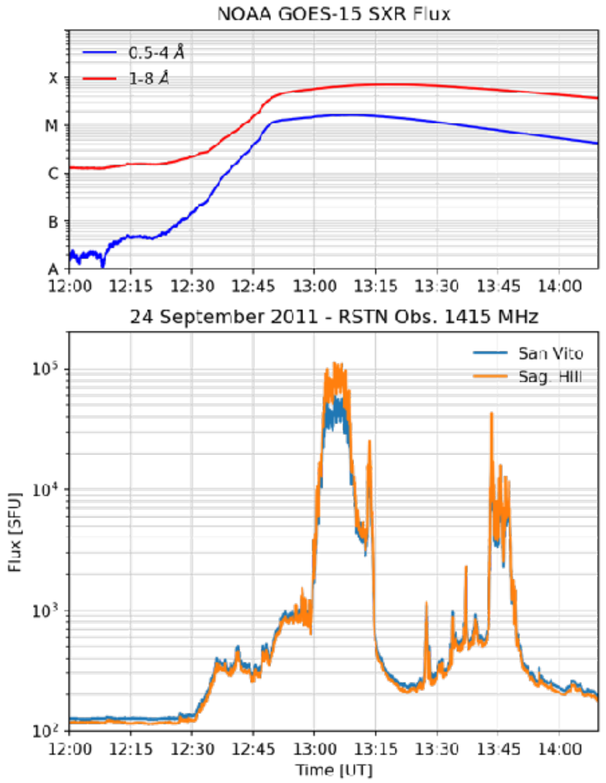

- M7.1 flare, max @ 13:20 UT
- AR 11302, Ekc, $\beta\gamma$
- ★110000 SFU @13:02 UT [Sag. Hill]
- ★60000 SFU [San Vito]
- Dm type IV burst (Bleien, Ondrejov)

C/N0 degradation

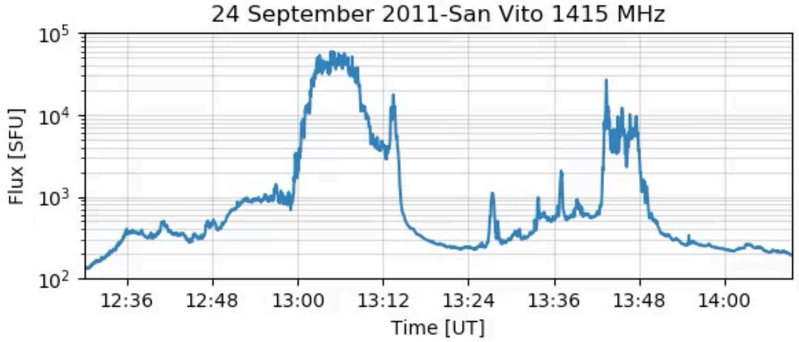

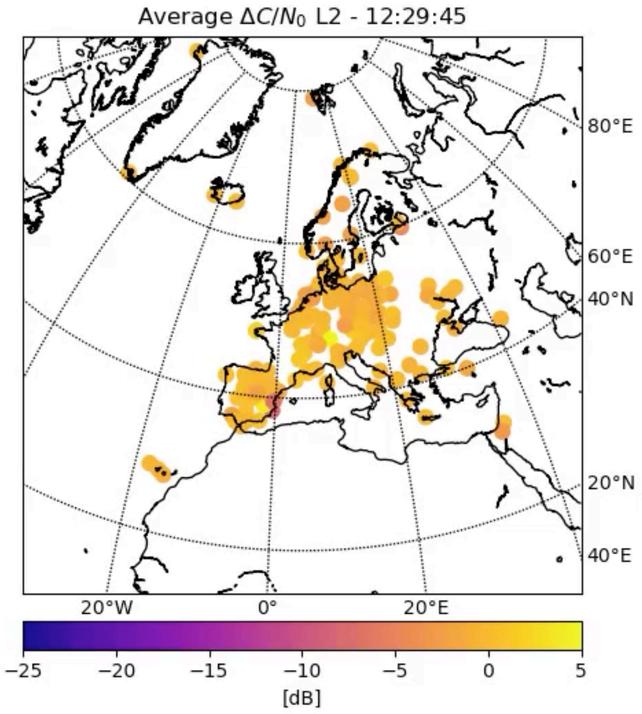

C/N0 DEGRADATION

L1 1575 MHz

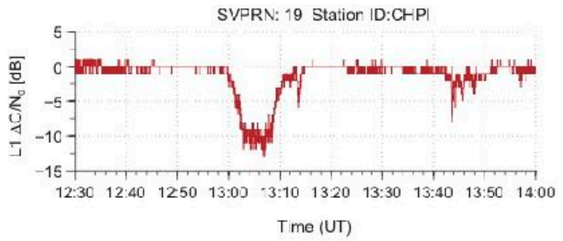

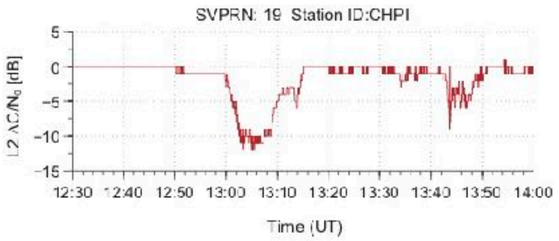

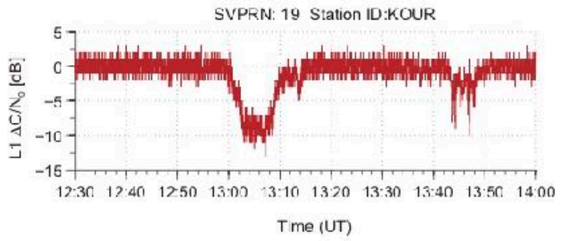

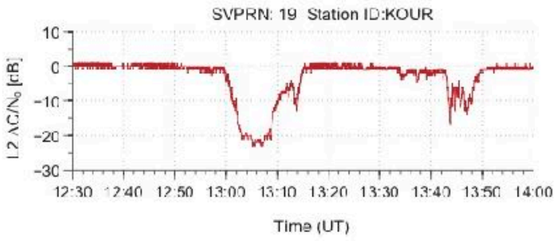

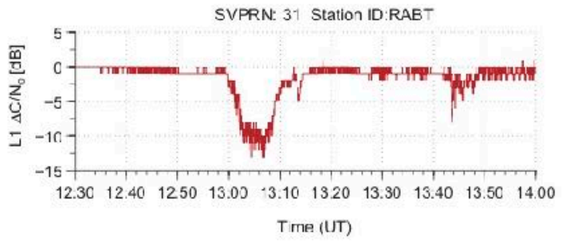

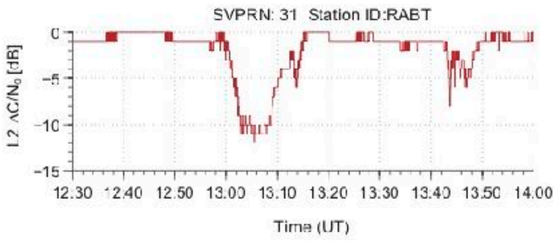

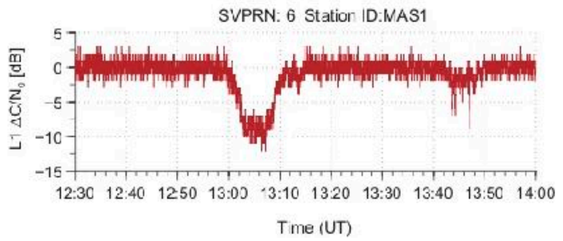

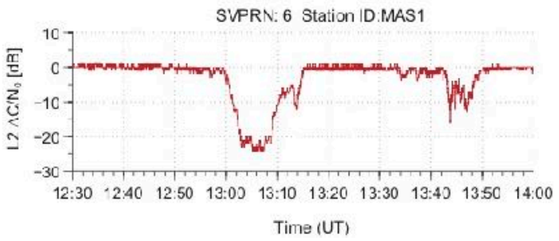

L2 1228 MHz

Muhammad et al., 2015

September 6 2017

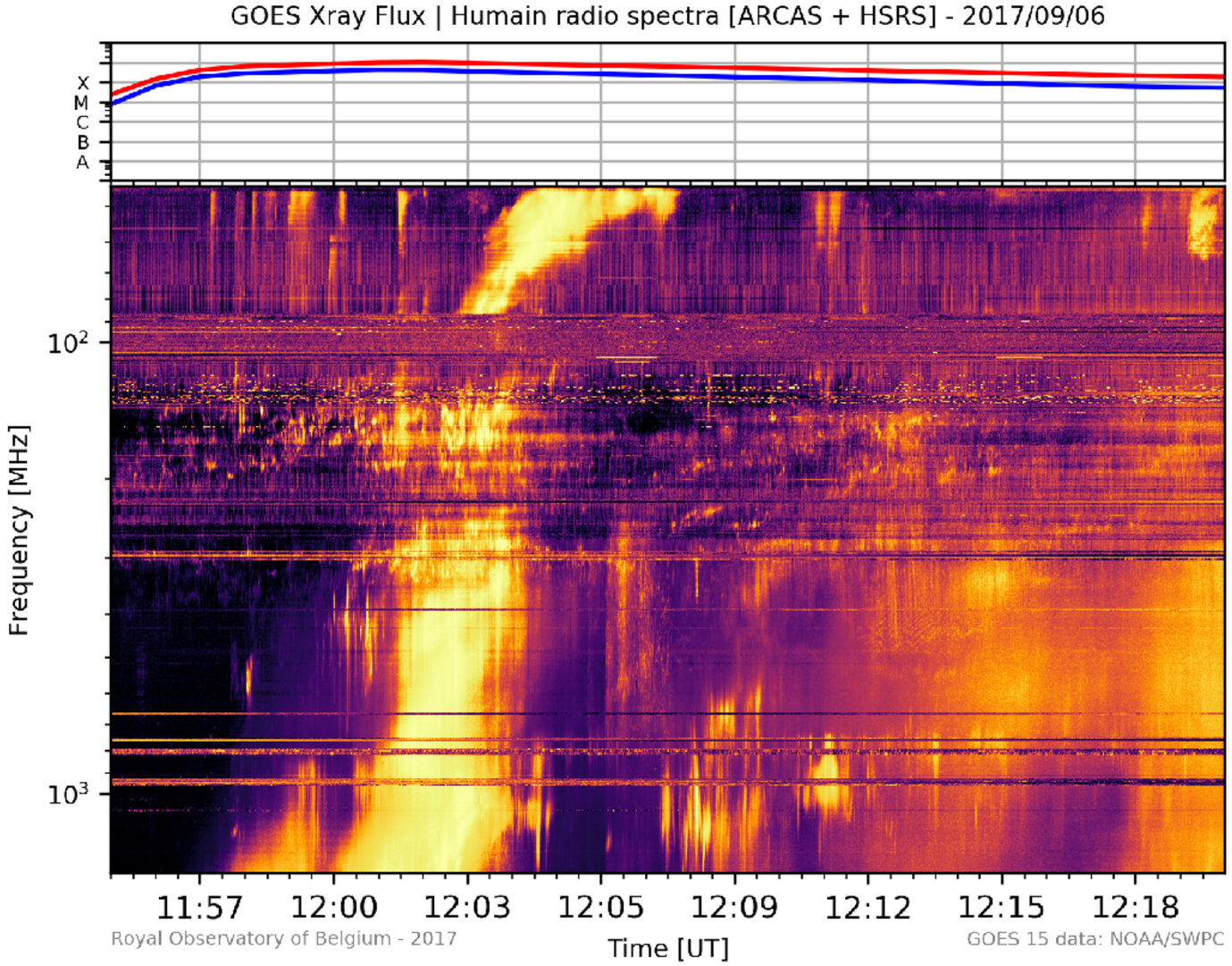

Flux density > 20 kSFU @ L2

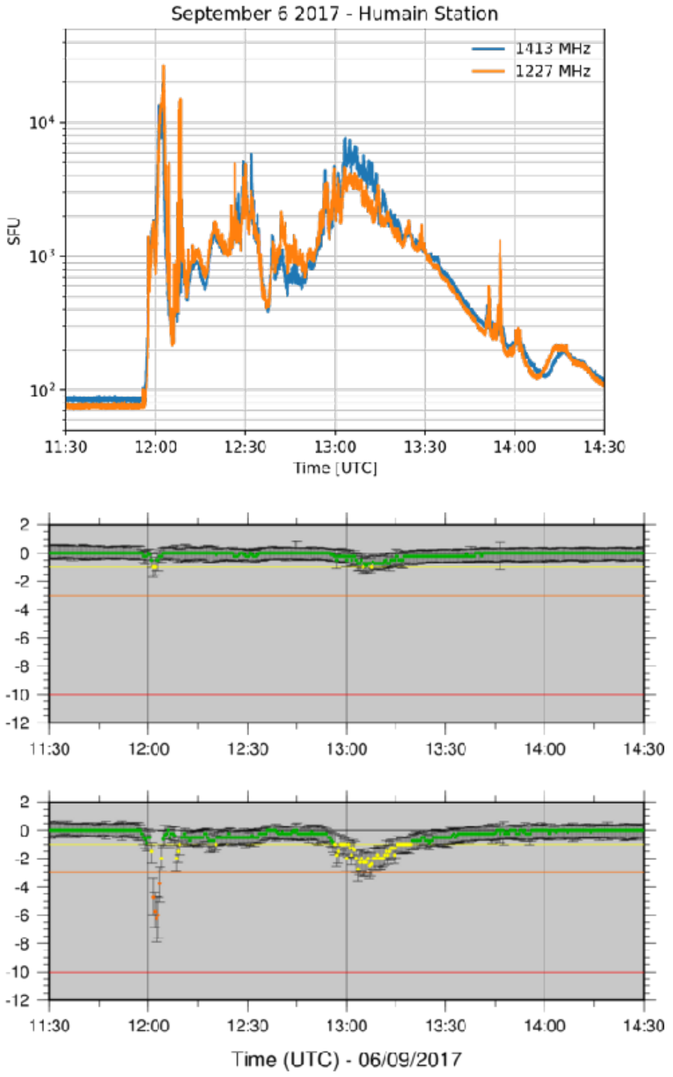

Complex dm type IV + fine structures

Chevalier & Bergeot

September 6 2017

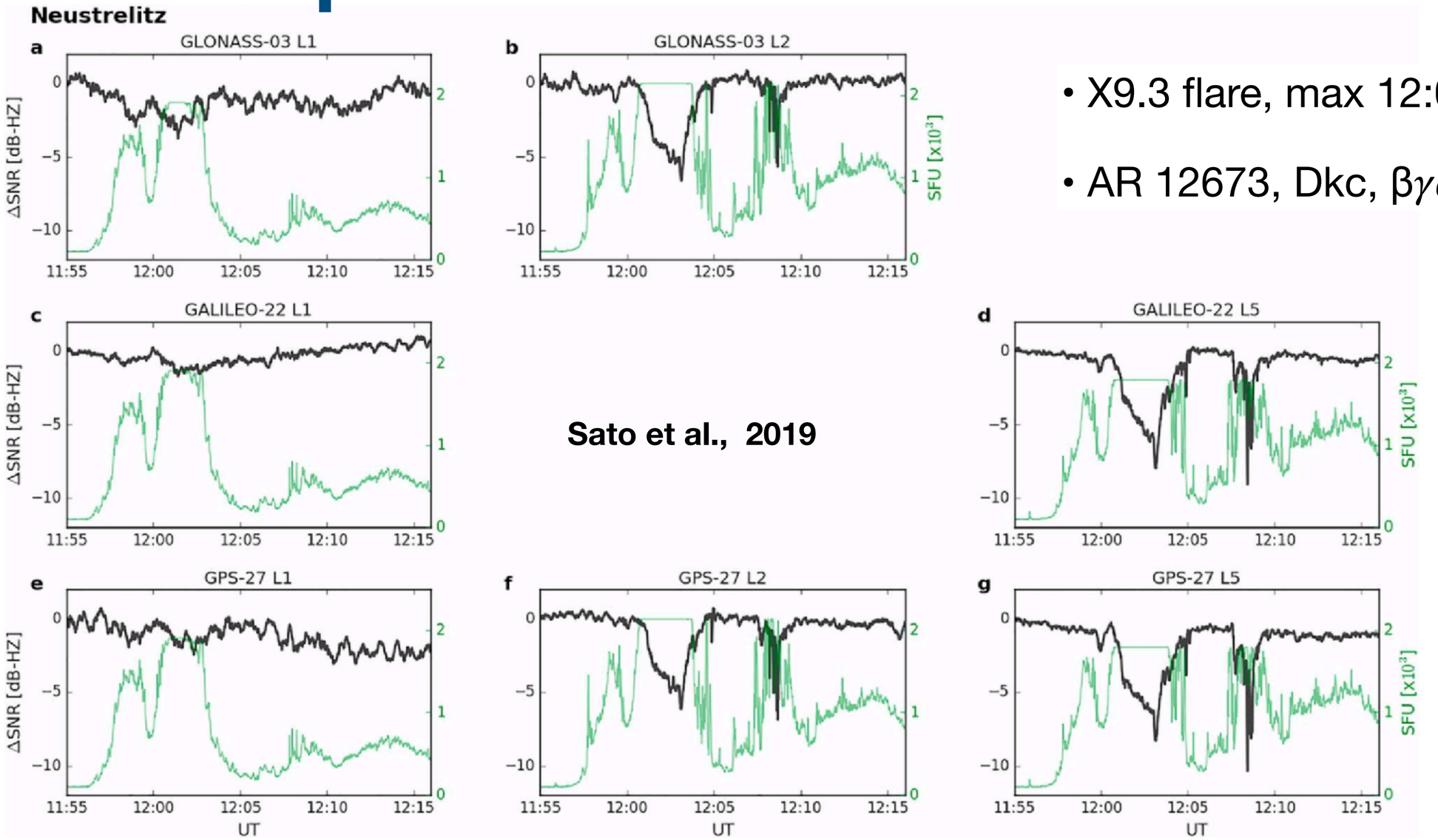

Sato et al., 2019

- X9.3 flare, max 12:02 UT
- AR 12673, Dkc, $\beta\gamma\delta$

Impact on WAAS/EGNOS systems

December 6 2006 event

- X6 flare producing an intense SRB (type IV) at 1415 MHz (10^6 SFU - RHCP)

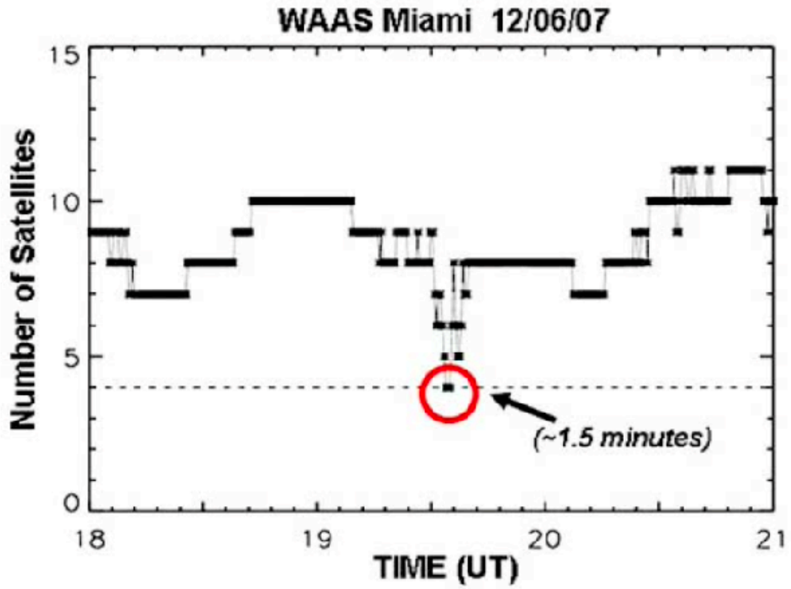

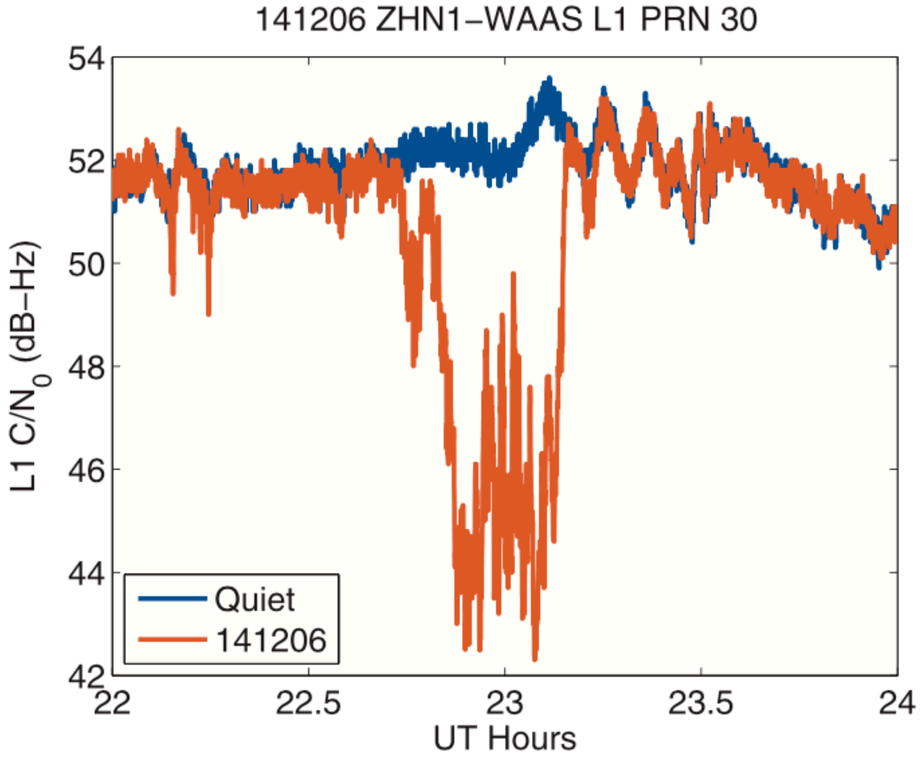

Cerruti et al., 2008

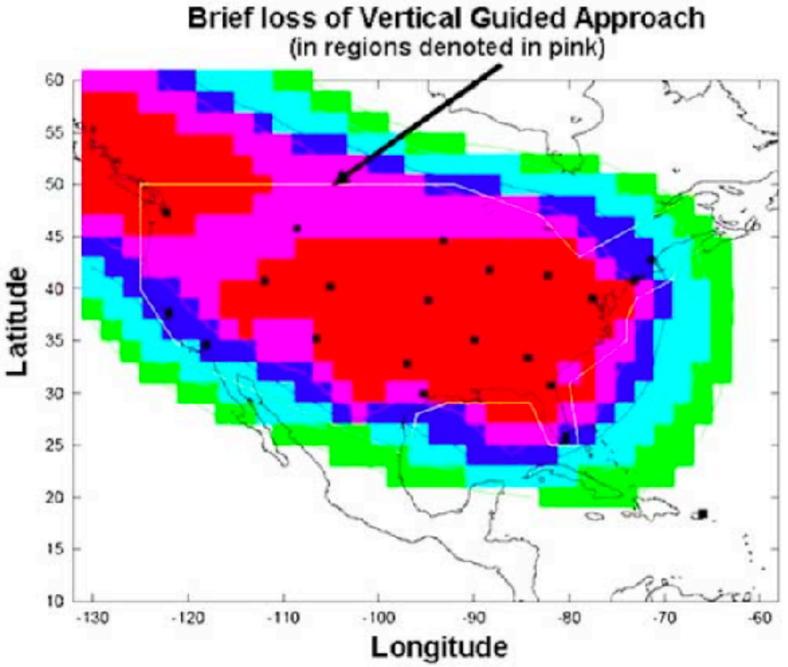

Radar altimeters

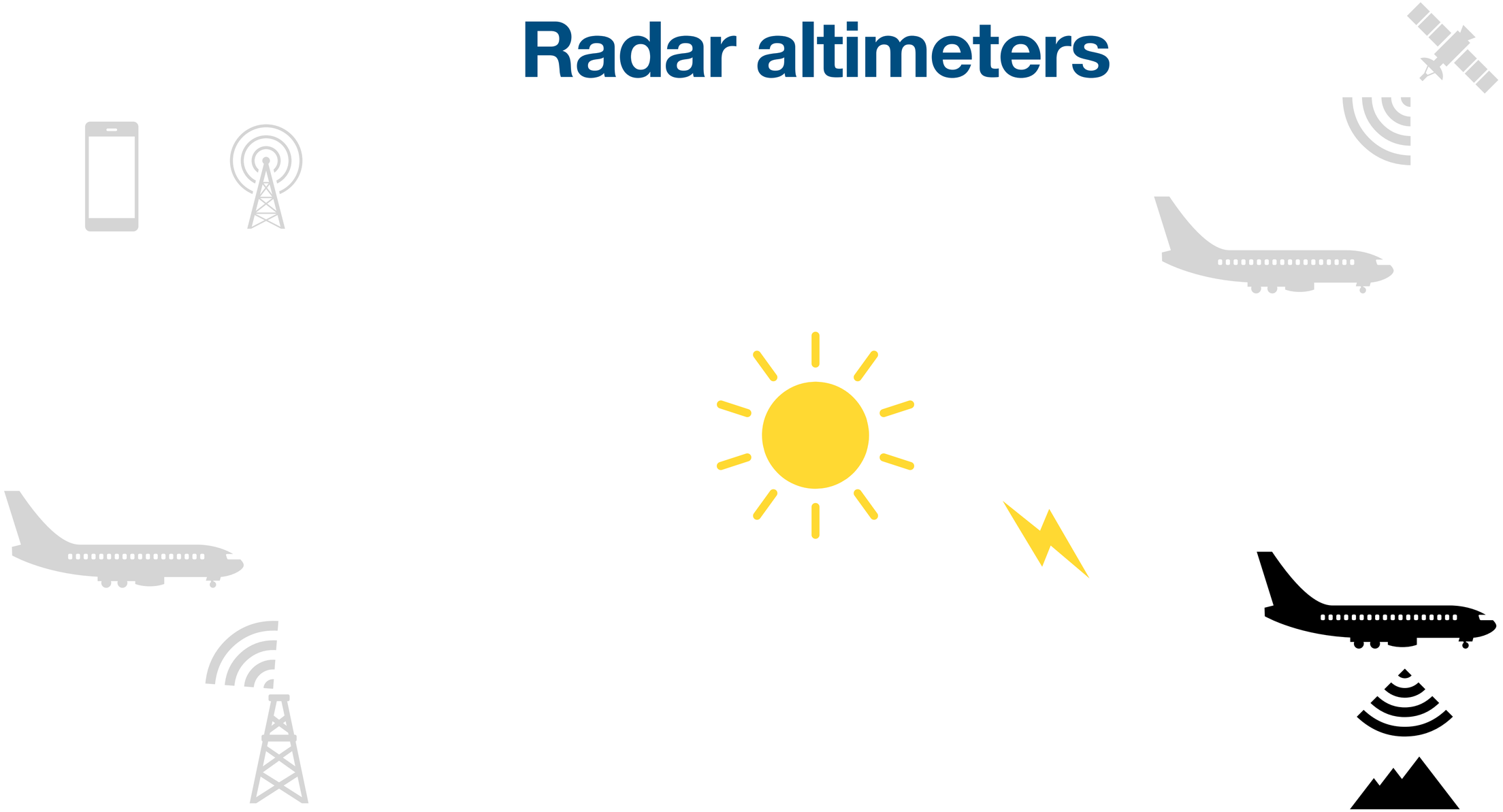

Radar altimeter

Estimated susceptibility

- Measurement of height Above Ground Level
- 4.2 - 4.4 GHz
- Devices on the plane belly

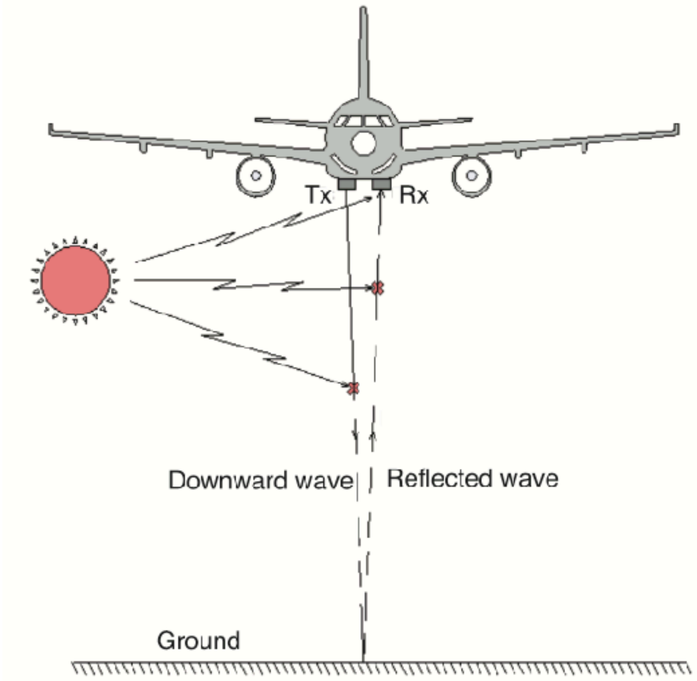

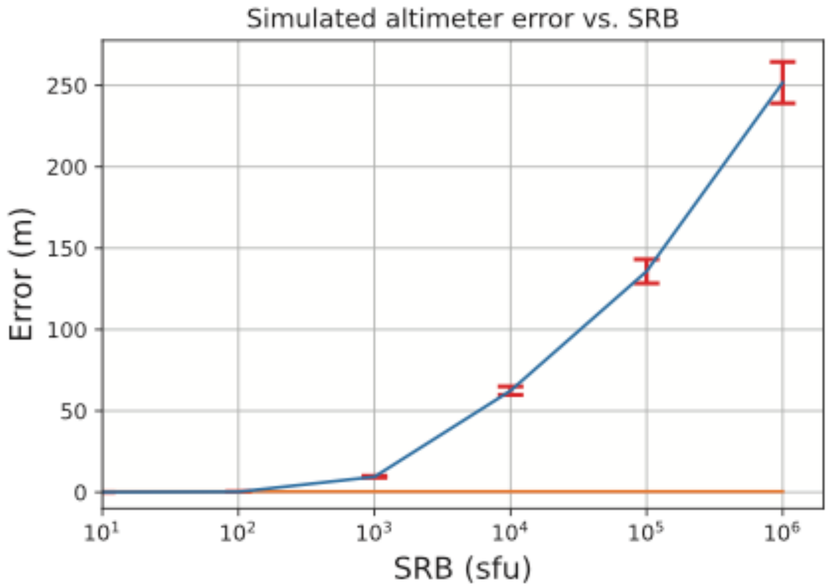

Mc Kee et al., 2023

Should we worry ?

TABLE 2

SINGLE FREQUENCY RADIO BURST MAXIMA 1956—PRESENT

Symbol	Observatory	Frequency MHz	Date	Peak Flux Units 10^{-22} W m^{-2} Hz^{-1}
A	Nagoya	1000	March 29, 1960	247000
B	Nagoya	2000	March 29, 1960	49000
C	Nagoya	3750	March 29, 1960	8250
D	Tokyo	9500	March 29, 1960	~ 25000*
E	Hollandia	545	March 29, 1960	~100000
F	Hollandia	200	March 29, 1960	38000
G	Nagoya	9400	February 23, 1956	31400†
H	Nagoya	9400	July 10, 1959	26500
I	Nagoya	9400	November 15, 1960	24000
J	Nagoya	3750	February 23, 1956	18000†
K	Nagoya	3750	April 5, 1960	14200
L	Nagoya	3750	November 15, 1960	11600
M	Nagoya	3750	September 3, 1960	12000
N	Nagoya	3750	September 15, 1960	8080
O	Nagoya	2000	November 11, 1960	9600
P	Tokyo	3000	September 3, 1960	5600
Q	Nagoya	1000	November 11, 1960	47000
R	Hollandia	545	July 14, 1959	40000
S	Hollandia	200	August 26, 1958	85000
T	Nagoya	1000	July 14, 1959	10600
U	Nagoya	1000	September 15, 1963	13800
V	Nagoya	1000	April 5, 1960	18000
W	Netherlands	200	April 8, 1959	~500000

* Estimated mean data

† See Kundu (1965) p. 201.

Castelli, 1968

Table 3. Peak flux densities in SFU for the strongest radio bursts since 2000 (peak flux greater than 50 000 SFU at 1415 MHz) tabulated by NOAA[i] (RSTN network at 1415 MHz) and by the Nobeyama Observatory[ii] (1000 and 2000 MHz)

Date	Flux at 1000 MHz	Flux at 1415 MHz	Flux at 2000 MHz
2001 April 15	N/A	54 000	N/A
2002 April 21	150 000	110 000	9000
2006 December 06	N/A	139 000[a b]	N/A
2006 December 13	440 000	130 000[a]	302 000
2006 December 14	N/A	55 600	N/A
2011 February 15	46 000	54 000	1500
2011 September 24	N/A	110 000	N/A
2012 March 05	502 000	20 000[c]	19 000

(i) ftp://ftp.swpc.noaa.gov/pub/warehouse/

(ii) http://solar.nro.nao.ac.jp/norp/index.html (a) Saturation limit (b) Cliver et al. (2011) report for that event a peak flux density of ~ 10^6 SFU from OVSA observations between 1 and 1.6 GHz (c) End of observations at peak flux; probably underestimated

Our own study, 2018

Impact of SRBs

- Long duration and intense radio bursts (type IV) are to be monitored
- ATC radar and GNSS (WAAS/EGNOS) systems used by the aviation industry are susceptible to interferences from Solar Radio Bursts
- Radar altimeters may be susceptible
- These systems may be degraded during critical parts of flights (landing, traffic around airports etc...)
- Communication services are also susceptible to be interfered with (we would like to hear from users !)
- Awareness of operators and pilots is critical

Antenna & telescopes

Gain and radiation pattern

- Isotropic antenna: a perfect antenna that would radiate (or received) equally in all directions ($4\pi\ sr$)
- A real antenna radiates in a preferential direction determined by its geometry and electrical properties ($\Omega\ sr$)
- Its gain is: $G = \frac{4\pi}{\Omega}$

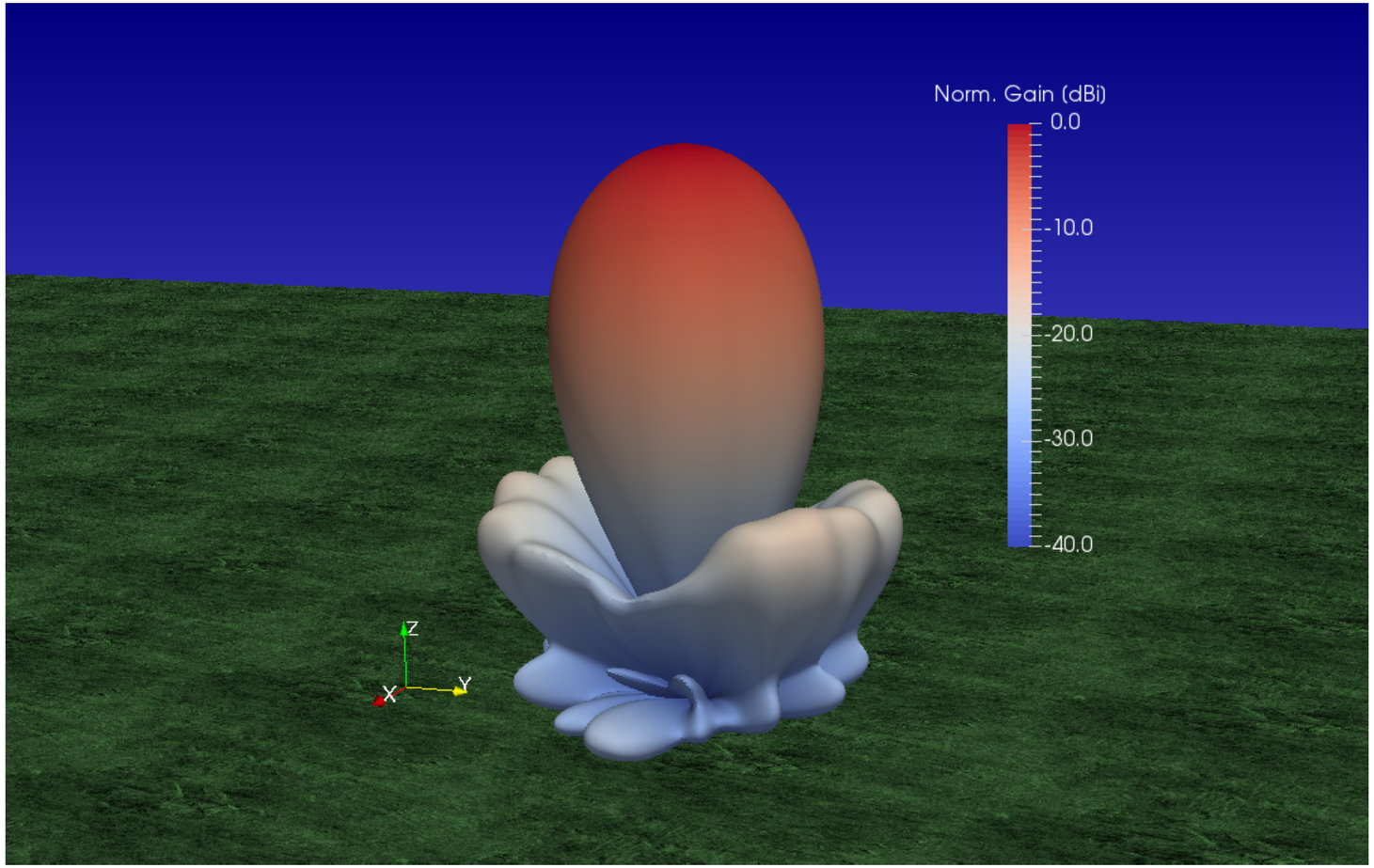

Martinez, A.

We define the efficient area: $A_{eff} = \frac{G\lambda^2}{4\pi} \approx Aperture$

Dipole antenna

- Detection of the Electric component of the E.M Wave
- Half-wave dipole : tuned to a given frequency
- Resonant element

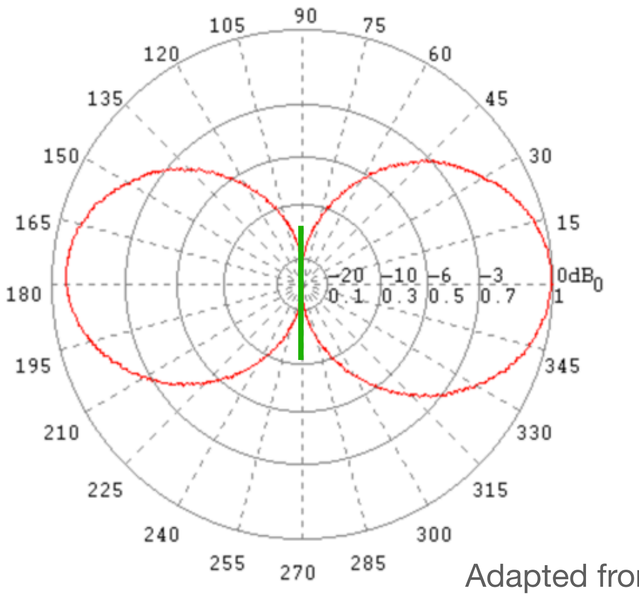

Adapted from Schwarsbeck

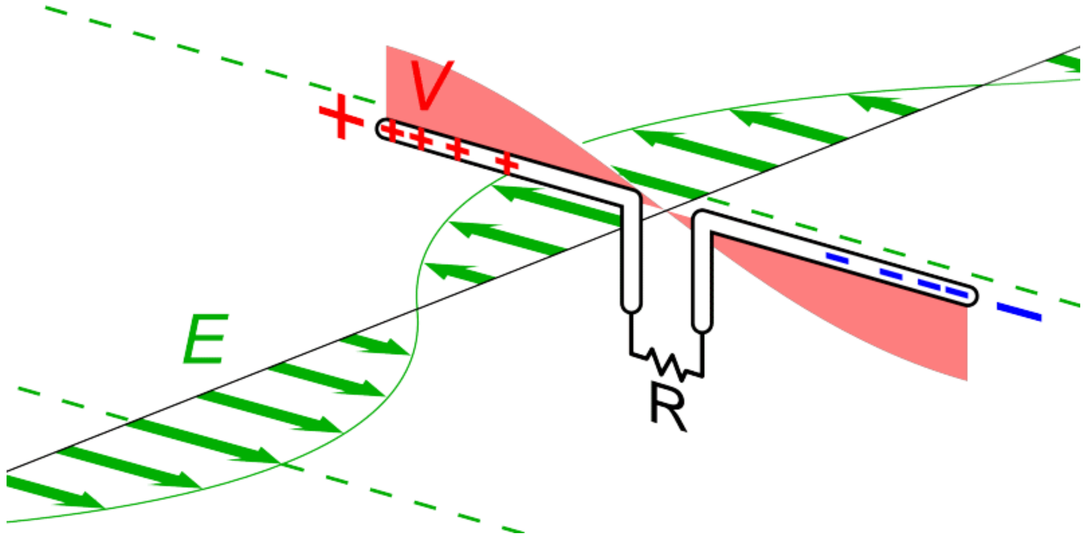

Wikipedia

Dipole antenna

- Detection of the Electric component of the E.M Wave
- Half-wave dipole : tuned to a given frequency
- Resonant element

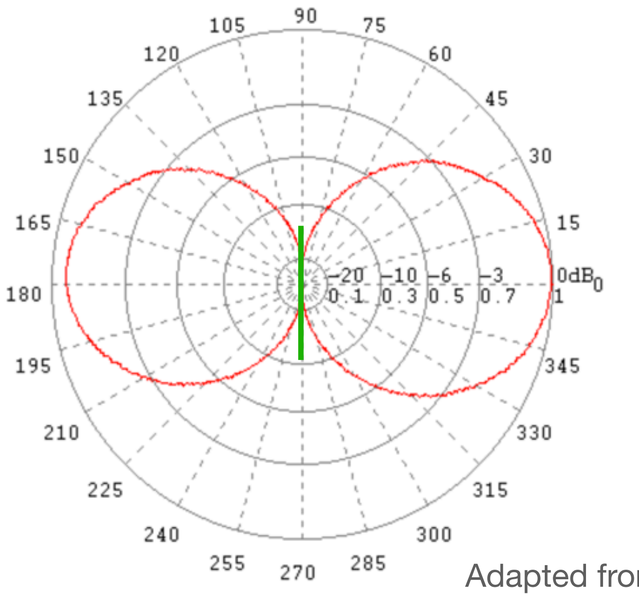

Adapted from Schwarsbeck

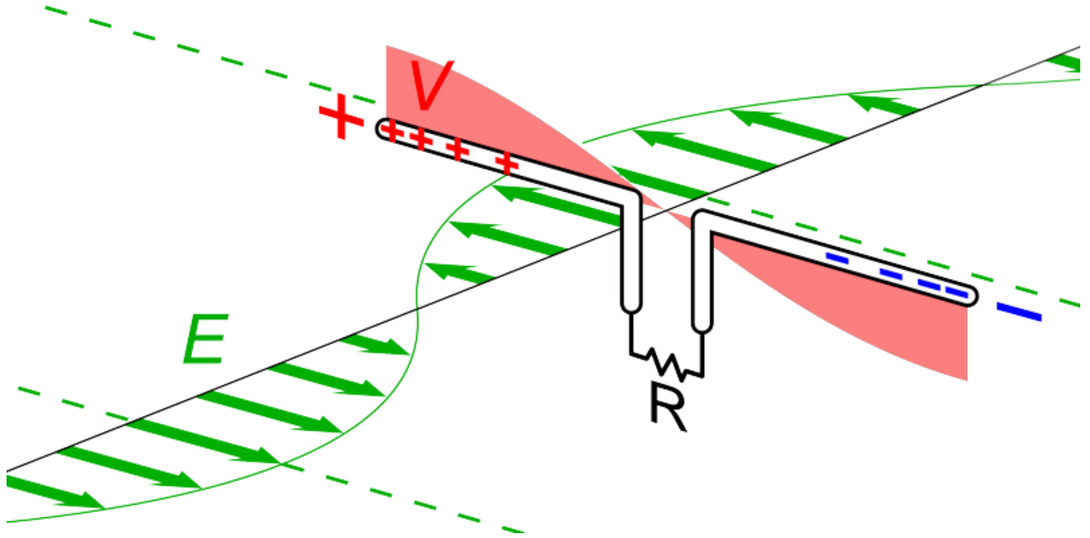

Wikipedia

Yagi antenna

- One “active” element
- Passive elements drive waves interfering additively forward and destructively backward
- Tuned for one frequency



Martinez, A.

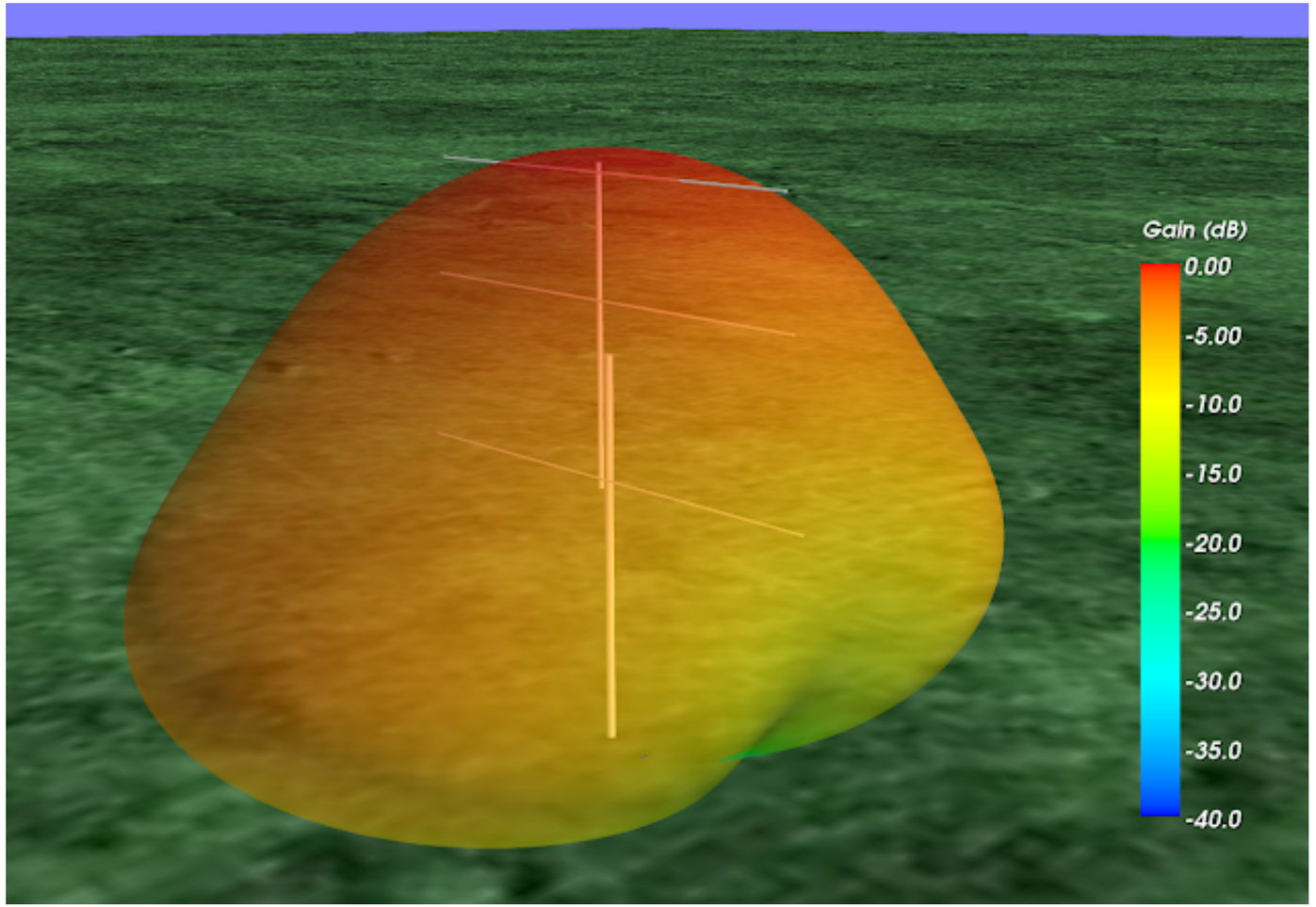

Logperiodic antenna

- All elements “actives”
- successive elements connected out-of-phase
- Constructive interferences forward
- “Flat” gain & broadband



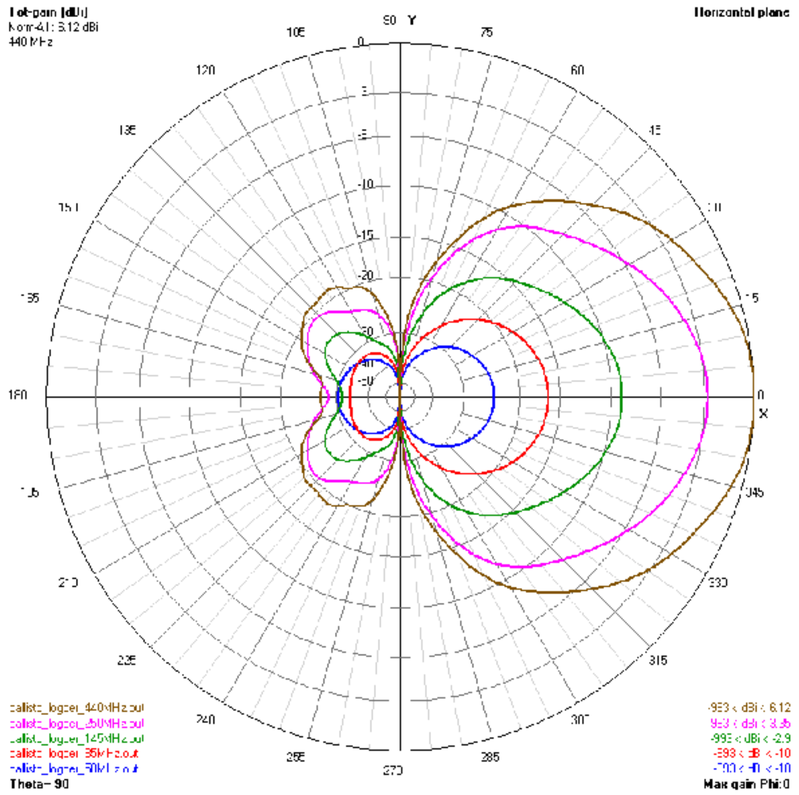

Adapted from Schwarzbeck

Horn antenna

- Provide a “soft” transition between free-space electrical conditions to the ones of wave guide and electronics
- Radiation characteristics can be easily (analytically) calculated
- High gain and lower side lobes
- Used as feed systems and absolute calibration system

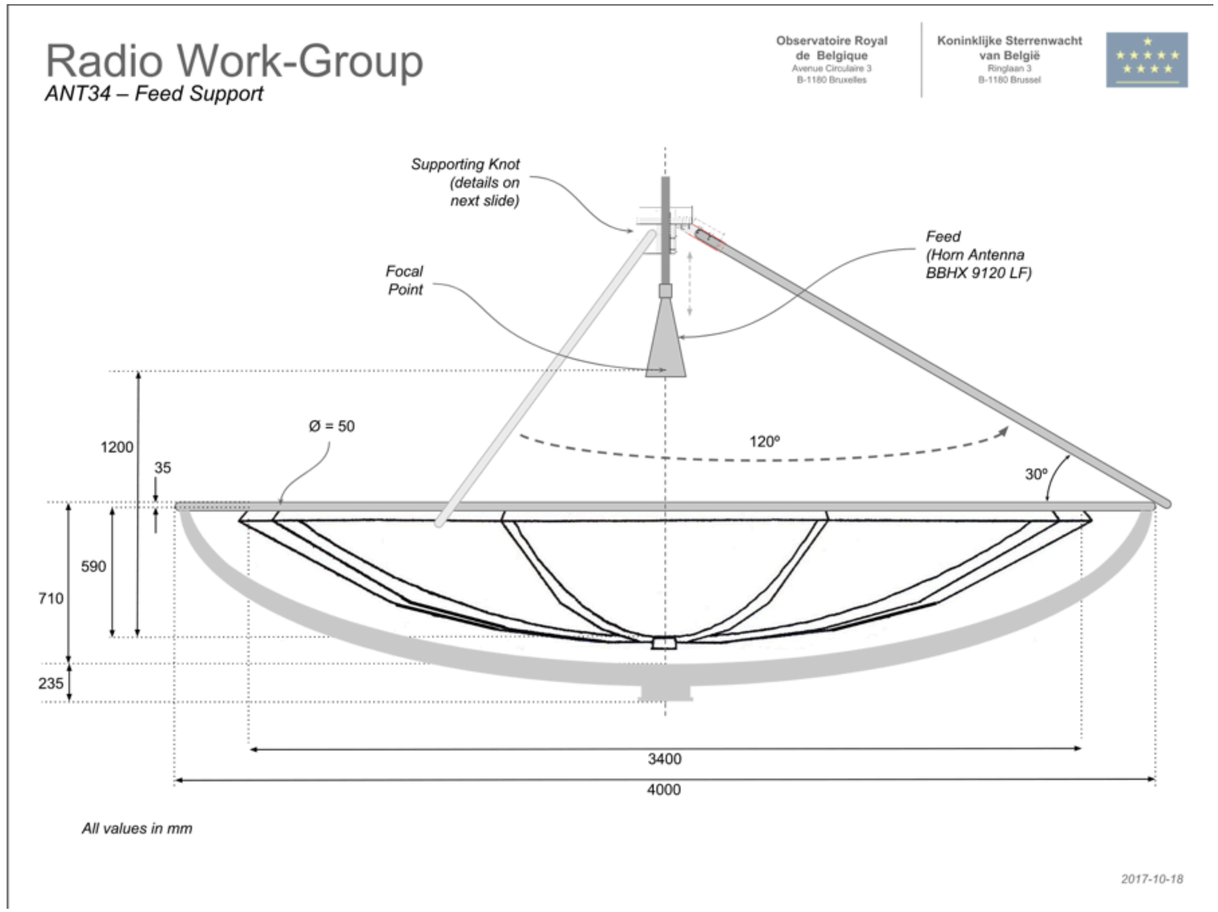

Solar telescopes

- Beam width $\sim 70° \frac{\lambda}{D}$

- Flux and spectral monitoring are made with small instruments that see the full Sun (30')

- Analogy with optical telescopes: parabolic prime mirror, focal plane

- Mirror can be plain or mesh (λ/10 rule)

- Compromise between mirror size, beam size and heat load (e.g. ALMA test antenna sub reflector heat up to 100 C during solar observation)

Tapping, K.





Marqué, C.



Kennewell, J.

Solar telescopes

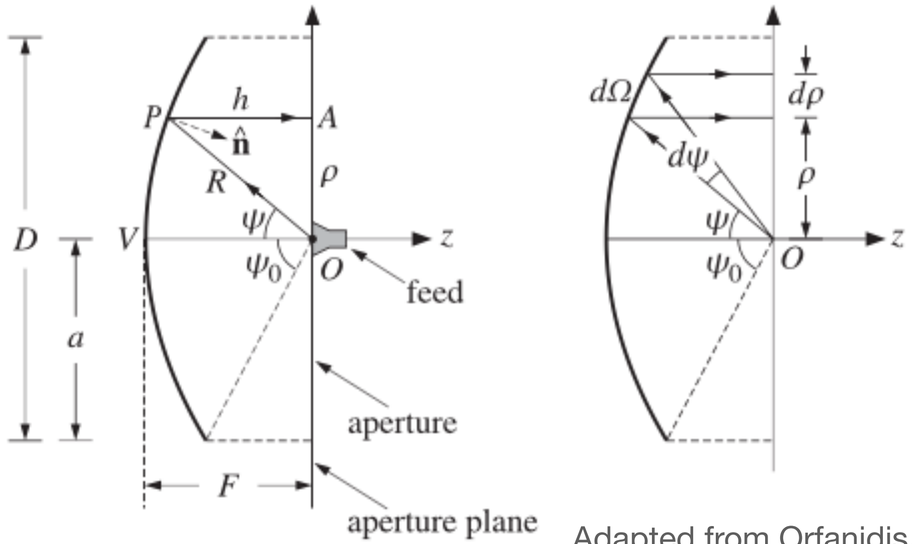

Adapted from Orfanidis, S. J.

Beam width

$$70\frac{\lambda}{D} = 70 \times \frac{0.1}{3.6} = 1.94\ ^\circ$$

Gain

$$0.6 \times \frac{3.14^2 \times 3.6^2}{0.1^2} \approx 12800 \approx 38.8\ dB$$

Gain of parabola :

$$G = \eta\frac{4\pi A}{\lambda^2}$$

where eta is a factor ~0.6, accounts for illumination, edge effects, spill over…

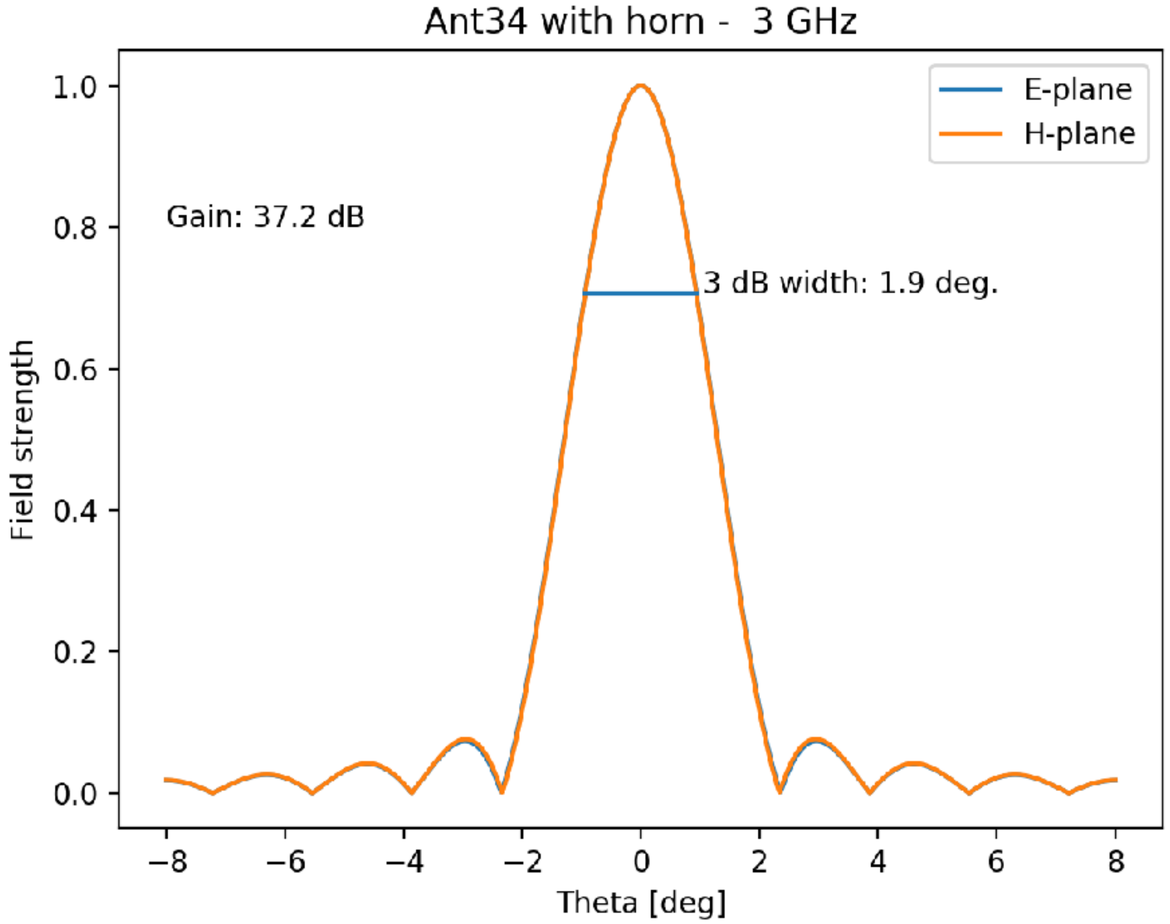

Receiving systems

What do we measure?

- Output of receiver is a power (W)
- Radio astronomers use the concept of temperature:

$$T = \frac{P_\nu[W/Hz]}{k[J/K]}$$

Measured power is:

$$T_{meas} = T_{ant} + T_{sys}$$

with

$$T_{ant} = T_{sun} + T_{sky} + T_{atm} + T_{ground} + \ldots$$

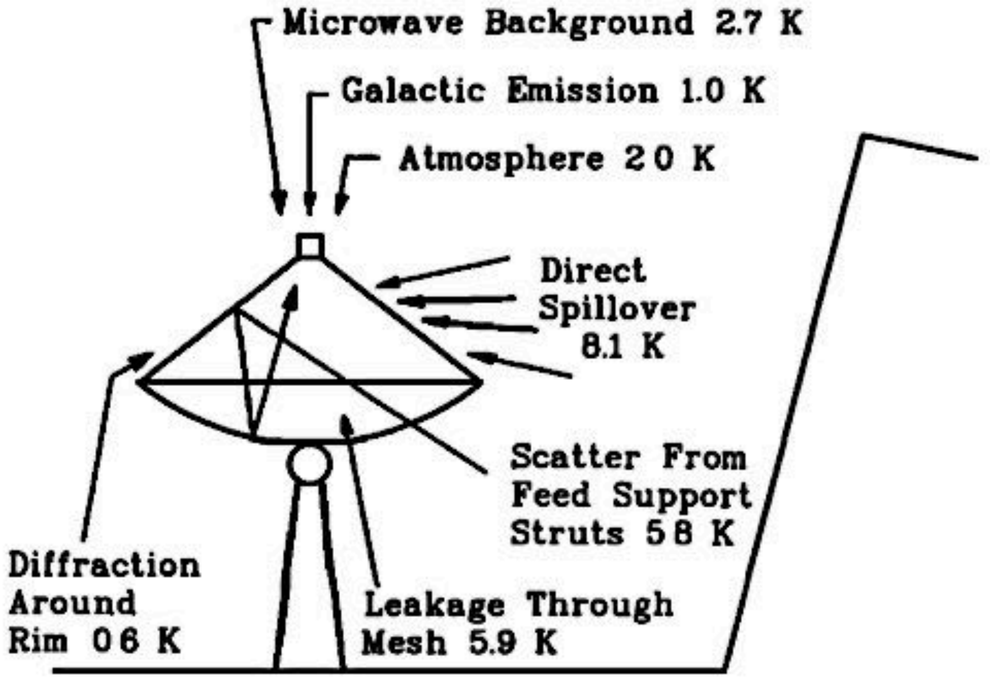

Fig. 5. Pictorial representation of the contributions to antenna temperature.

Anderson et al. 1991

From power to flux density

- One of the solar activity parameters is the Sun's flux density $S_\nu[W\,.\,m^{-2}\,.\,Hz^{-1}]$
- 1 Solar Flux Unit (SFU) = $10^{-22}W\,.\,m^{-2}\,.\,Hz^{-1}$
- We measure a Power density $P_\nu[W\,.\,Hz^{-1}]$

$$P_\nu = \frac{1}{2}A_{eff}S_\nu \quad \Rightarrow \quad S_\nu = \frac{2P_\nu}{A_{eff}} = \frac{2kT_{sun}}{G\lambda^2} \times 4\pi = \frac{2kT_{sun}}{\lambda^2} \times \Omega$$

System noise

Receiving chain is made of:

amplifiers, filters, attenuators, couplers, mixers, cables

Each contributes to add extra noise.

Total contribution is calculated with

the Friis formula

Example in Humain (6-m telescope)

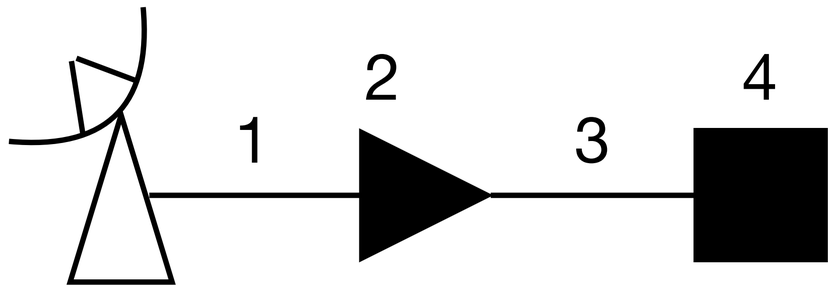

(1) (3), cables with attenuation L,
(2) Amplifier, with gain G, and noise figure NF, (4) receiver, with noise figure NF

$$T_{sys} = T_1 + L_1 T_2 + \frac{L_1}{G_2} T_3 + \frac{L_1 L_3}{G_2} T_4$$

$$T_{1,3} = (L_{1,3} - 1) T_0 \qquad T_{2,4} = (NF_{2,4} - 1) T_0 \qquad T_0 \approx 290\ K$$

Example: 04-11-2015 1415 MHz

$$T_{track} = \alpha T_{off}$$

$$T_{track} = T_{sun} + T_{sky} + T_{sys}$$

$$T_{off} = T'_{sky} + T_{sys}$$

$$T_{sun} = \alpha \times (T'_{sky} + T_{sys}) - (T_{sky} + T_{sys})$$

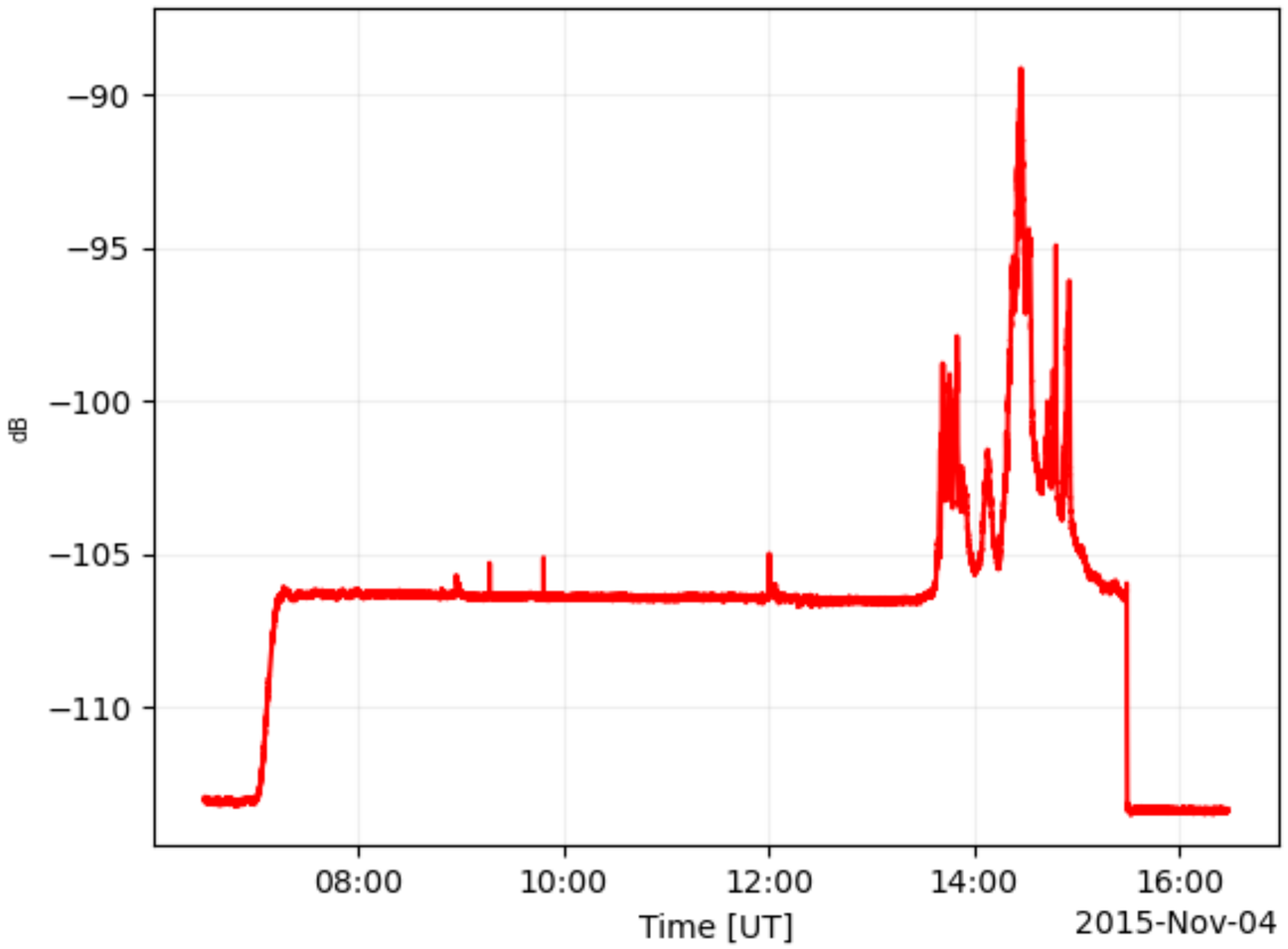

Example: 04-11-2015 1415 MHz

$$T_{track} = \alpha T_{off}$$

$$T_{track} = T_{sun} + T_{sky} + T_{sys}$$

$$T_{off} = T'_{sky} + T_{sys}$$

$$T_{sun} = \alpha \times (T'_{sky} + T_{sys}) - (T_{sky} + T_{sys})$$

$$M_{track} = -106.49\ dB$$

$$M_{off} = -113.38\ dB$$

$$T_{sys} = 1516\ K \quad T_{sky} = 3\ K$$

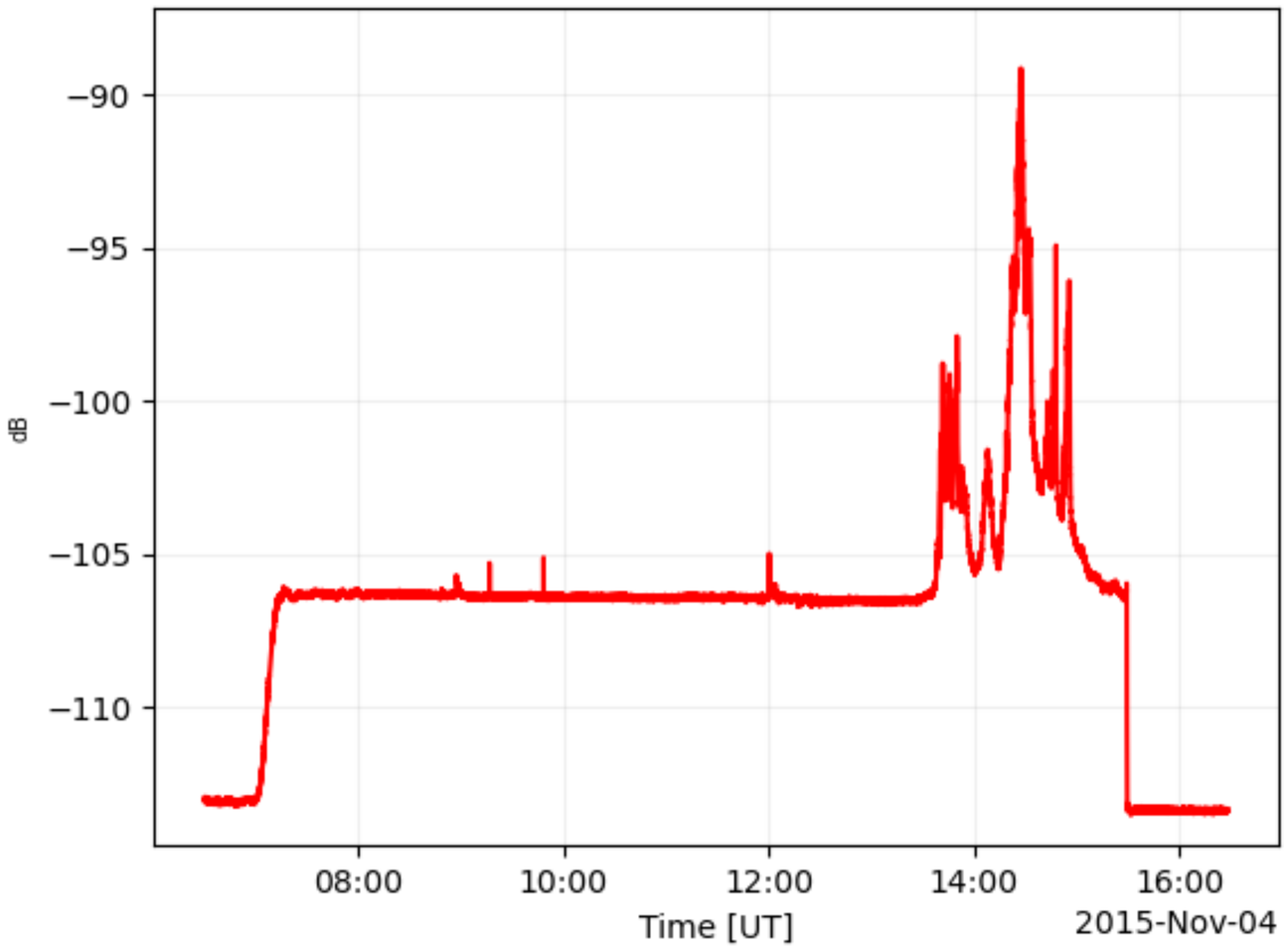

Example: 04-11-2015 1415 MHz

$$T_{track} = \alpha T_{off}$$

$$T_{track} = T_{sun} + T_{sky} + T_{sys}$$

$$T_{off} = T'_{sky} + T_{sys}$$

$$T_{sun} = \alpha \times (T'_{sky} + T_{sys}) - (T_{sky} + T_{sys})$$

$M_{track} = -106.49\ dB$

$M_{off} = -113.38\ dB$

$T_{sys} = 1516\ K \quad T_{sky} = 3\ K$

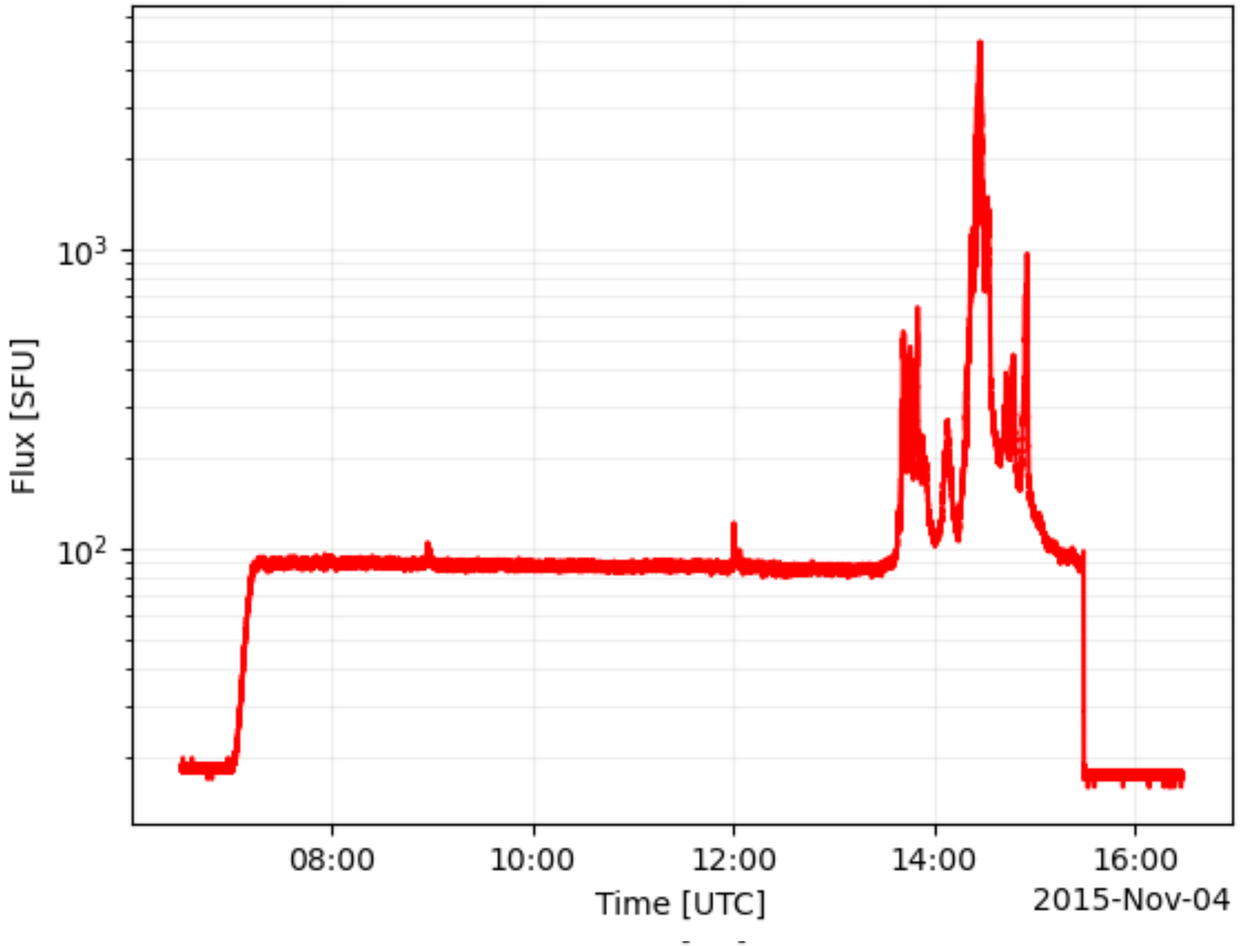

$\alpha = 4.88 \quad T_{sun} = 5905\ K \quad S_{\nu} = 87\ SFU \quad S_{\nu,peak} = 4900\ SFU$

The radio astronomy station of Humain

Humain station



Users of Humain

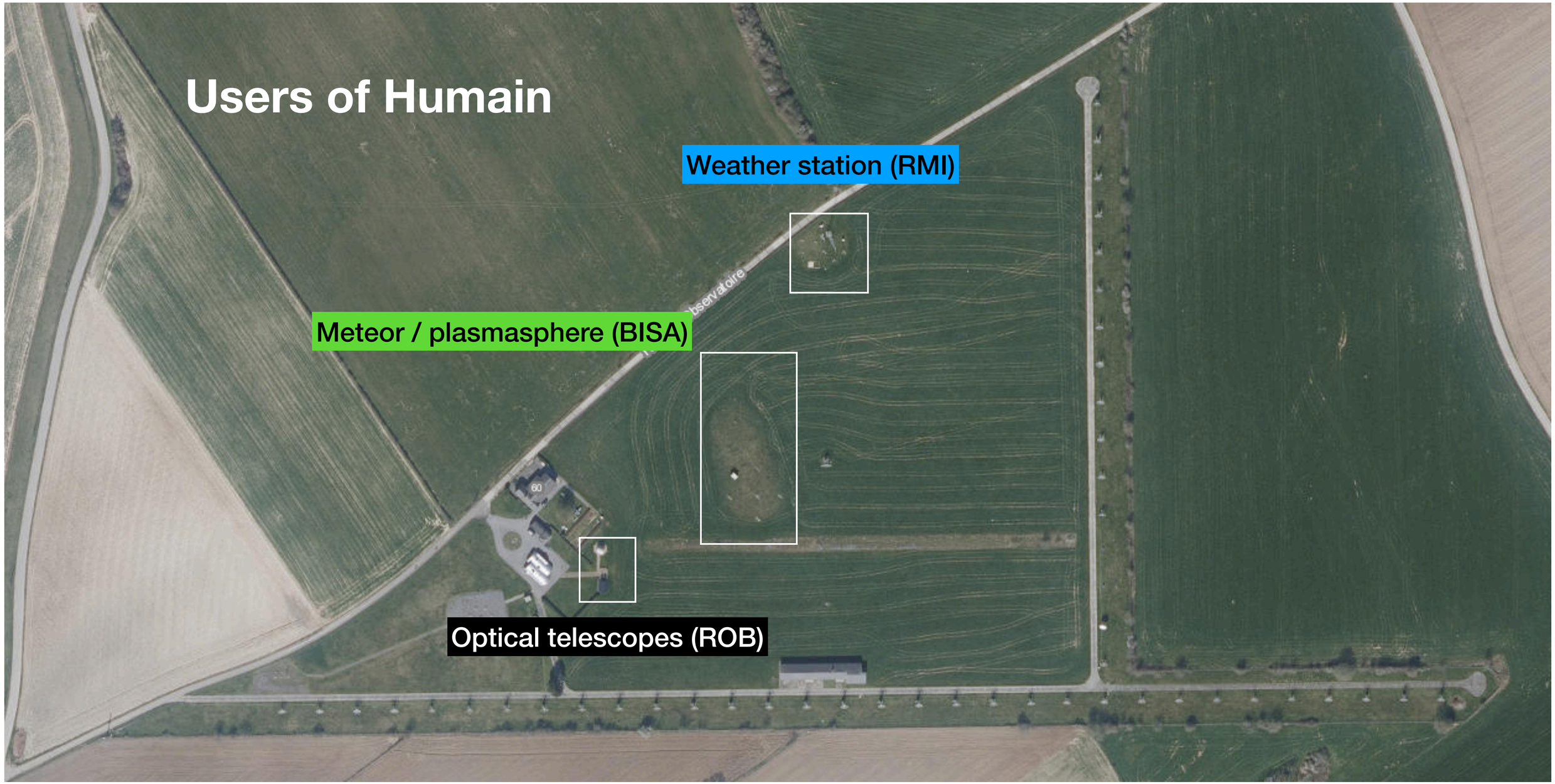

Radioastronomy



Source: WalOnMap


SPADE

SPADE

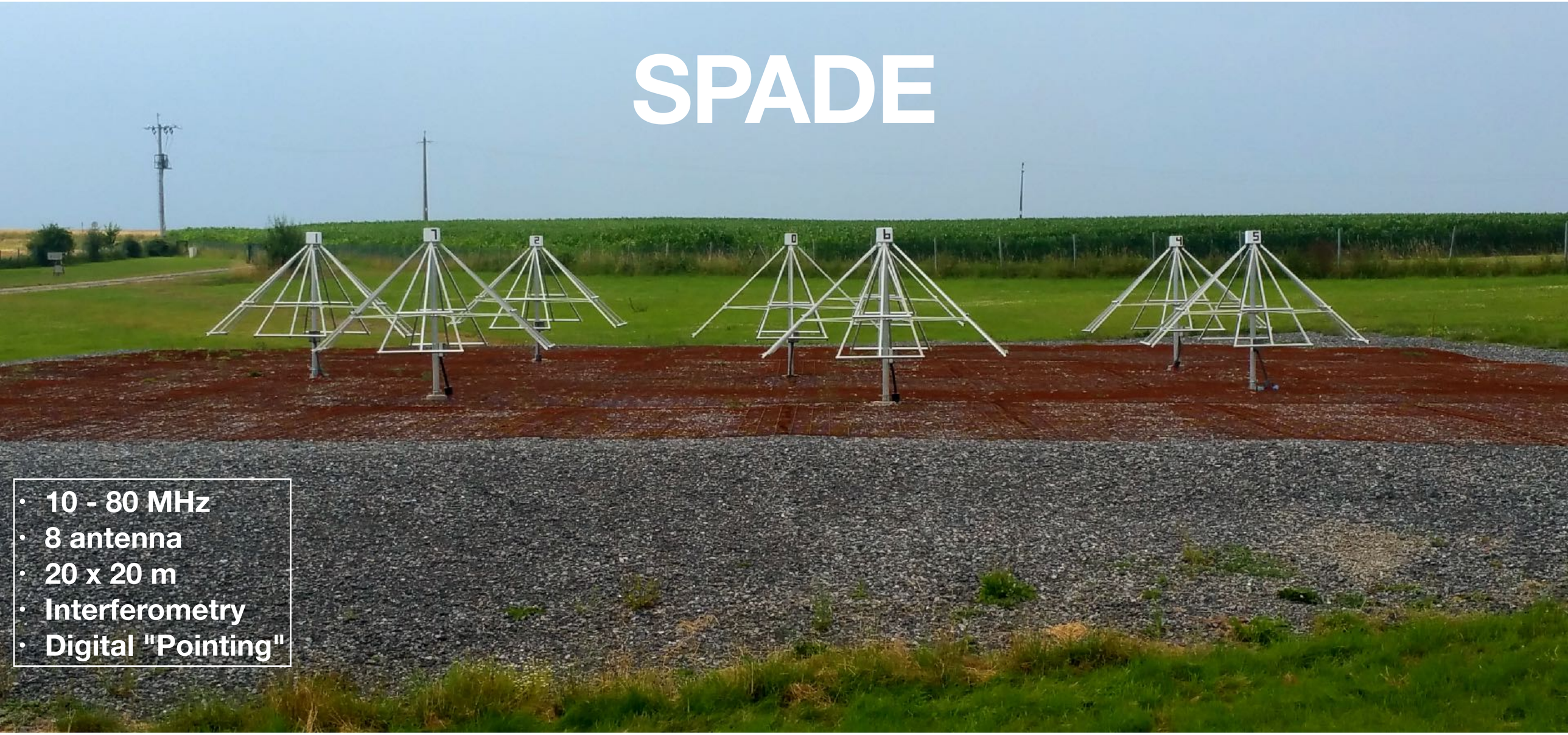

- 10 - 80 MHz
- 8 antenna
- 20 x 20 m
- Interferometry
- Digital "Pointing"

- Addition in "phase" of the signal from each antenna
- By playing digitally with the phase we can point the telescope in the sky

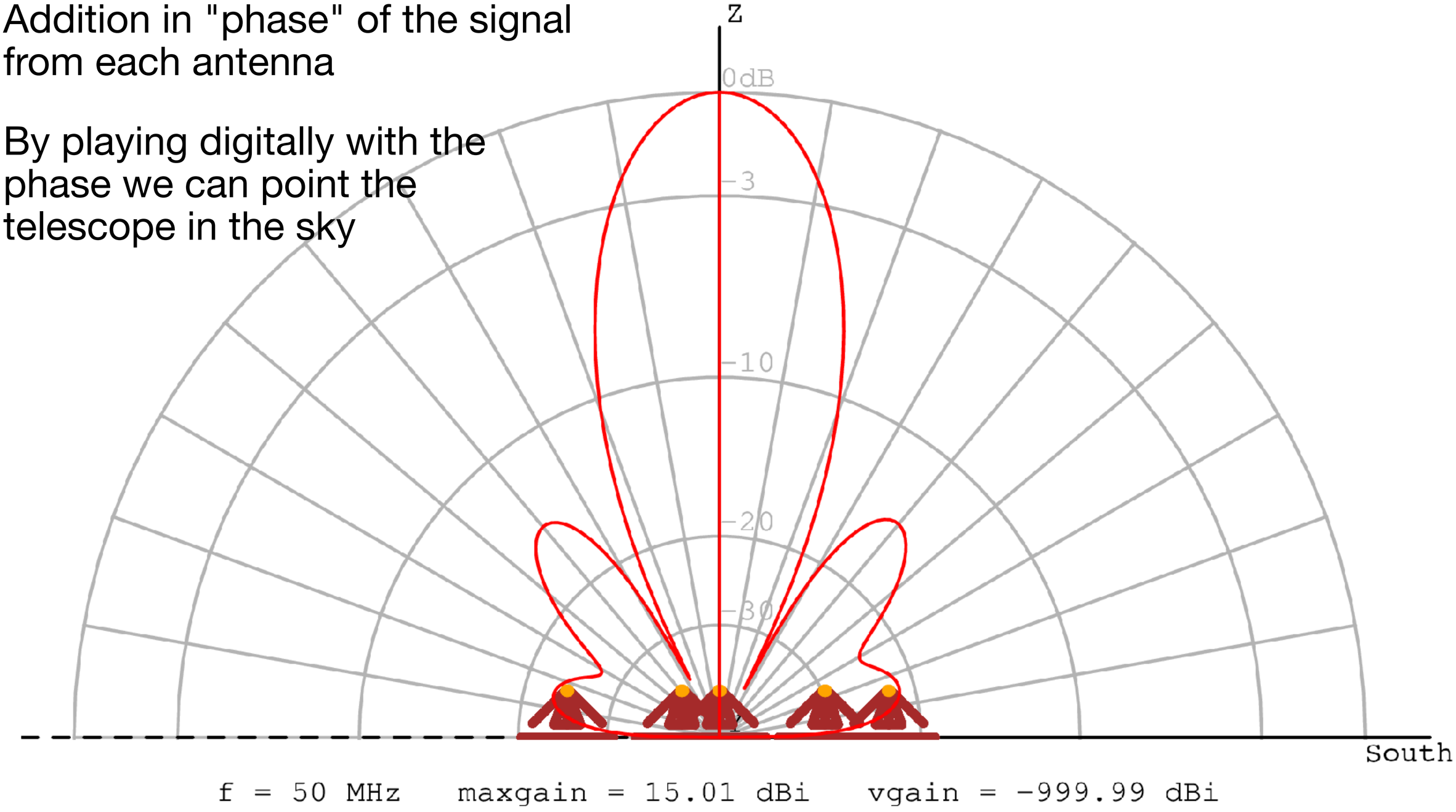

- Addition in "phase" of the signal from each antenna
- By playing digitally with the phase we can point the telescope in the sky

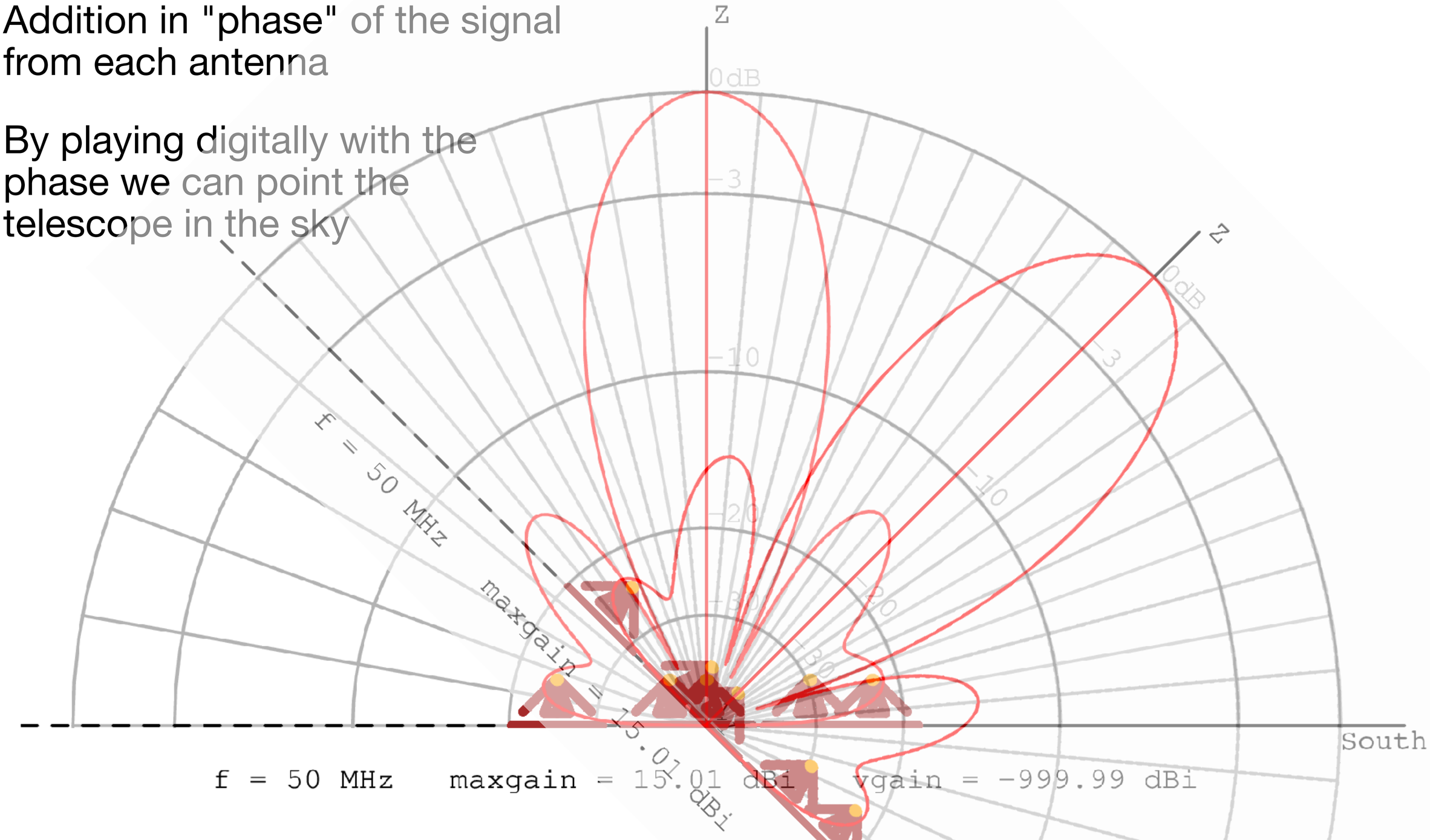














HITACHI

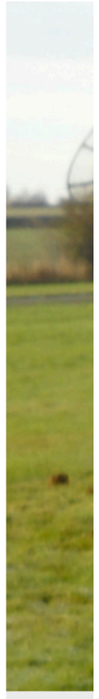















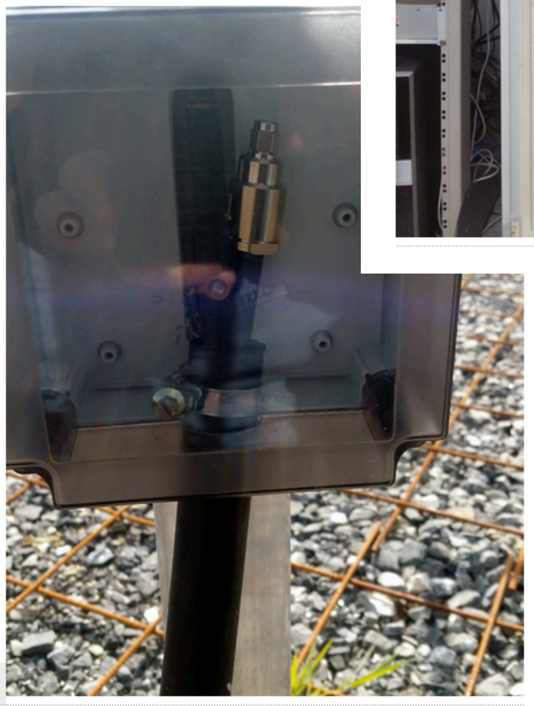









SPADE

4 months of regular solar observations

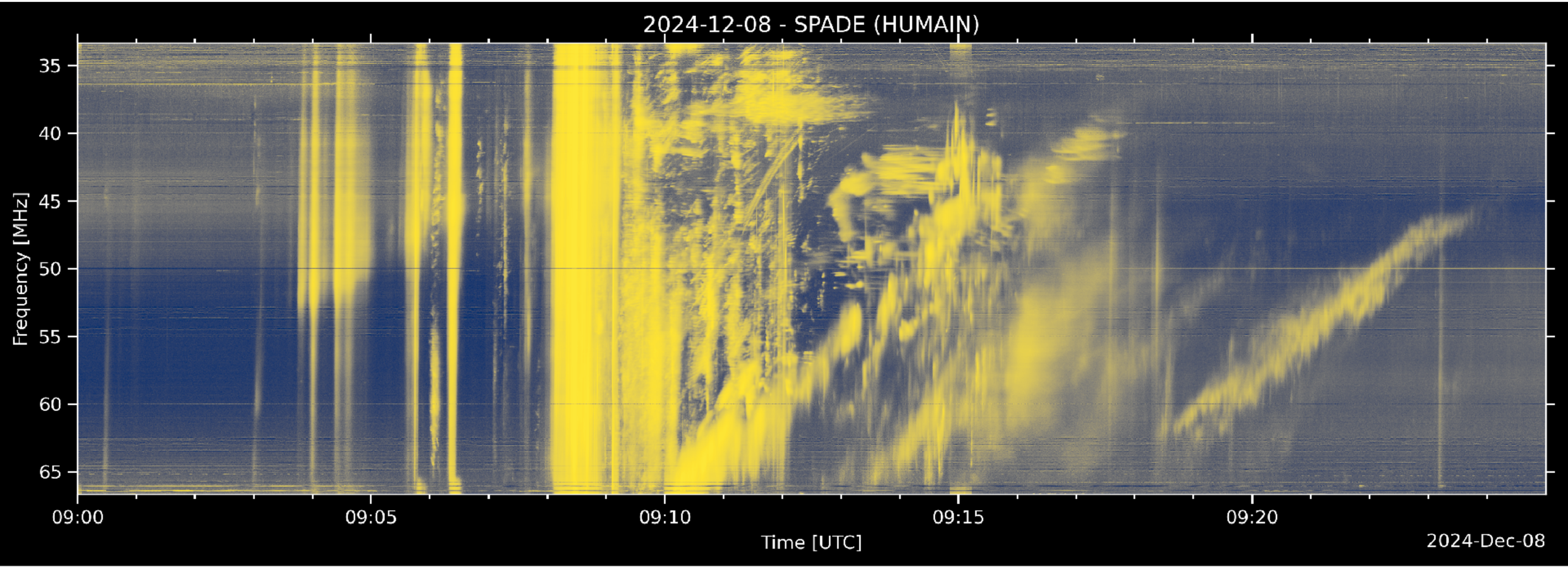

SPADE

Jovian observations

- Mainly modulated by Io's position w/r Jupiter magnetic field & Earth's viewpoint
- Space weather may have a weaker impact
- Possibility of coordinated observations

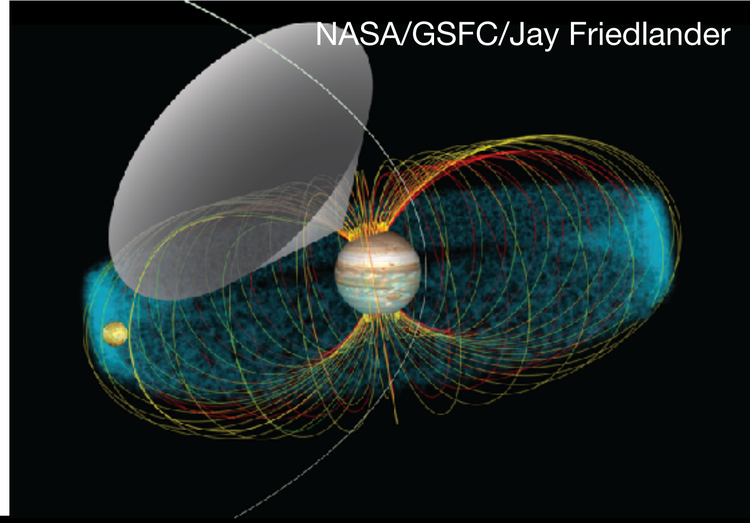

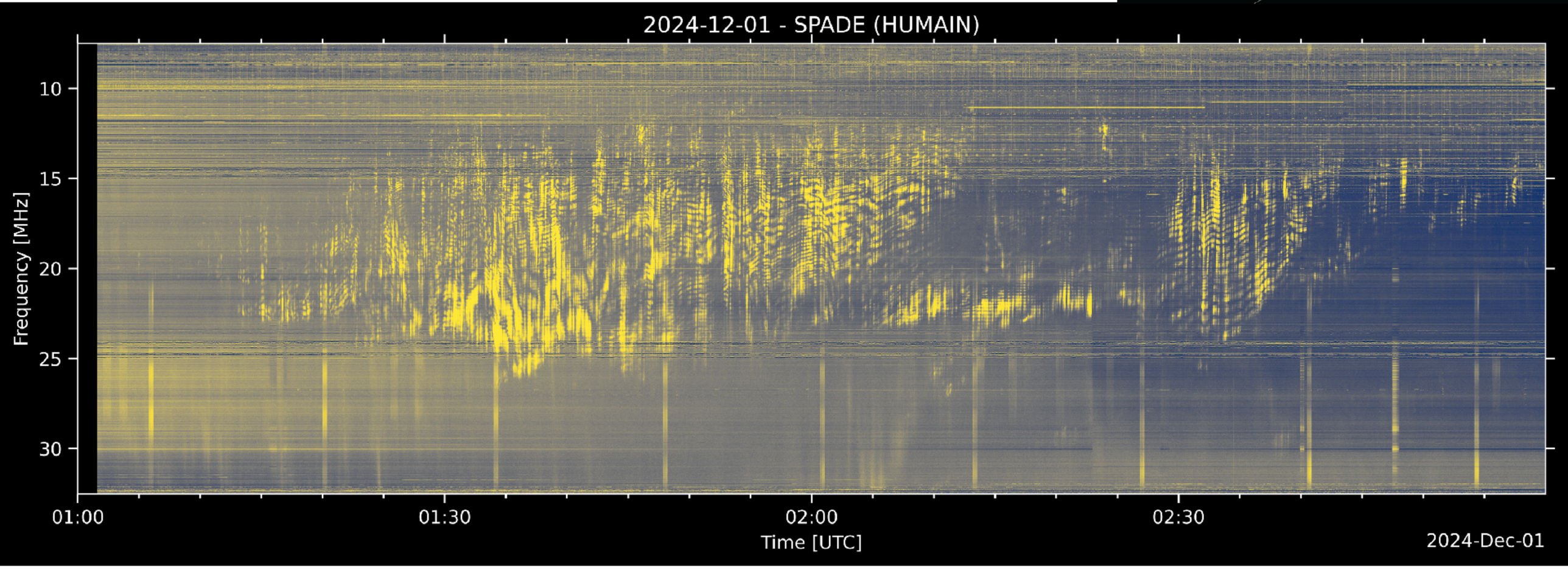

SPADE

Jovian observations

- Mainly modulated by Io's position w/r Jupiter magnetic field & Earth's viewpoint
- Space weather may have a weaker impact
- Possibility of coordinated observations

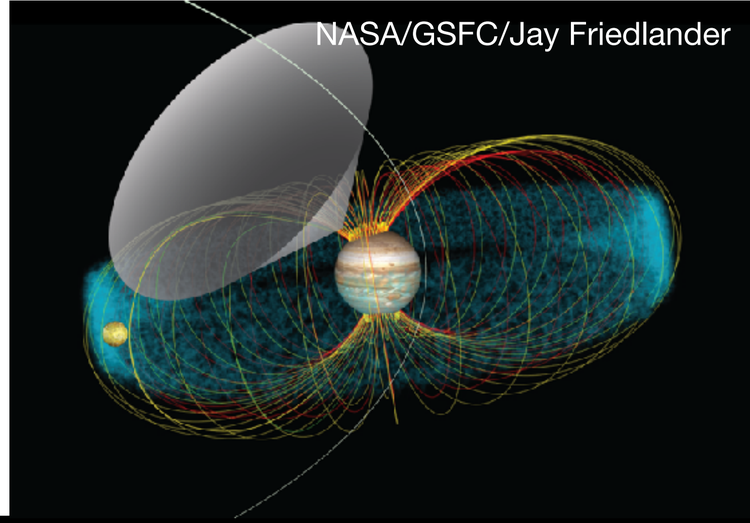

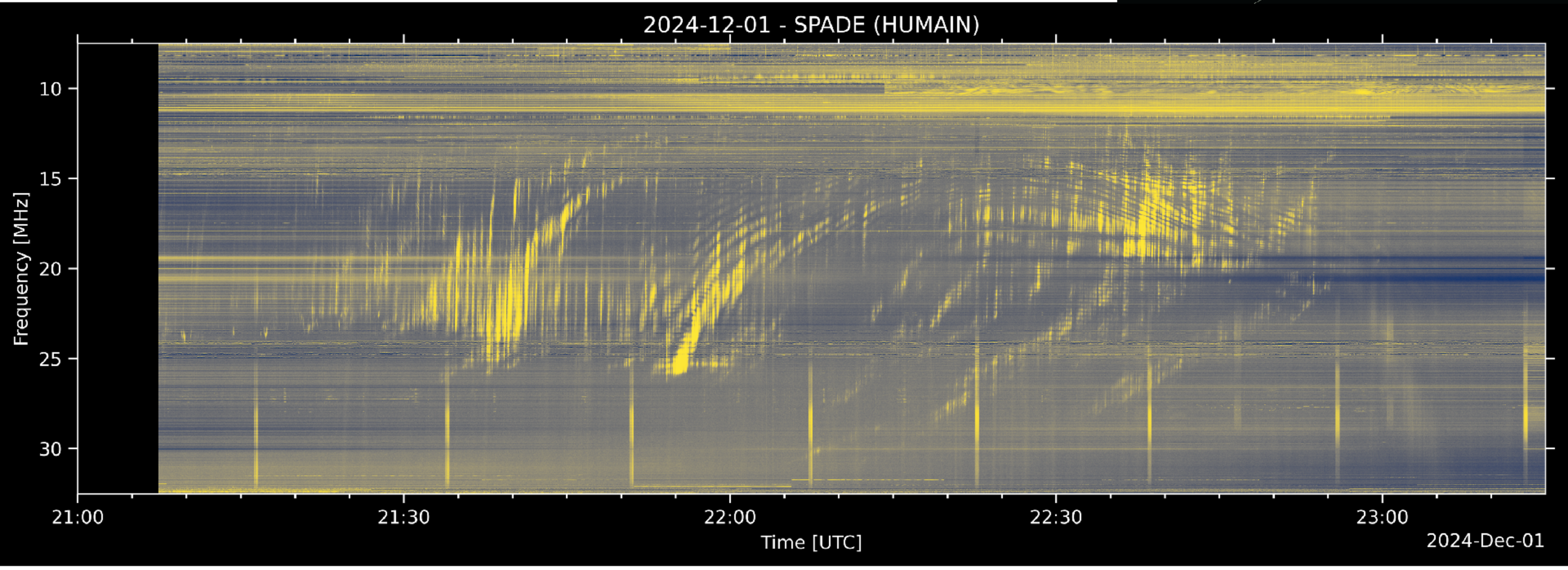

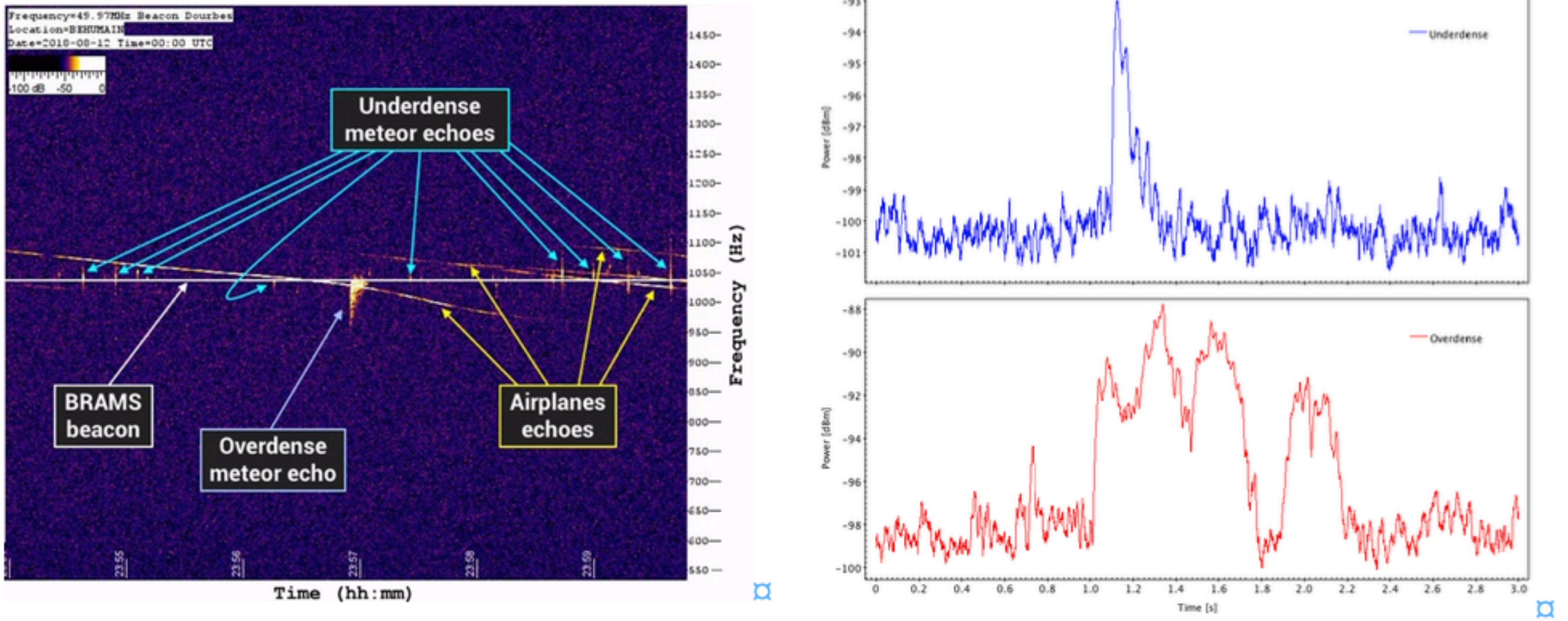

Figure 12 Meteor observation with one of the SPADE antennas. Left, dynamic spectrum; right, profile recorded with a spectrum analyzer (from Martinez & Marqué, 2018 in prep)


ANT61

ANT61

45 MHz

Callisto
ARCAS

275 MHz

HSRS

1500 MHz



Spectrograph

Analog ones: e.g. CALLISTO

Parameter	Specification
Frequency range	45-870 MHz
Frequency resolution	62.5 kHz
Bandwidth	300 kHz (-3dB)
Dynamic range	~50 dB
Sensitivity	25±1 mV/dB
Noise figure	<10dB
Sampling rate	800-1000 samp/s
Weight	800g
Dimensions	11x8x20.5 cm

Monstein, C.

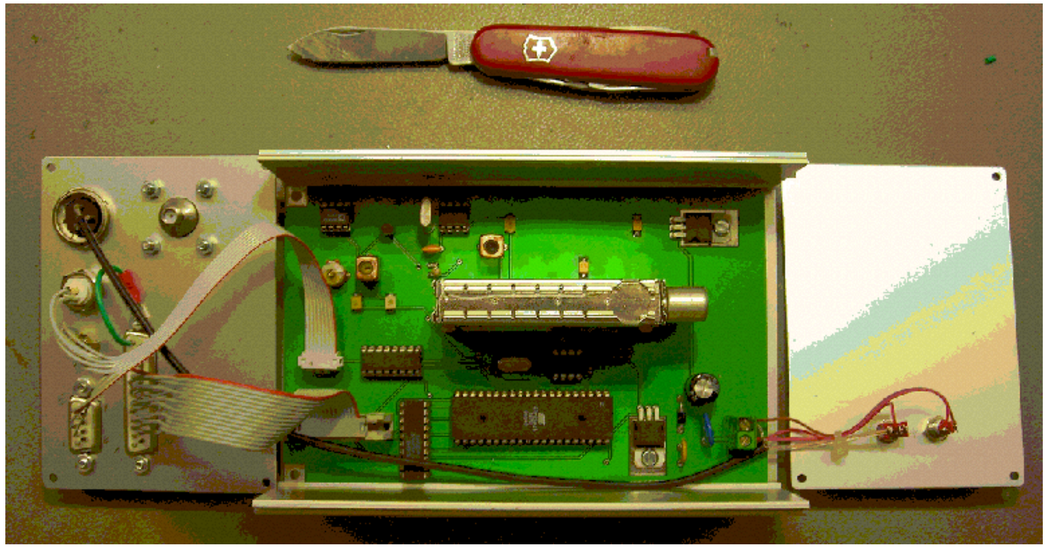

- Made from consumer electronics hardware PC-controlled hardware with RS232 connection
- Software for automatic observations (frequency program, schedule…)
- Programmable frequencies

Digital spectrograph



- GNURADIO, Python, C
- Sweep FFT spectrometer
- Fully programmable
- upgradable according to new situation (interferences...)
- Same family of receivers used in Humain for SPADE, HSRS, ARCAS and SAFIRE

Last major event of cycle 24

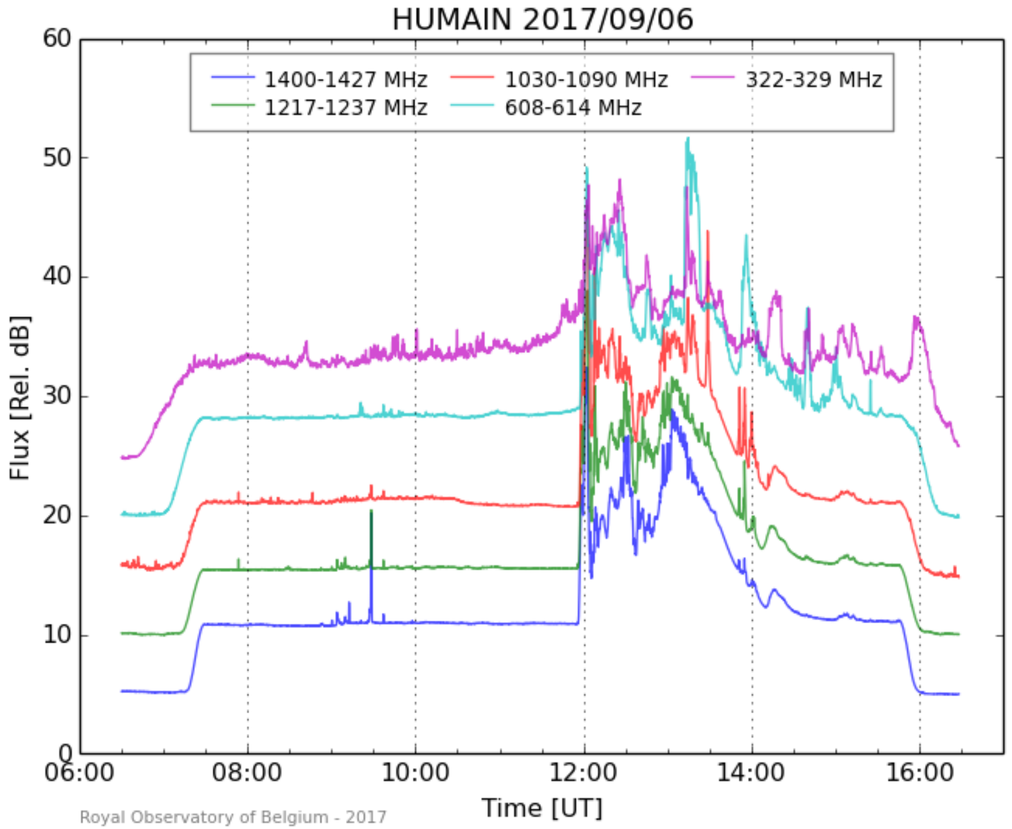

Data provided to ESA-SSA

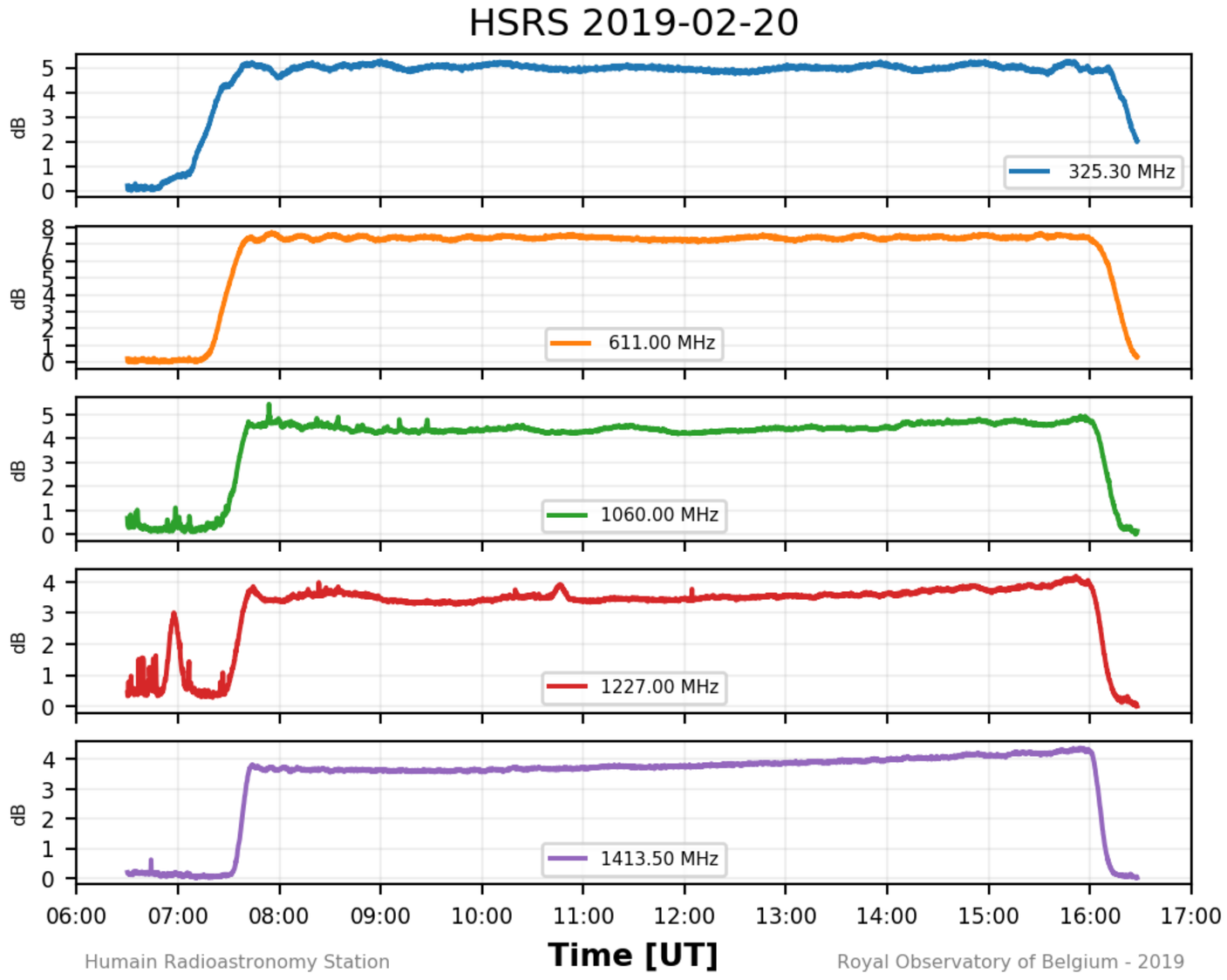

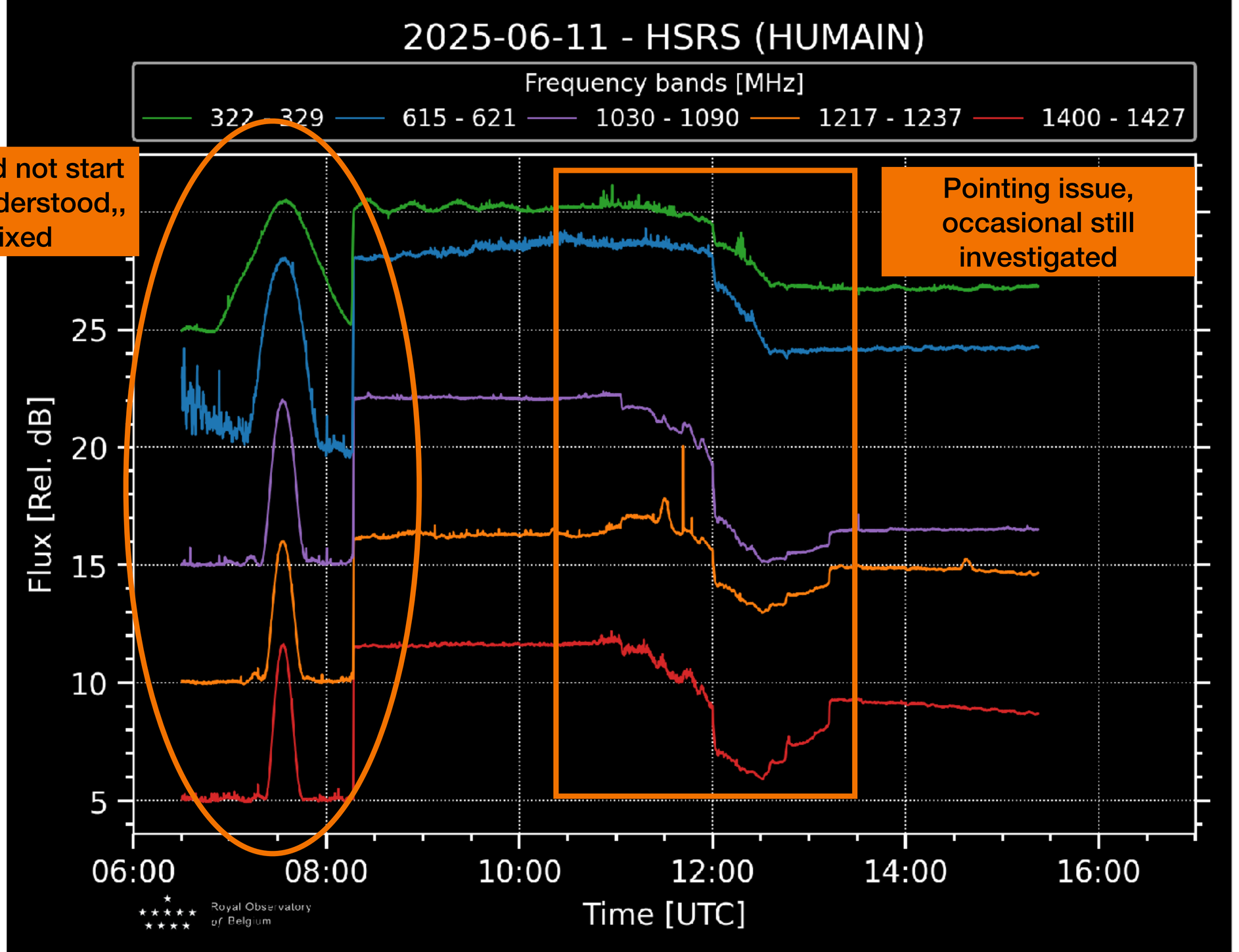
2025-06-11 - HSRS (HUMAIN)
Frequency bands [MHz]
322 - 329
615 - 621
1030 - 1090
1217 - 1237
1400 - 1427
Telescope did not start
Reason is understood,,
will be fixed
Pointing issue,
occasional still
investigated
Flux [Rel. dB]
25
20
15
10
5
06:00
08:00
10:00
12:00
14:00
16:00
Time [UTC]
Royal Observatory
of Belgium

Burst detection from Callisto

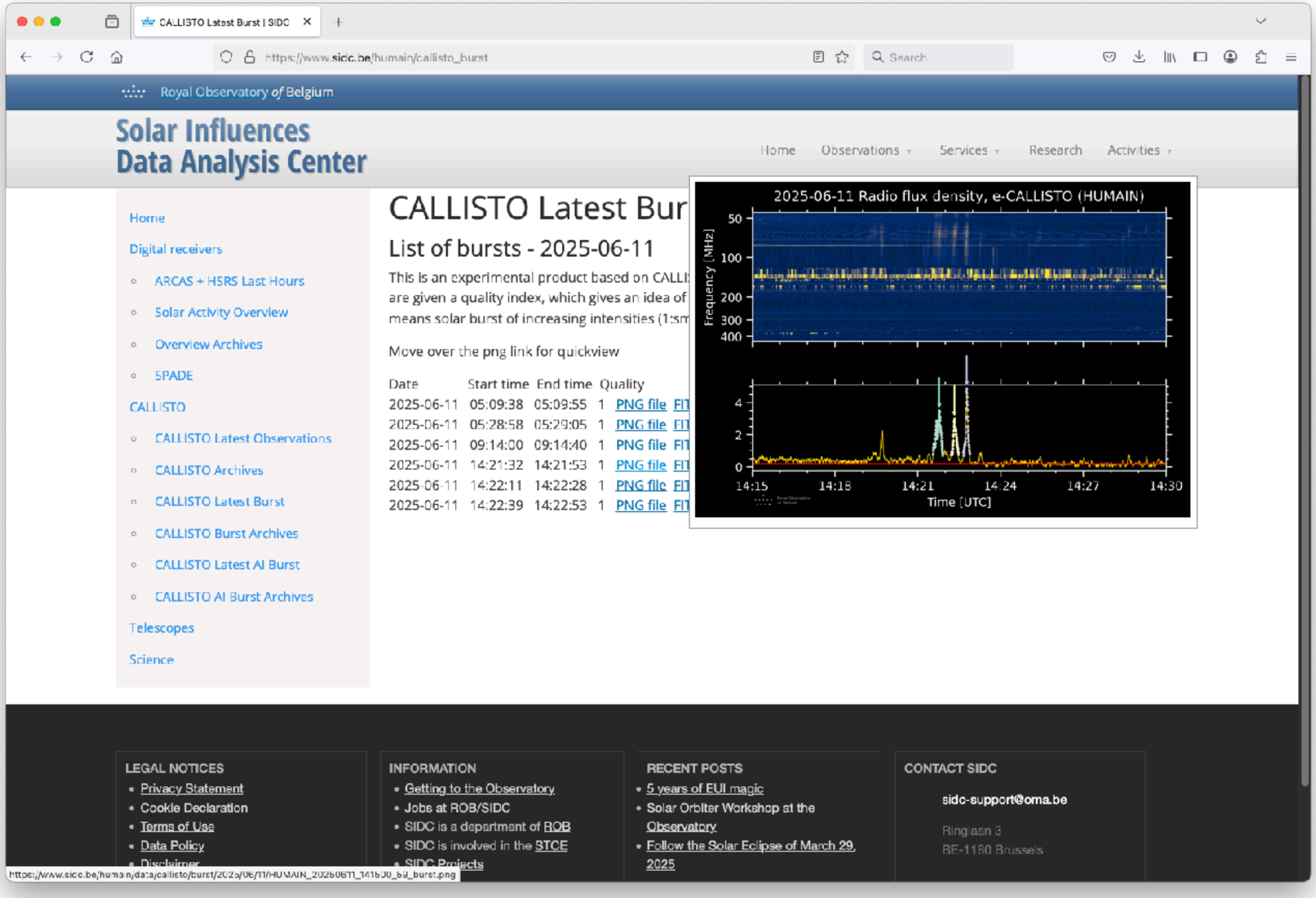

Burst detection from Callisto

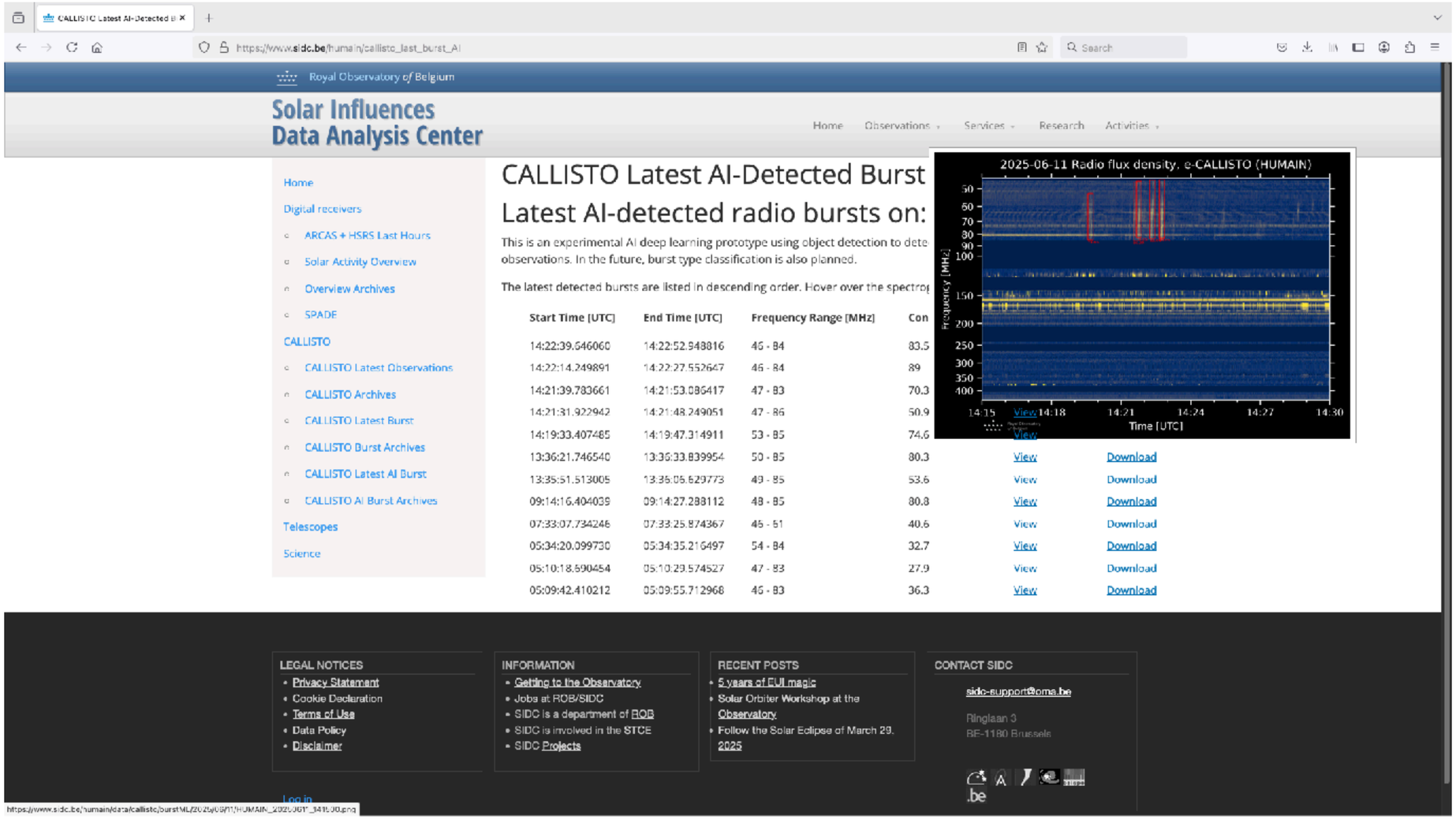

Burst detection from Callisto

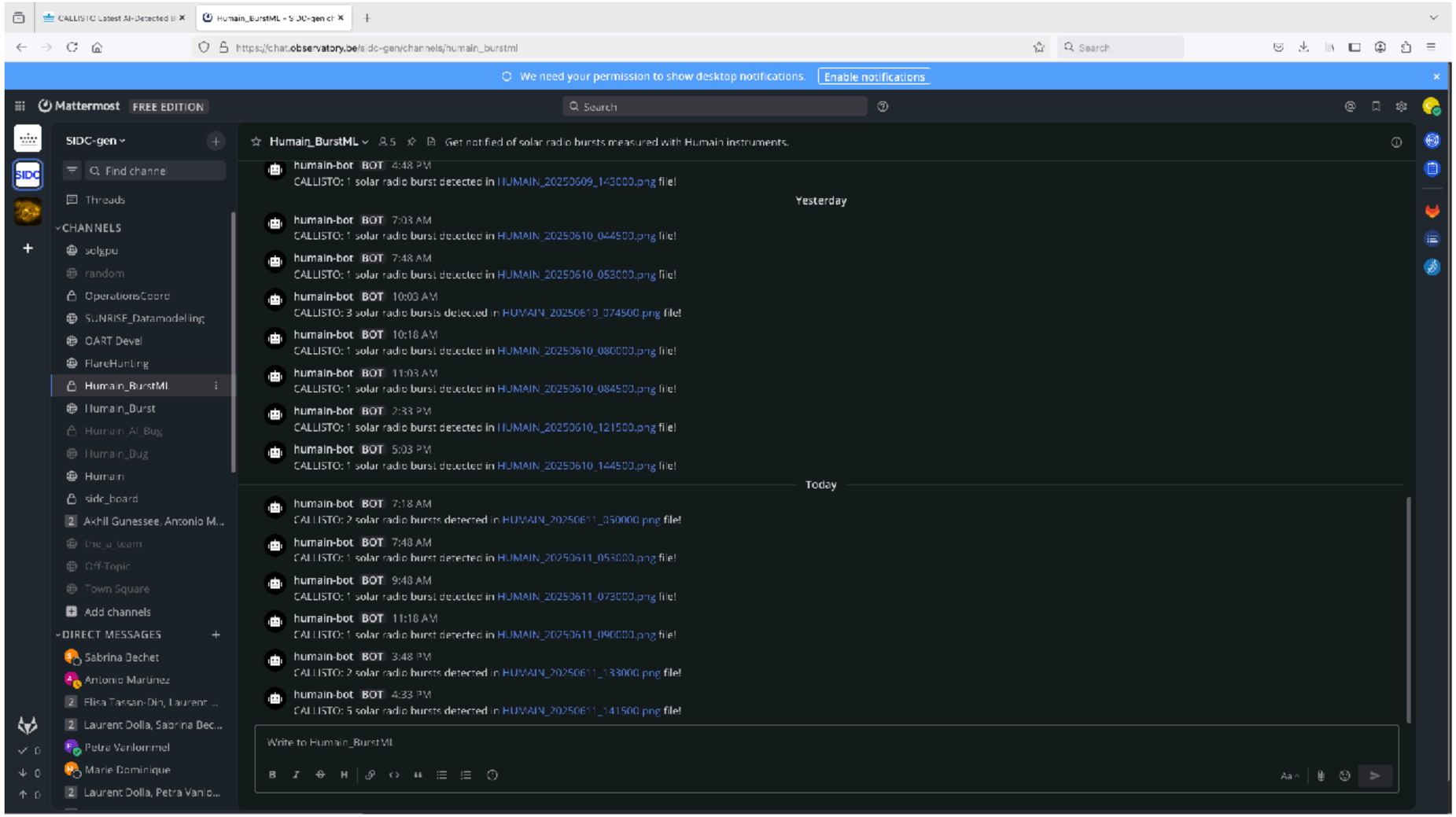


ANT34

ANT34

SAFIRE Instrument
Solar Flux between 1 & 5 GHz

1000	1060	1176	1228	1413	1575	1664
					2695	2800
			3350			
						4995

Orbitography, ATC radars, GNSS, R.A

Instrument & control system
developed at ROB



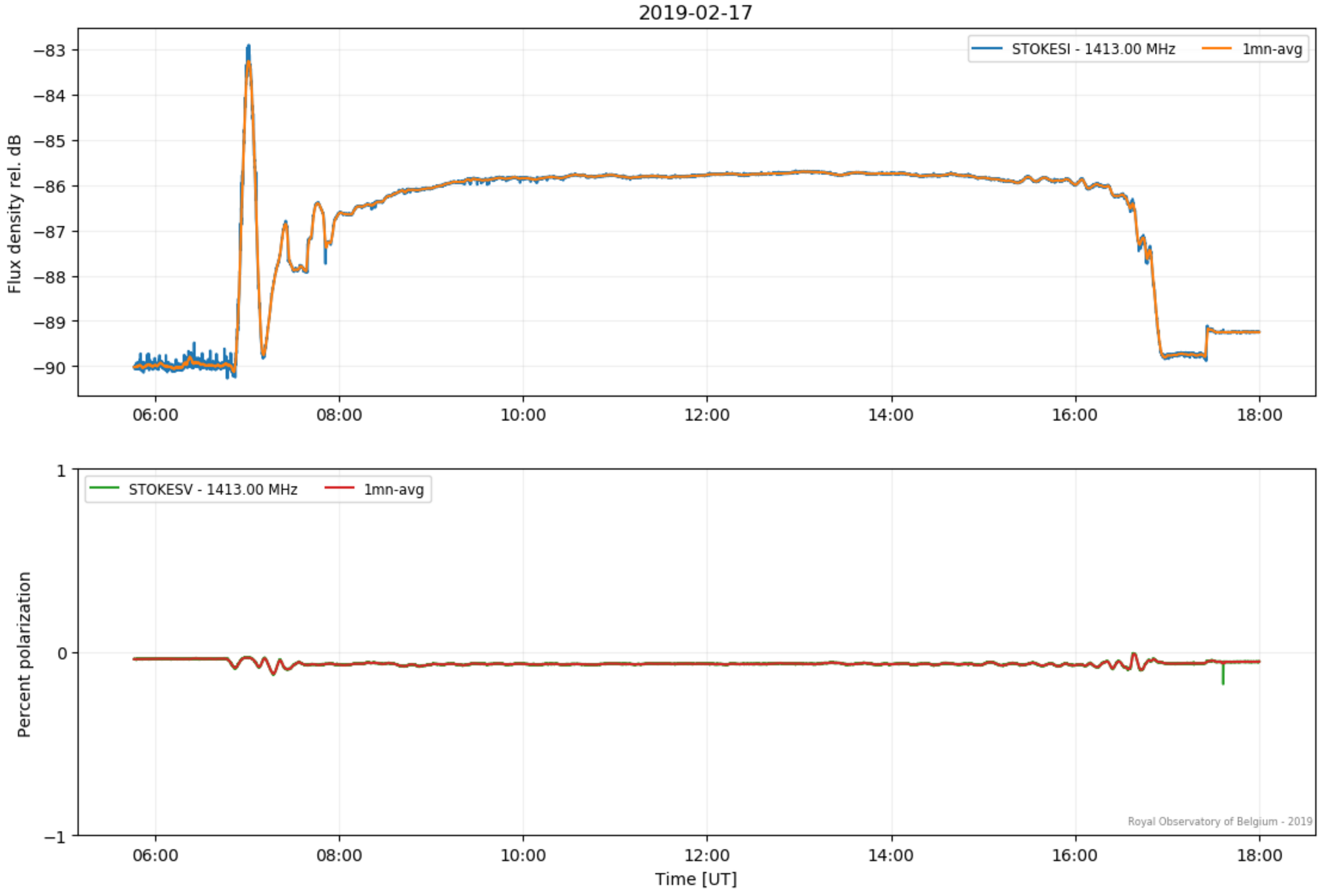
2019-02-17
STOKESI - 1413.00 MHz
1mn-avg
Flux density rel. dB
−83
−84
−85
−86
−87
−88
−89
−90
06:00
08:00
10:00
12:00
14:00
16:00
18:00
STOKESV - 1413.00 MHz
1mn-avg
Percent polarization
1
0
−1
Royal Observatory of Belgium - 2019
Time [UT]

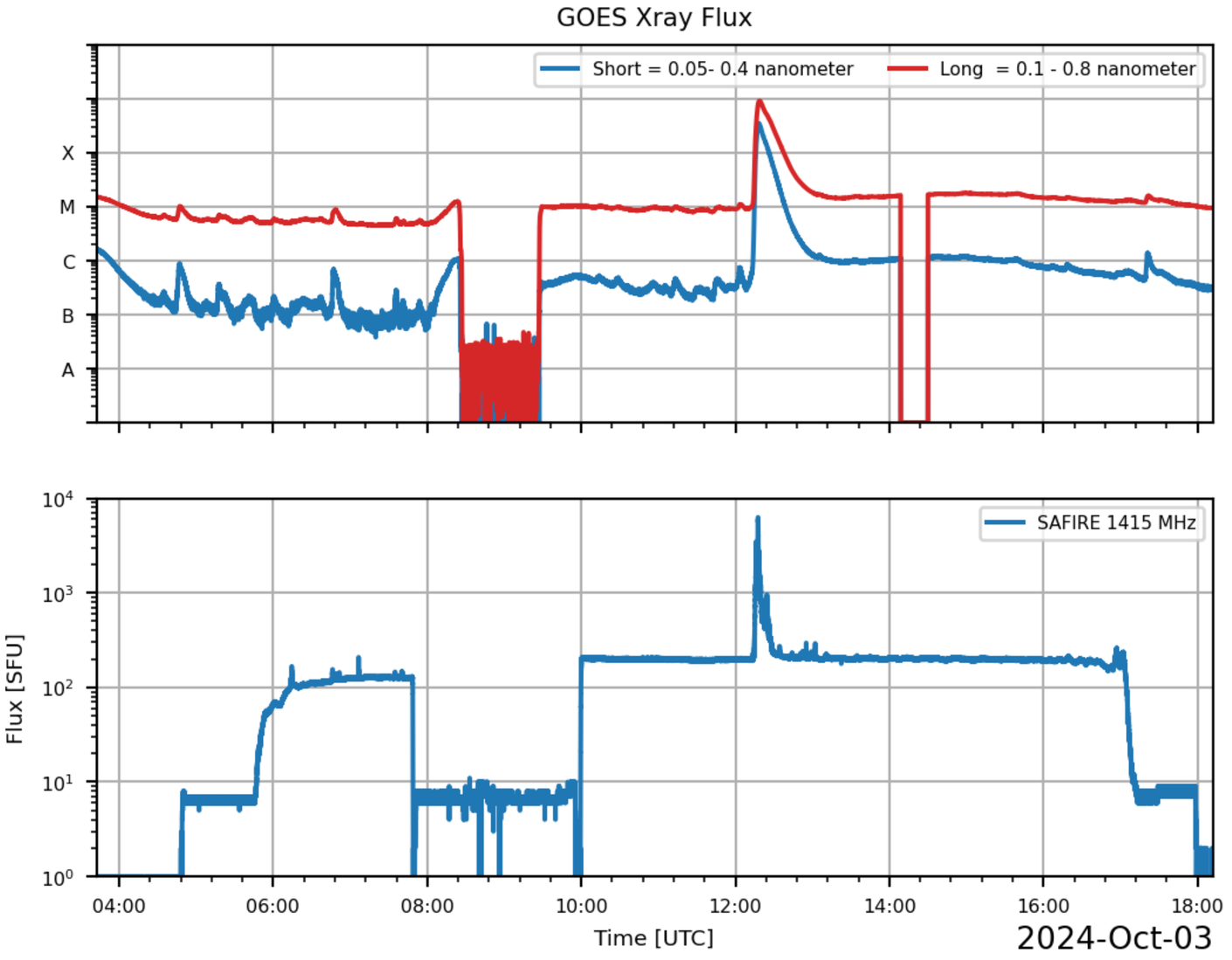
GOES Xray Flux
Short = 0.05- 0.4 nanometer
Long = 0.1 - 0.8 nanometer
X
M
C
B
A
SAFIRE 1415 MHz
Flux [SFU]
10^4
10^3
10^2
10^1
10^0
04:00
06:00
08:00
10:00
12:00
14:00
16:00
18:00
Time [UTC]
2024-Oct-03

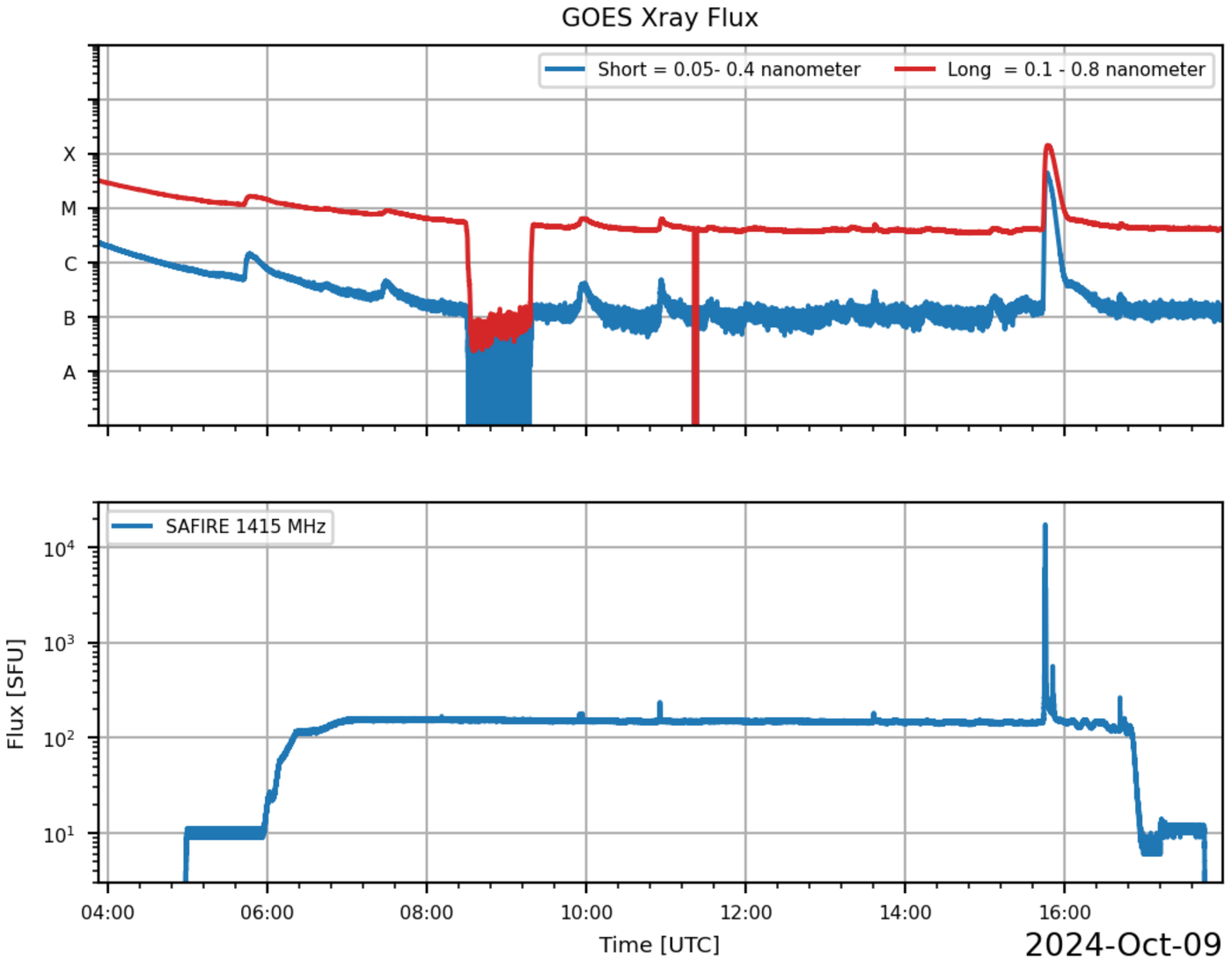
GOES Xray Flux
Short = 0.05- 0.4 nanometer
Long = 0.1 - 0.8 nanometer
X
M
C
B
A
SAFIRE 1415 MHz
Flux [SFU]
10^4
10^3
10^2
10^1
04:00
06:00
08:00
10:00
12:00
14:00
16:00
Time [UTC]
2024-Oct-09

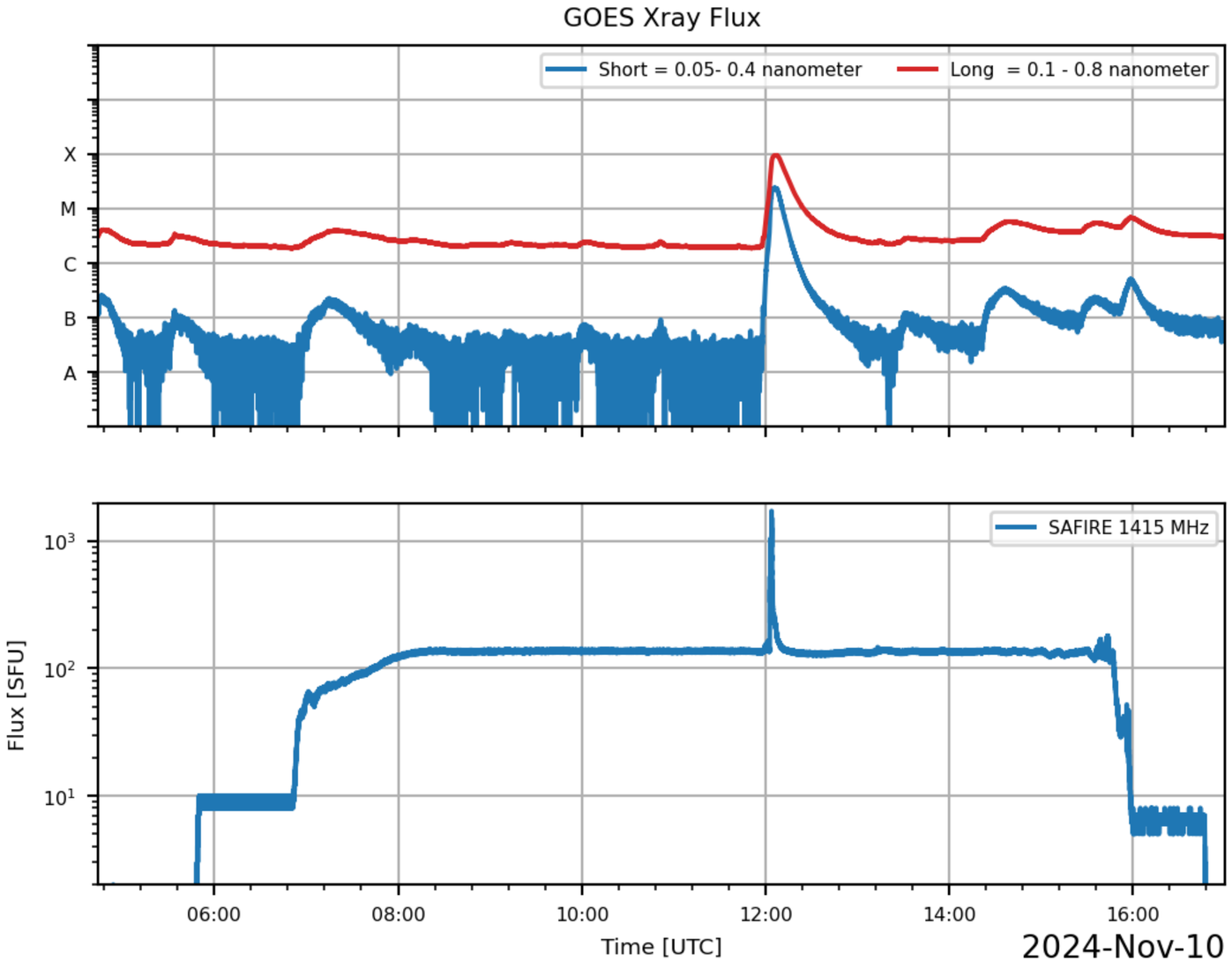
GOES Xray Flux
Short = 0.05- 0.4 nanometer
Long = 0.1 - 0.8 nanometer
X
M
C
B
A
SAFIRE 1415 MHz
Flux [SFU]
10^3
10^2
10^1
06:00
08:00
10:00
12:00
14:00
16:00
Time [UTC]
2024-Nov-10